ORNL/SR-2015/377

AGC-1 IRRADIATION INDUCED PROPERTY CHANGES ANALYSIS REPORT: ELECTRICAL RESISTIVITY AND COEFFICIENT OF THERMAL EXPANSION

Tim Burchell

Oak Ridge National Laboratory

February 2016

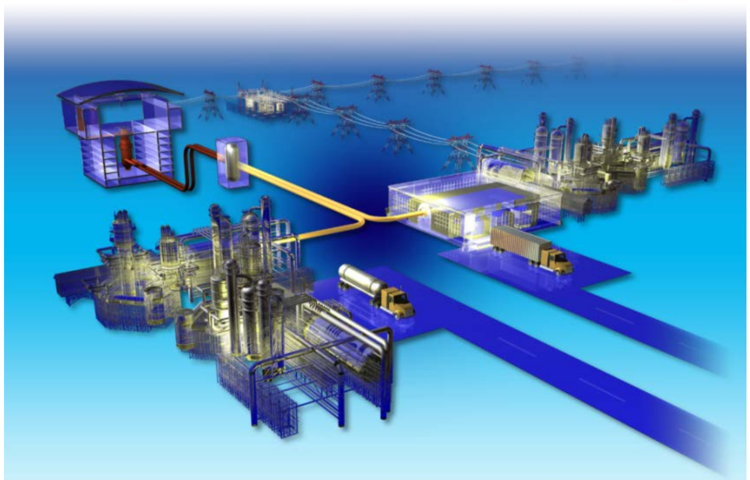

Prepared for
Office of Nuclear Energy Science and Technology
U.S. Department of Energy
Under Memorandum Purchase Order No. 00153522 with
Idaho National Laboratory

Prepared by
OAK RIDGE NATIONAL LABORATORY
Oak Ridge, Tennessee 37831
managed by
UT-BATTELLE, LLC
for the
U.S. DEPARTMENT OF ENERGY
Under DOE Contract No. DE-AC05-00OR22725

UT-BATTELLE
Oak Ridge National Laboratory

ORNL/SR-2015/377

AGC-1 IRRADIATION INDUCED PROPERTY CHANGES ANALYSIS REPORT: ELECTRICAL RESISTIVITY AND COEFFICIENT OF THERMAL EXPANSION

Tim Burchell
Oak Ridge National Laboratory

February 2016

Contents

Figures viii

Tables x

Abbreviations and Acronyms xii

Summary xiv

1. Introduction 1

2. Experimental 1

2.1 Electrical Resistivity 1

2.2 Coefficient of Thermal Expansion (CTE) 1

2.3 Irradiation Conditions 1

2.4 Error Analysis and Significance Testing 2

2.4.1 Error Analysis 2

2.4.2 Statistical Significance Testing 3

3. Results 4

3.1 Electrical Resistivity 4

3.1.1 Grade A, NBG-17 6

3.1.2 Grade B, NBG-18 7

3.1.3 Grade C, H-451 8

3.1.4 Grade D, PCEA 9

3.1.5 Grade E, IG-110 10

3.1.6 Grade F, IG-430 11

3.1.7 Grade Anisotropy Effects on Resistivity 12

3.2 Coefficient of Thermal Expansion 13

3.2.1 Grade A, NBG-17 14

3.2.2 Grade B, NBG-18 17

3.2.3 Grade C, H-451 18

3.2.4 Grade D, PCEA 19

3.2.5 Grade E, IG-110 20

3.2.6 Grade F, IG-430 21

3.2.7 Stress Direction and Isotropy Effects on Coefficient of Thermal Expansion 22

3.2.8 The Development of CTE with Creep Strain 23
4 Discussion 27
4.1 Electrical Resistivity 27
4.1.1 Grade A, NBG-17 28
4.1.2 Grade B, NBG-18 28
4.1.3 Grade C, H-451 29
4.1.4 Grade D, PCEA 29
4.1.5 Grade E, IG-110 30
4.1.6 Grade F, IG-430 30
4.1.7 Electrical Resistivity Statistical Testing 31
4.2 Coefficient of Thermal Expansion 35
4.2.1 Grade A, NBG-17 37
4.2.2 Grade B, NBG-18 37
4.2.3 Grade C, H-451 38
4.2.4 Grade D, PCEA 38
4.2.5 Grade E, IG-110 39
4.2.6 Grade F, IG-430 39
4.2.7 CTE Statistical Testing 40
5 Quality Assurance 45
6 Conclusions 45
7 Acknowledgements 45
8 Appendices 46
8.1 Electrical Resistivity 46
8.1.1 NBG-17 46
8.1.2 NBG-18 47
8.1.3 H-451 48
8.1.4 PCEA 49
8.1.5 IG-110 50
8.1.6 IG-430 51
8.2 Coefficient of Thermal Expansion 52
8.2.1 NBG-17 52
8.2.2 NBG-18 53

8.2.3 H-451 54
8.2.4 PCEA 55
8.2.5 IG-110 56
8.2.6 IG-430 57
9 Distribution 58
10 References 58

Figures

Figure 1 Variation of electrical resistivity with irradiation dose for NBG-17 graphite 6
Figure 2 Variation of electrical resistivity with compressive creep strain for NBG-17 graphite.................. 6
Figure 3 Variation of electrical resistivity with irradiation dose for NBG-18 graphite 7
Figure 4 Variation of electrical resistivity with compressive creep strain for NBG-18 graphite.................. 7
Figure 5 Variation of electrical resistivity with irradiation dose for H-451 graphite 8
Figure 6 Variation of electrical resistivity with compressive creep strain for H-451 graphite 8
Figure 7 Variation of electrical resistivity with irradiation dose for PCEA graphite 9
Figure 8 Variation of electrical resistivity with compressive creep strain for PCEA graphite....................... 9
Figure 9 Variation of electrical resistivity with irradiation dose for IG-110 graphite 10
Figure 10 Variation of electrical resistivity with compressive creep strain for IG-110 graphite 10
Figure 11 Variation of electrical resistivity with irradiation dose for IG-430 graphite 11
Figure 12 Variation of electrical resistivity with compressive creep strain for IG-430 graphite 11
Figure 13 Mean increase in electrical resistivity 13
Figure 14 The variation of Average CTE with temperature for NBG-17 (AW) creep specimen AW 10-03 (6.00dpa, -1.893% creep strain, T_{irr} = 670°C) and control specimen 12-03 (5.43 dpa, T_{irr} = 594°C) 15
Figure 15 The variation of mean $CTE_{(25\text{-}500°C)}$ with dose for NBG-17(WG) control samples 16
Figure 16 The variation of mean $CTE_{(25\text{-}500°C)}$ with compressive creep strain for NBG-17(WG) creep samples 16
Figure 17 The variation of $CTE_{(25\text{-}500°C)}$ with dose for NBG-18 (WG) control samples 17
Figure 18 The variation of mean $CTE_{(25\text{-}500°C)}$ with compressive creep strain for NBG-18 (WG) creep samples 17
Figure 19 The variation of $CTE_{(25\text{-}500°C)}$ with dose for H-451(WG) control samples 18
Figure 20 The variation of mean $CTE_{(25\text{-}500°C)}$ with compressive creep strain for H-451(WG) creep samples 18
Figure 21 The variation of mean $CTE_{(25\text{-}500°C)}$ with dose for PCEA (WG) control samples 19
Figure 22 The variation of mean $CTE_{(25\text{-}500°C)}$ with compressive creep strain for PCEA (WG) creep samples 19
Figure 23 The variation of mean $CTE_{(25\text{-}500°C)}$ with dose for IG-110 control samples 20
Figure 24 The variation of mean $CTE_{(25\text{-}500°C)}$ with compressive creep strain for IG-110 creep samples 20
Figure 25 The variation of mean $CTE_{(25\text{-}500°C)}$ with dose for IG-430 control samples 21
Figure 26 The variation of $CTE_{(25\text{-}500°C)}$ with compressive creep strain for IG-430 creep samples 21
Figure 27 Temperature dependence of mean CTE for various levels of compressive creep strain for NBG-17 (AW) 23
Figure 28 Temperature dependence of mean CTE for various levels of compressive creep strain for NBG-18 (BW) 23
Figure 29 Temperature dependence of mean CTE for various levels of compressive creep strain for H-451 (WG) 24
Figure 30 Temperature dependence of mean CTE for various levels of compressive creep strain for PCEA (WG) 24

Figure 31 Temperature dependence of mean CTE for various levels of compressive creep strain for IG-110 25
Figure 32 Temperature dependence of mean CTE for various levels of compressive creep strain for IG-430 25
Figure 33 Fractional changes in resistivity for control and creep specimen of NBG-17 (AL) and NBG-17 (AW) 28
Figure 34 Fractional changes in resistivity for control and creep specimen of NBG-18 (BL) and NBG-18 (BW) 28
Figure 35 Fractional changes in resistivity for control and creep specimen of H-451 (WG) 29
Figure 36 Fractional changes in resistivity for control and creep specimen of PCEA (AG) and PCEA (WG)29
Figure 37 Fractional changes in resistivity for control and creep specimen of IG-110........ 30
Figure 38 Fractional changes in resistivity for control and creep specimen of IG-430........ 30
Figure 39 Fractional changes in CTE for control and creep specimen of NBG-17 (AW) and NBG-17 (AL) . 37
Figure 40 Fractional changes in CTE for control and creep specimen of NBG-18 (BW) and NBG-18 (BL).. 37
Figure 41 Fractional changes in CTE for control and creep specimen of H-451 (WG)........ 38
Figure 42 Fractional changes in CTE for control and creep specimen of PCEA (AG) and PCEA (WG)........ 38
Figure 43 Fractional changes in CTE for control and creep specimen of IG-110 39
Figure 44 Fractional changes in CTE for control and creep specimen of IG-430 39

Tables

Table 1 3σ expressed as a percentage of mean for unirradiated electrical resistivity 2
Table 2 3σ expressed as a percentage of mean for unirradiated Mean Coefficient of Thermal Expansion (25-500°C) 2
Table 3 Significance Level and their associated "p" values 3
Table 4 Electrical resistivity values for the unirradiated graphite specimens 5
Table 5 the mean electrical resistivity's and mean percentage increase for the major grades irradiated in AGC-1 12
Table 6 Statistical significance test questions 31
Table 7 Unirradiated resistivity means and the three highest dose creep and control specimens and their electrical resistivity for each grade of graphite in AGC-1 32
Table 8 "t' tests results for the specimen irradiation dose 33
Table 9 Significance testing results for the electrical resistivity data 34
Table 10 Unirradiated $CTE_{(25\text{-}500°C)}$ and the three largest values doses specimens and their corresponding values of $CTE_{(25\text{-}500°C)}$ for the creep and control specimens for each major grade of graphite in AGC-1 41
Table 11 Significance testing results for the mean coefficient of thermal expansion (25-500°C) with largest dose from AGC-1 42
Table 12 Unirradiated $CTE_{(25\text{-}500°C)}$ and the three largest values of $CTE_{(25\text{-}500°C)}$ for the creep and control specimens and their doses for each major grade of graphite in AGC-1 43
Table 13 "t' tests results for the specimen irradiation dose of the three specimens with the largest $CTE_{(25\text{-}500°C)}$ 44
Table 14 Significance testing results for the three largest mean coefficient of thermal expansion (25-500°C) from AGC-1 44
Table 15 Electrical resistivity data for irradiated and crept samples of NBG-17 graphite 46
Table 16 Electrical resistivity data for irradiated and crept samples of NBG-18 graphite 47
Table 17 Electrical resistivity data for irradiated and crept samples of H-451 graphite 48
Table 18 Electrical resistivity data for irradiated and crept samples of PCEA graphite 49
Table 19 Electrical resistivity data for irradiated and crept samples of IG-110 graphite 50
Table 20 Electrical resistivity data for irradiated and crept samples of IG-430 graphite 51
Table 21 Average Coefficient of Thermal Expansion (α) over the temperature range RT - 500°C for irradiated and crept NBG-17 Graphite 52
Table 22 Average Coefficient of Thermal Expansion (α) over the temperature range RT - 500°C for irradiated and crept NBG-18 Graphite 53
Table 23 Average Coefficient of Thermal Expansion (α) over the temperature range RT - 500°C for irradiated and crept H-451 Graphite 54
Table 24 Average Coefficient of Thermal Expansion (α) over the temperature range RT - 500°C for irradiated and crept PCEA Graphite 55
Table 25 Average Coefficient of Thermal Expansion (α) over the temperature range RT - 500°C for irradiated and crept IG-110 Graphite 56
Table 26 Average Coefficient of Thermal Expansion (α) over the temperature range RT - 500°C for irradiated and crept IG-430 Graphite 57

Abbreviations and Acronyms

AGC	Advanced graphite creep
ATR	Advanced Test Reactor
ER	Electrical resistivity
CTE	Coefficient of thermal expansion
DOE	Department of Energy
dpa	displacements per atom
INL	Idaho National Laboratory
ORNL	Oak Ridge National Laboratory

Summary

The analysis of some of the test property data from the AGC-1 creep capsule is reported. Specifically, the analysis of the electrical resistivity (ER) and coefficient of thermal expansion (CTE) is reported. AGC-1 was operated at ~640°C and the irradiated specimen CTE (α) over the temperature range 25°C to 550°C was experimentally measured. Consequently, the mean CTE value for the temperature range 25°C – 500°C was analyzed. Both the ER and mean $CTE_{(25\text{-}500°C)}$ have been examined as a function of specimen dose (control specimens) and creep strain, %, (creep specimen). A direct comparison of the property changes was made for the creep and control specimens by plotting their respective fractional changes as a function on neutron dose. Statistical "t" testing was applied to any observed differences in property (ER or CTE) as a function of dose for the creep and control specimens of each graphite grade in the AGC-1 capsule. For electrical resistivity the irradiated value was shown to be greater than the unirradiated value for all graphite grades. However, the additional change due to creep strain was not found to be statistically significant. The coefficient of thermal expansion was seen to increase with dose for both the creep and control specimens. This increase was clearly seen in the fractional changes in CTE plot. The creep specimens were seen to increase their CTE above that noted for the control samples. The values of mean $CTE_{(25\text{-}500°C)}$ was statistically "t" tested and the differences between the creep and control CTE increases were shown to be statistically significant. Thus, creep strain is shown to have no additional effect upon ER but does increase the CTE over that observed from dose alone. The additional increase of CTE due to creep, is attributed to the closure of a larger fraction of the aligned porosity by compressive creep.

1. Introduction

This report, along with its companion report[1], represent the final detailed data assessments from capsule AGC-1,[2,3] the first and prototype irradiation creep capsule of the AGC experiment. Preirradiation data[4] and post irradiation data[5] were previously reported. Analysis of the dimensional change, volume change and creep strain data is given in ORNL/TM-2014/255[6]. In this report, property change data, specifically electrical resistivity, ρ, and coefficient of thermal expansion, α, as a function of irradiation induced creep strain at a nominal temperature of 641 °C, and to a peak dose of 7 displacements per atom (dpa) from capsule AGC-1, are analyzed. The data from this report shall be supplied to the NDMAS database and the Gen IV Handbook. The electrical resistivity and coefficient of thermal conductivity are reported as a function of neutron dose, dpa, and compressive creep strain, %. By convention, a compressive stress causes a negative strain. The % stain data are highlighted yellow in sections 8.1.1 to 8.1.6 and 8.2.1 to 8.2.6.

2. Experimental

2.1 Electrical Resistivity

Previously the experimental methods and techniques used to measure electrical resistivity were reported[4].

2.2 Coefficient of Thermal Expansion (CTE)

The experimental methods used to determine the coefficient of thermal expansion (CTE) were previously reported[4].

2.3 Irradiation Conditions

The AGC-1 creep capsule was irradiated in the Advanced Test Reactor (ATR) at INL over the dose range ≈3-7 dpa. The temperatures varied along the capsule length and the capsule ran hotter with each subsequent cycle. The specimen temperatures thus varied from 470 to 716 °C. Full details of the specimen irradiation history have previously been reported[6].

2.4 Error Analysis and Significance Testing

2.4.1 Error Analysis

An effort has been made to quantify the experimental errors and display them as error bars on the property versus dose plots, and the property versus creep strain plots. An estimate of the uncertainty, arising from both experimental errors and material variability, was taken to be plus or minus three standard deviations (±3σ) of the distribution of the unirradiated property values (from pre-irradiation examination of the specimens[4]). This ±3σ quantity was expressed as a percentage of the unirradiated mean and applied (as a percentage) to both the unirradiated and irradiated specimen populations. The error values applied for each grade and orientation are shown in Table 1 and Table 2 for the electrical resistivity and CTE, respectively.

Table 1 3σ expressed as a percentage of mean for unirradiated electrical resistivity

Unirradiated Values					
Grade/Orientation	Electrical Resistivity, μΩm				Error fraction (3SD/mean), %
	Mean	St. Dev.	3 x S.D.	n	
NBG-17 (AL)	9.87	0.43	1.28	8	13.0
NBG-17 (AW)	10.22	0.24	0.71	30	6.9
NBG-18 (BL)	9.27	0.23	0.69	8	7.5
NBG-18 (BW)	9.47	0.21	0.64	30	6.9
H-451 (WG)	6.98	0.62	1.87	22	26.8
PCEA (AG)	8.72	0.53	1.6	7	18.4
PCEA (WG)	8.05	0.08	0.25	31	3.1
IG-110	12.2	0.62	1.87	22	15.3
IG-1430	9.68	0.69	2.06	34	21.3

Table 2 3σ expressed as a percentage of mean for unirradiated Mean Coefficient of Thermal Expansion (25-500°C)

Unirradiated Values					
Grade/Orientation	Mean CTE $x10^{-6}\,^{\circ}C^{-1}$, 25-500°C				Error fraction (3SD/mean), %
	Mean	St. Dev.	3 x S.D.	n	
NBG-17 (AL)	5.53	0.086	0.258	8	4.7
NBG-17 (AW)	5.34	0.104	0.312	30	5.8
NBG-18 (BL)	5.4	0.176	0.528	8	9.8
NBG-18 (BW)	5.31	0.163	0.489	30	9.2
H-451 (WG)	3.75	0.096	0.288	22	7.7
PCEA (WG)	4.76	0.057	0.171	33	3.6
PCEA (AG)	5.2	0.038	0.114	5	2.2
IG-110	4.66	0.109	0.327	22	7.0
IG-1430	5.01	0.229	0.687	34	13.7

Based on previous ATR operating experience, the irradiation dose error was assumed to be ±5%. However, arriving at an estimated error for the creep strain was more challenging. If the specimen pairs were exactly matched in both irradiation temperature and dose the creep error would only arise from the differences in dimensional measurements. Since the specimens dimensions are measured with high precision and accuracy, the errors would be very small. However, AGC-1 was a prototype capsule, and the temperature control was not optimal. There was a significant temperature gradient along the length of the capsule, and the capsule mean temperature increased with each successive ATR cycle. Consequently, there is considerable uncertainty regarding the exact specimen temperatures. Similarly, there is some uncertainty associated with the specimen irradiation dose (±5%) and a larger concern as to whether the matched pair of creep and control sample received identical irradiation doses. Given the uncertainties associated with the irradiation conditions of the matched pairs in AGC-1 it is unlikely we can know the exact specimen creep strain to better than ±10%. Consequently, the creep strain error bars on the property versus creep strain plots (Figure 2, Figure 4, Figure 6, Figure 8, Figure 10, Figure 12 and Figure 16, Figure 18, Figure 20, Figure 22, Figure 24 and Figure 26) was set to ±10%.

2.4.2 Statistical Significance Testing

Later in the report, we make extensive use of Significance Testing to establish whether there is a difference between selected properties of the irradiated (control) specimen and the irradiated and stressed (creep) specimens. Moreover, we have compared the irradiation doses of each specimen property data group to first establish that they are indeed similar irradiation doses. The statistical significance was tested by calculating the "P" statistic (P is a function of the mean, standard deviation and population size (n)) and compared it to the probabilities defined in Students[7] "t" distribution. The "P" statistic was calculated and significance testing carried out using GraphPad[8] software.

The levels of significance used, their exact terminology, and the associated "P" values are given in Table 3.

Table 3 Significance Level and their associated "p" values

"P" Value	Terminology
Less than 0.0001	**Extremely Significant**
0.0001 to 0.001	**Extremely Significant**
0.001 to 0.01	**Very Significant**
0.01 to 0.05	**Significant**
Greater than or equal to 0.05	**Not significant**

Determinations are made as to whether Creep specimen material properties are different from Control specimen material properties based entirely on the reported "P" values, and hence the statistical significance of any observed difference.

3. Results

3.1 Electrical Resistivity

Values for the electrical resistivity (ρ) of the non-irradiated graphite specimens[4] are summarized in Table 4. The unirradiated means are plotted with the irradiated and crept specimen data at zero dose or strain as the "all specimen zero dose data". The post irradiation data[5] for the creep and control specimens from AGC-1 are given in Figure 1 to Figure 12 and in Appendices (Table 15 to Table 20). Inspection of Figure 1 to Figure 12 indicates the electrical resistivity increases substantially on irradiation with or without stress (i.e., control and creep specimens). Moreover, there appear to be little, or no, additional effect of creep strain on electrical resistivity. To quantitatively determine the effect that irradiation or creep may have on electrical resistivity, statistical significance testing is used to evaluate the potential differences between unirradiated, irradiated, and specimens that have undergone irradiation induced creep.

Table 4 Electrical resistivity values for the unirradiated graphite specimens

Zero Dose Data Sets																	
NBG-17 AG		NBG-17 WG		NBG-18 AG		NBG-18 WG		H-451 WG		PCEA AG		PCEA WG		IG-110		IG-430	
Specimen ID	Resistivity μΩm	Specimen ID	Resistivity μΩm	Specimen ID	Resistivity μΩm	Specimen ID	Resistivity μΩm	Specimen ID	Resistivity μΩm	Specimen ID	Resistivity μΩm	Specimen ID	Resistivity μΩm	Specimen ID	Resistivity μΩm	Specimen ID	Resistivity μΩm
AL6-01	9.29	AW1-01	10.25	BL6-01	8.88	BW1-01	8.92	CW7-01	6.17	DA601	8.971144	DW1-01	8.05	EW2-01	10.93	FW1-01	10.32
AL6-02	9.45	AW1-02	9.85	BL6-02	9.66	BW1-02	9.72	CW7-03	7.15	DA602	9.189037	DW1-02	8.14	EW2-02	12.51	FW1-02	8.60
AL6-03	9.53	AW1-03	10.14	BL6-03	9.38	BW1-03	9.69	CW8-02	6.51	DA701	9.178562	DW1-03	8.16	EW2-03	12.46	FW1-03	10.35
AL8-01	9.89	AW2-01	10.00	BL7-01	9.26	BW2-01	9.65	CW8-03	6.86	DA702	7.963477	DW2-01	8.04	EW4-01	12.30	FW2-01	10.43
AL8-02	10.56	AW2-02	9.93	BL7-02	9.05	BW2-02	9.72	CW9-01	6.37	DA802	8.880019	DW2-02	8.16	EW4-02	12.03	FW2-02	9.37
AL8-03	9.93	AW2-03	9.50	BL7-03	9.28	BW2-03	9.28	CW9-02	7.28	DA801	7.958086	DW2-03	8.15	EW5-01	12.76	FW2-03	10.42
AL7-01	10.17	AW4-01	10.29	BL8-01	9.40	BW3-01	9.59	CW9-03	6.85	DA901	8.907307	DW3-01	8.06	EW5-02	12.66	FW3-01	9.38
AL7-02	10.13	AW4-02	10.03	BL8-02	9.28	BW3-02	9.65	CW10-01	6.90			DW3-02	8.04	EW5-03	11.74	FW3-02	10.11
		AW4-03	10.02			BW3-03	9.39	CW10-02	6.89			DW3-03	7.99	EW6-01	12.74	FW3-03	8.91
		AW5-01	10.19			BW5-01	9.50	CW10-03	6.56			DW4-01	8.16	EW6-02	11.56	FW4-01	9.98
		AW5-02	9.95			BW5-02	9.47	CW11-01	6.37			DW4-03	7.91	EW6-03	11.30	FW4-02	9.94
		AW5-03	10.53			BW5-03	9.23	CW11-02	6.71			DW5-01	8.06	EW7-01	12.62	FW4-03	9.65
		AW6-01	10.36			BW7-01	9.59	CW11-03	6.48			DW5-02	8.12	EW7-03	13.01	FW5-01	10.15
		AW6-02	10.44			BW7-02	9.60	CW12-01	6.36			DW5-03	8.21	EW8-01	12.42	FW5-02	8.66
		AW6-03	10.48			BW7-03	9.47	CW12-02	8.25			DW6-01	8.07	EW8-02	12.50	FW5-03	10.09
		AW7-01	10.19			BW8-01	9.19	CW13-01	6.54			DW6-02	8.08	EW8-03	12.70	FW7-01	9.92
		AW7-02	10.32			BW8-02	9.69	CW13-02	7.75			DW6-03	8.15	EW9-01	12.41	FW7-02	10.17
		AW7-03	10.25			BW8-03	9.36	CW13-03	6.64			DW7-01	8.05	EW9-02	11.71	FW7-03	10.11
		AW9-01	10.36			BW9-01	9.27	CW14-01	7.04			DW7-02	8.02	EW9-03	12.87	FW8-01	9.89
		AW9-02	10.02			BW9-02	9.43	CW14-02	7.58			DW7-03	8.07	EW10-01	10.77	FW8-02	9.06
		AW9-03	10.23			BW9-03	9.10	CW15-01	8.15			DW8-01	8.08	EW10-02	12.46	FW8-03	9.24
		AW10-01	10.40			BW10-01	9.86	CW15-02	8.08			DW8-02	7.95	EW10-03	11.97	FW9-01	10.10
		AW10-02	10.42			BW10-02	9.74					DW8-03	8.01			FW9-02	10.15
		AW10-03	10.35			BW10-03	9.32					DW9-01	8.00			FW9-03	9.85
		AW12-01	10.46			BW11-01	9.57					DW9-02	8.01			FW10-01	9.34
		AW12-02	10.24			BW11-02	9.57					DW9-03	7.89			FW10-02	9.16
		AW12-03	10.21			BW11-03	9.59					DW10-01	8.01			FW10-03	10.16
		AW13-01	10.43			BW12-01	9.36					DW10-02	8.10			FW11-01	10.38
		AW13-02	10.09			BW12-02	9.35					DW10-03	7.91			FW11-02	9.69
		AW13-03	10.62			BW12-03	9.34					DW11-01	7.93			FW11-03	10.10
												DW11-02	7.99			FW12-01	10.05
																FW12-02	9.80
																FW13-01	7.77
																FW13-02	7.87
MEAN	9.87		10.22		9.27		9.47		6.98		8.72		8.05		12.20		9.68
S.D.	0.43		0.24		0.23		0.21		0.62		0.53		0.08		0.62		0.69
3S.D.	1.28		0.71		0.69		0.64		1.87		1.60		0.25		1.87		2.06
3S.D.%	12.95		6.94		7.48		6.78		26.76		18.35		3.13		15.34		21.30
n	8		30		8		30		22		7		31		22		34

3.1.1 Grade A, NBG-17

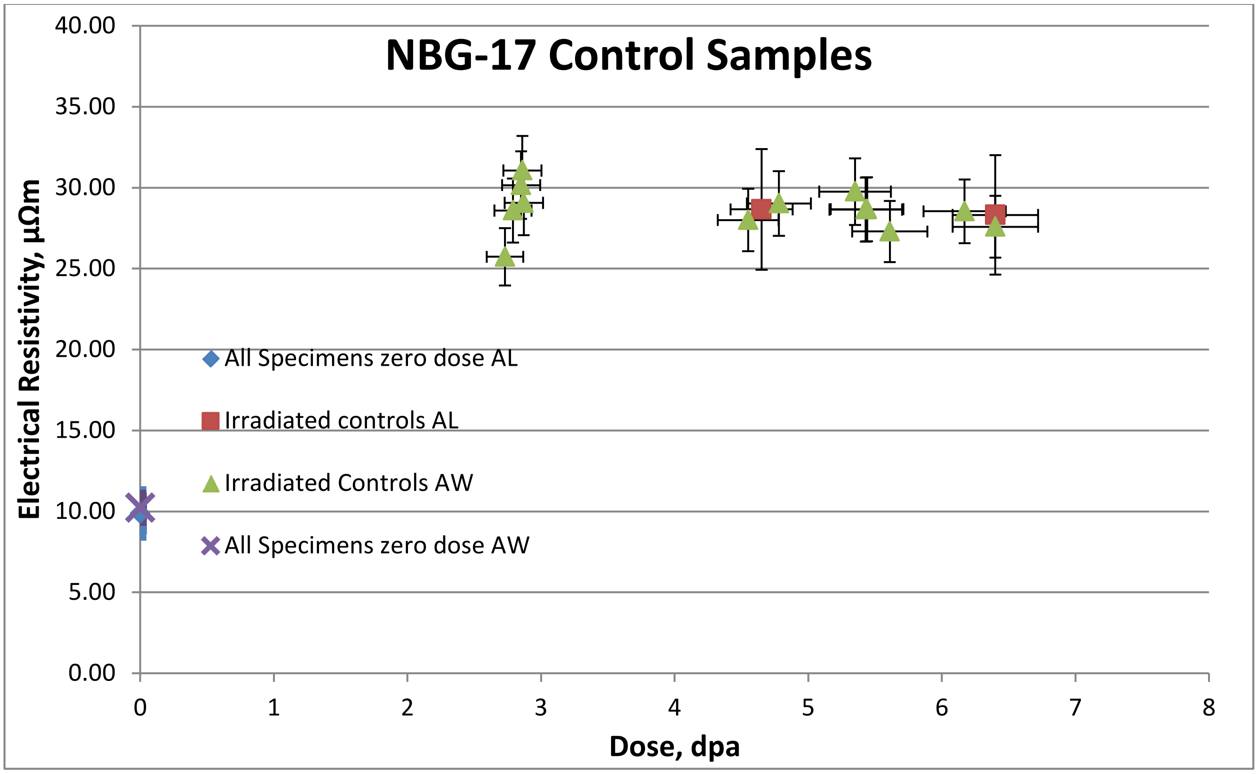

Figure 1 Variation of electrical resistivity with irradiation dose for NBG-17 graphite

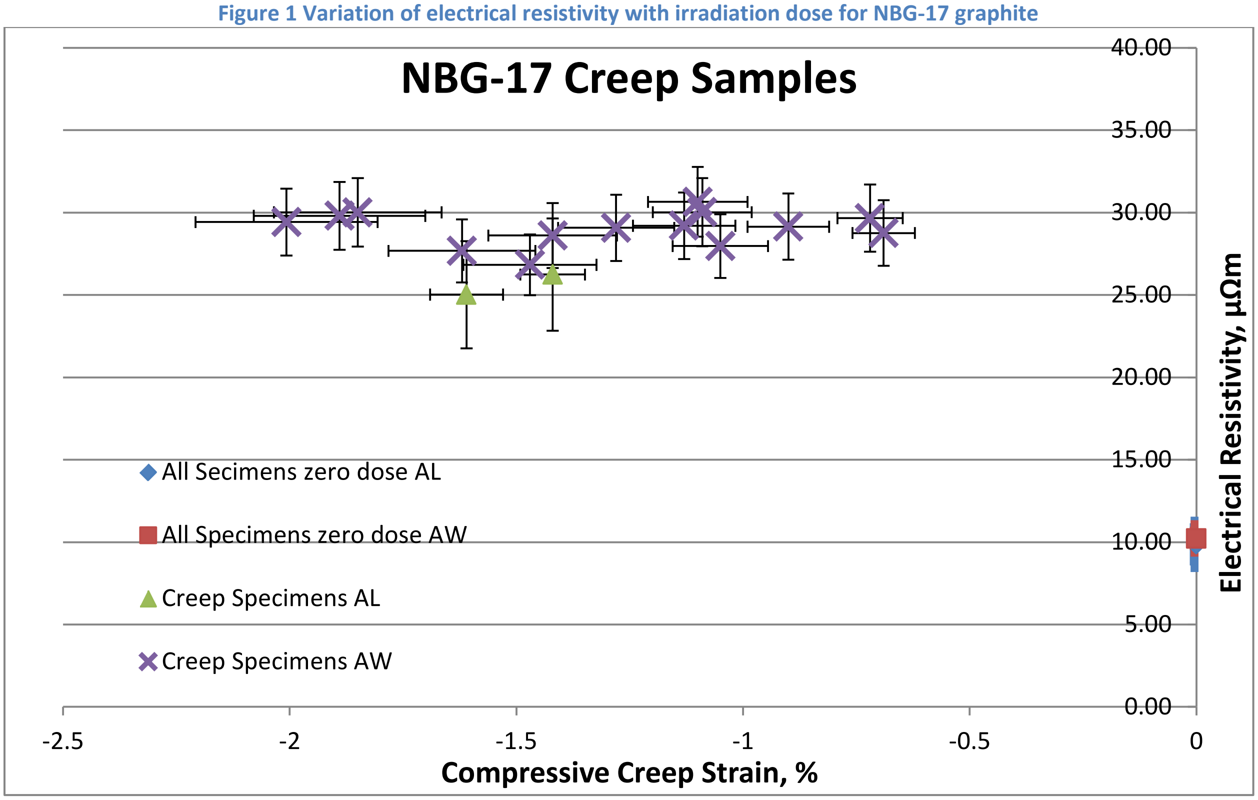

Figure 2 Variation of electrical resistivity with compressive creep strain for NBG-17 graphite

3.1.2 Grade B, NBG-18

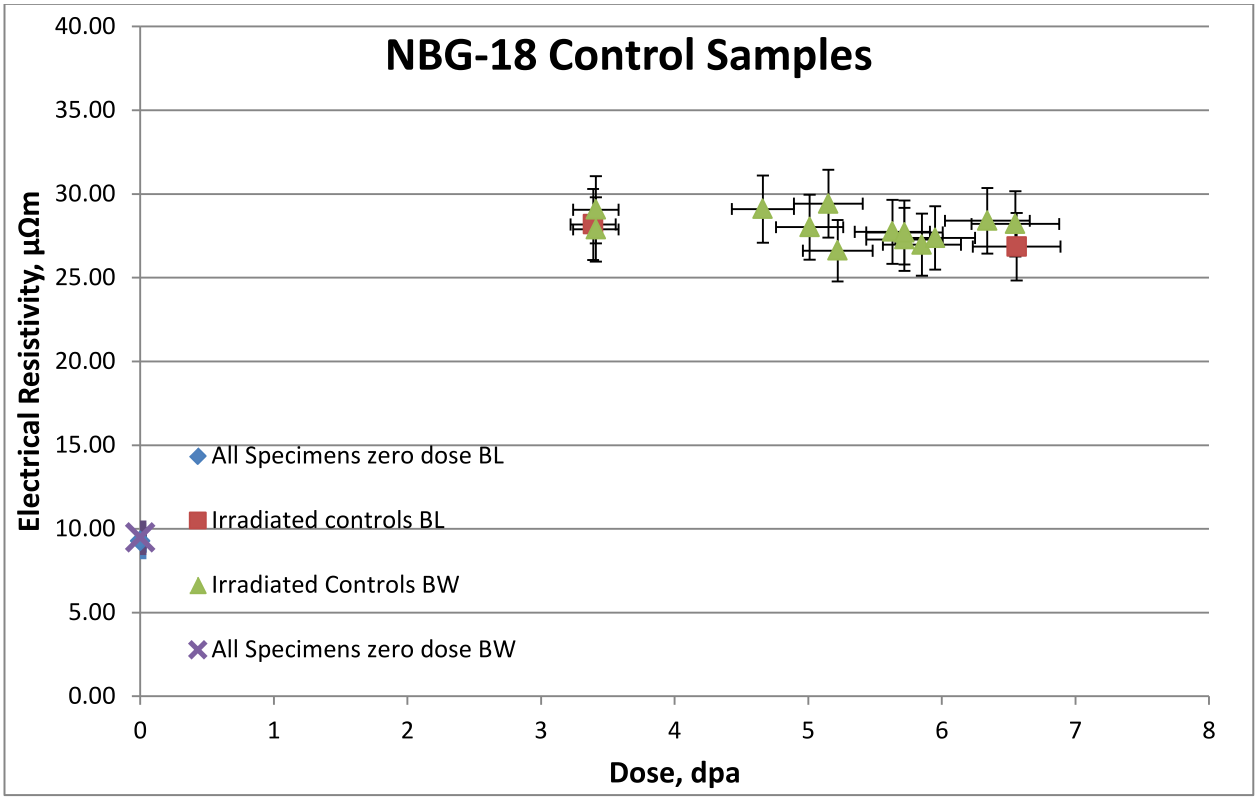

Figure 3 Variation of electrical resistivity with irradiation dose for NBG-18 graphite

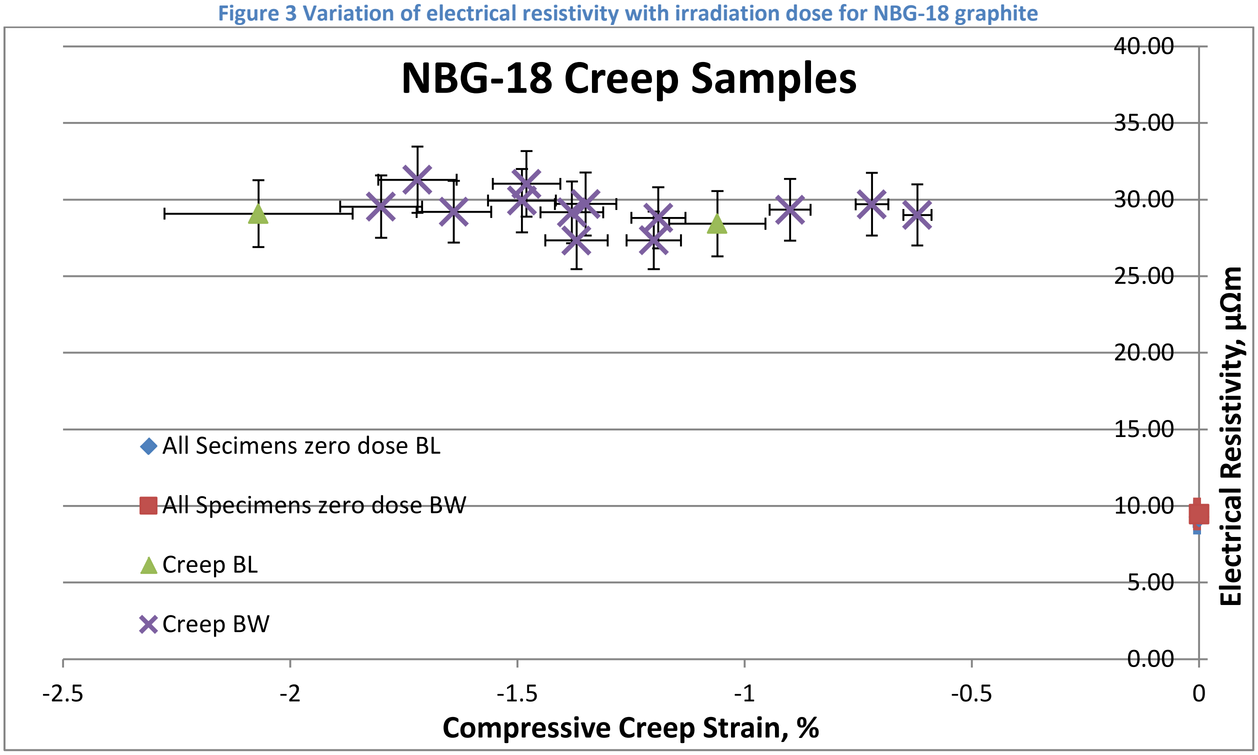

Figure 4 Variation of electrical resistivity with compressive creep strain for NBG-18 graphite

3.1.3 Grade C, H-451

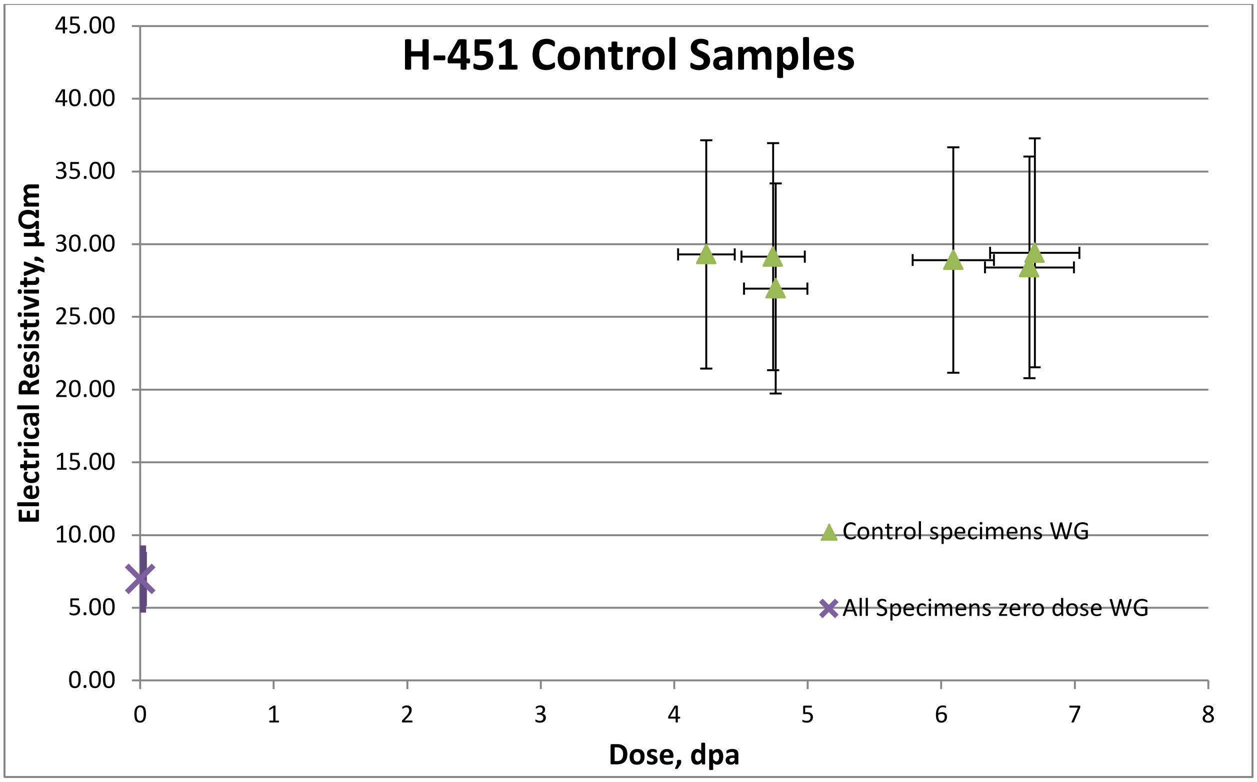

Figure 5 Variation of electrical resistivity with irradiation dose for H-451 graphite

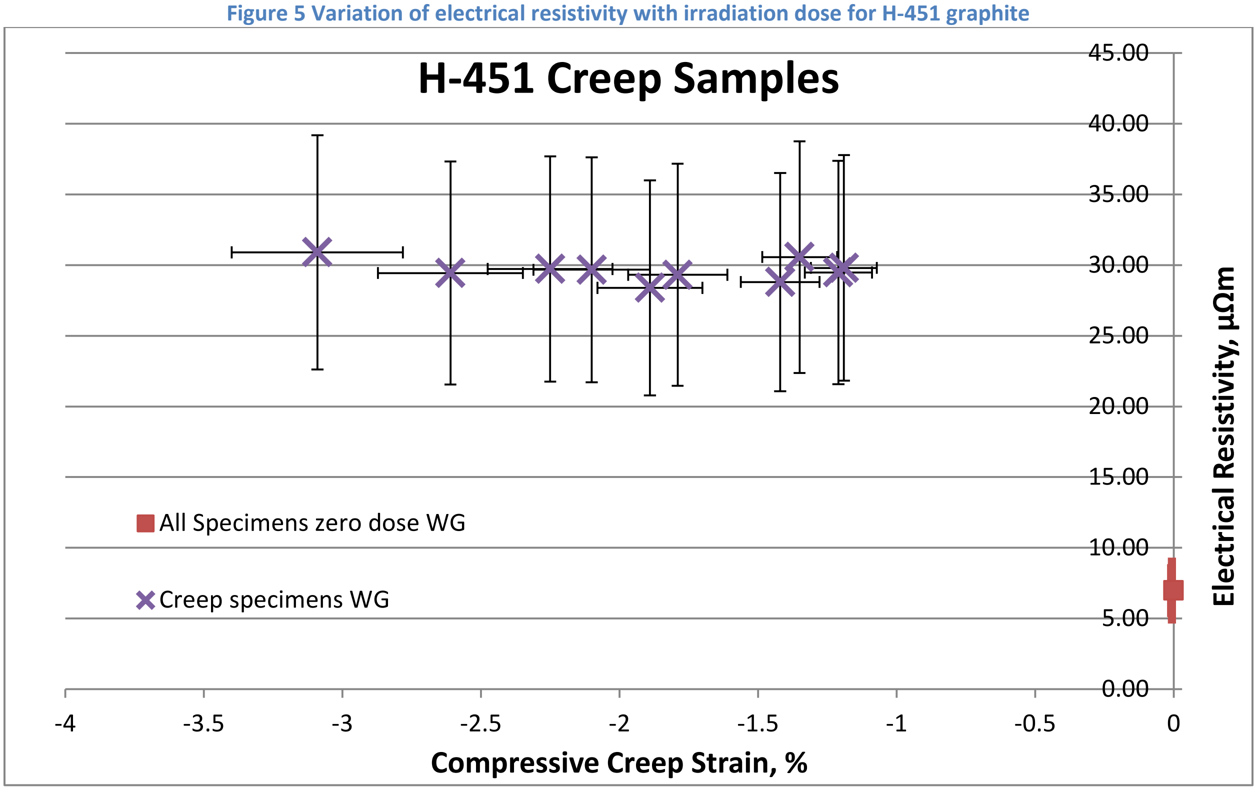

Figure 6 Variation of electrical resistivity with compressive creep strain for H-451 graphite

3.1.4 Grade D, PCEA

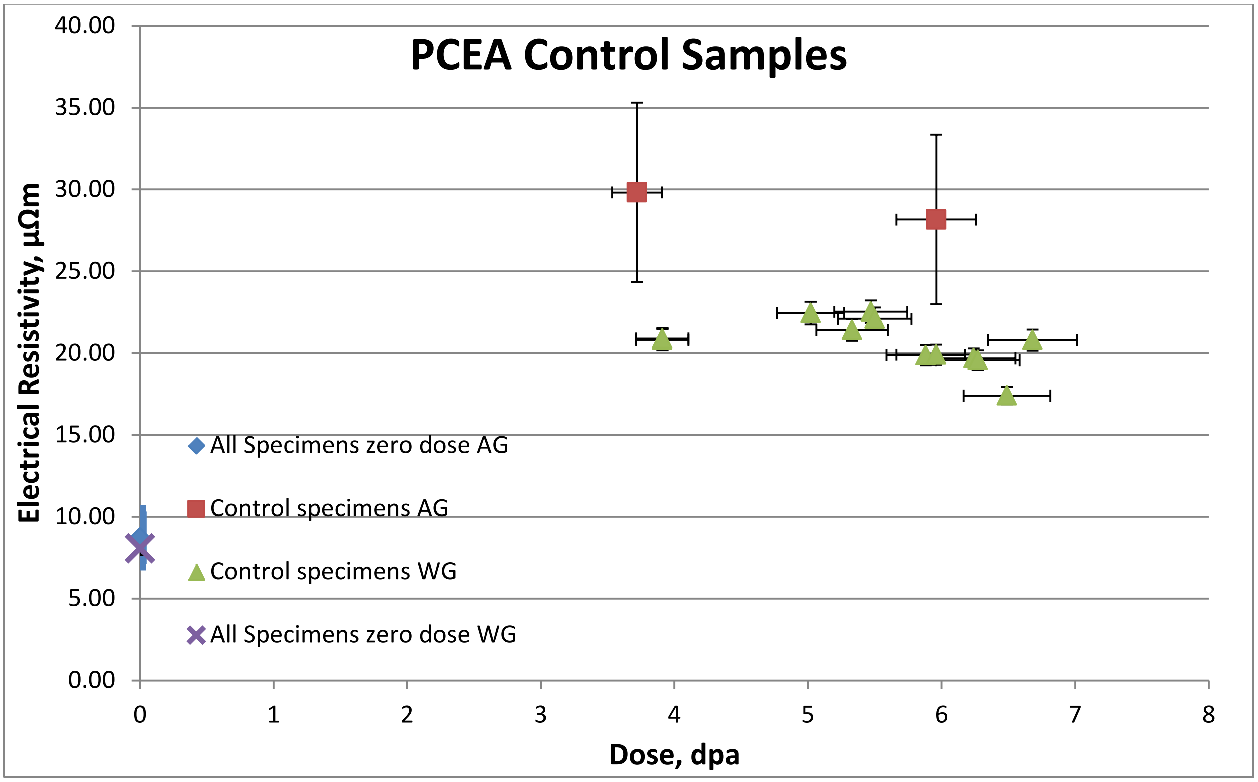

Figure 7 Variation of electrical resistivity with irradiation dose for PCEA graphite

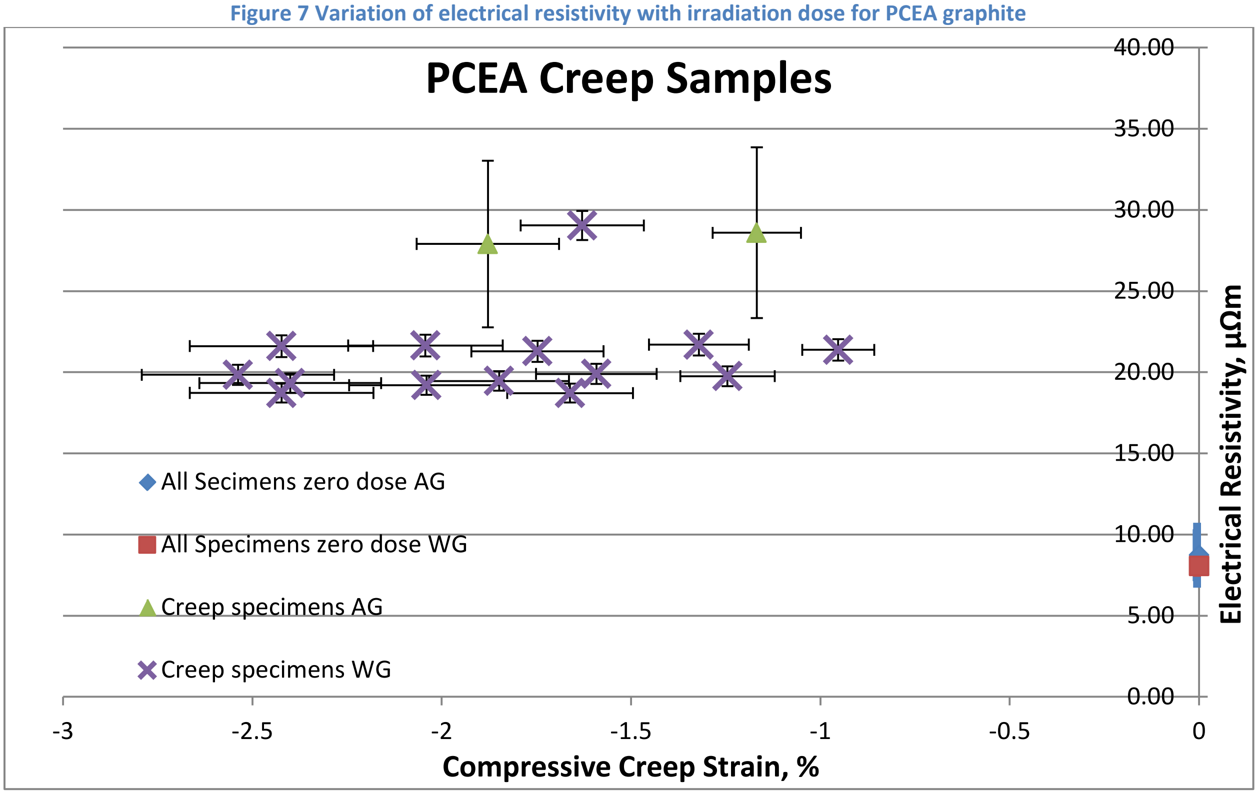

Figure 8 Variation of electrical resistivity with compressive creep strain for PCEA graphite

3.1.5 Grade E, IG-110

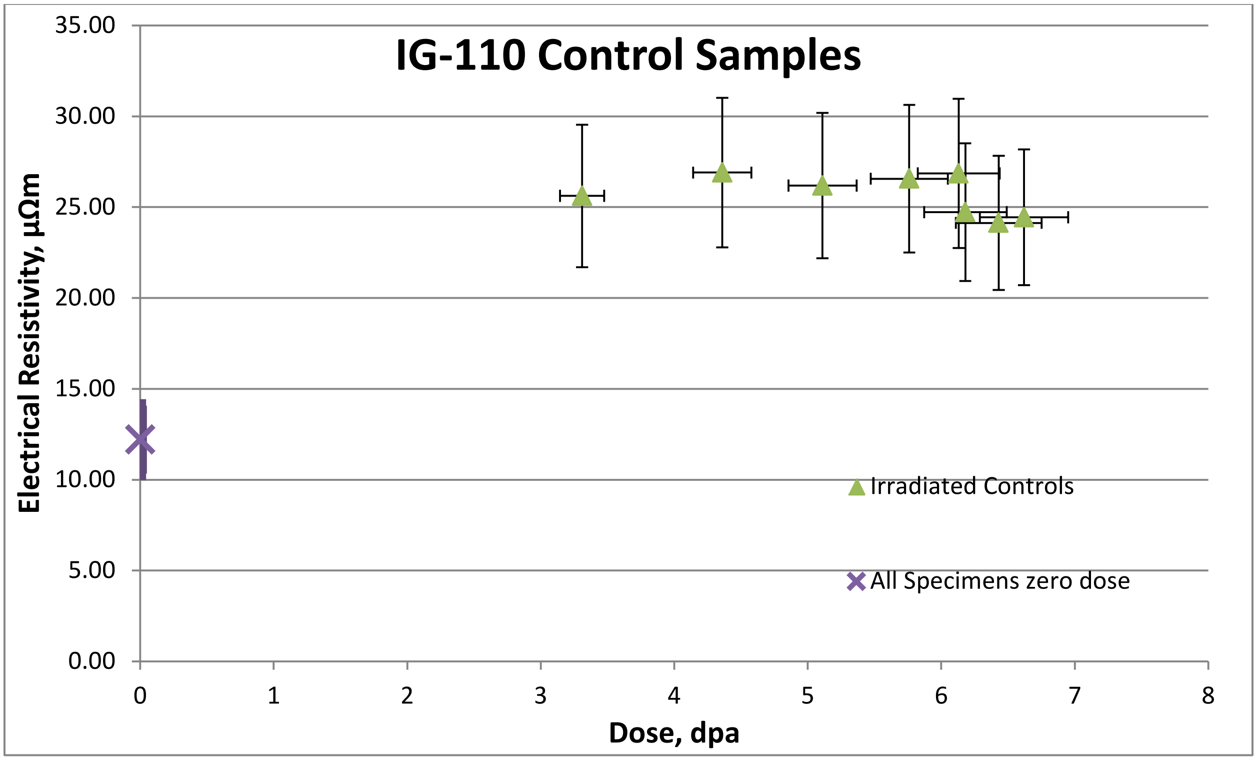

Figure 9 Variation of electrical resistivity with irradiation dose for IG-110 graphite

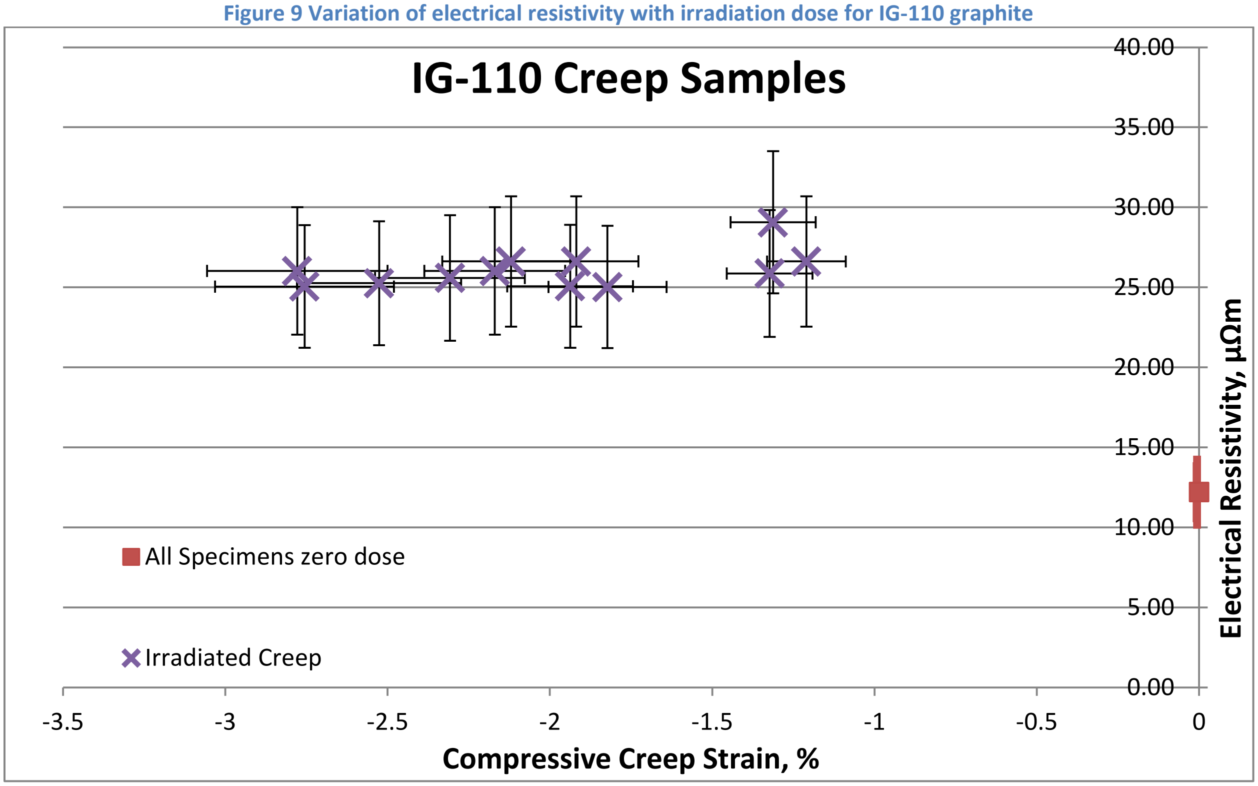

Figure 10 Variation of electrical resistivity with compressive creep strain for IG-110 graphite

3.1.6 Grade F, IG-430

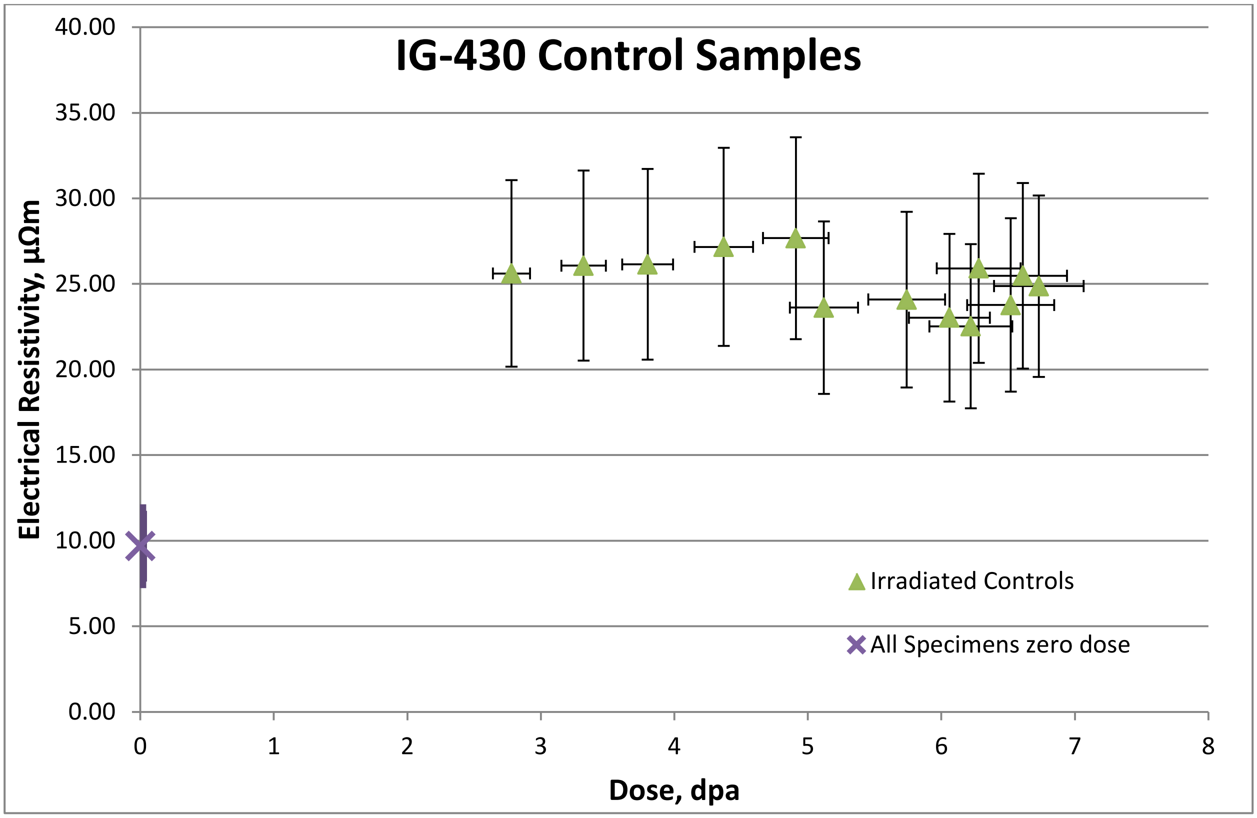

Figure 11 Variation of electrical resistivity with irradiation dose for IG-430 graphite

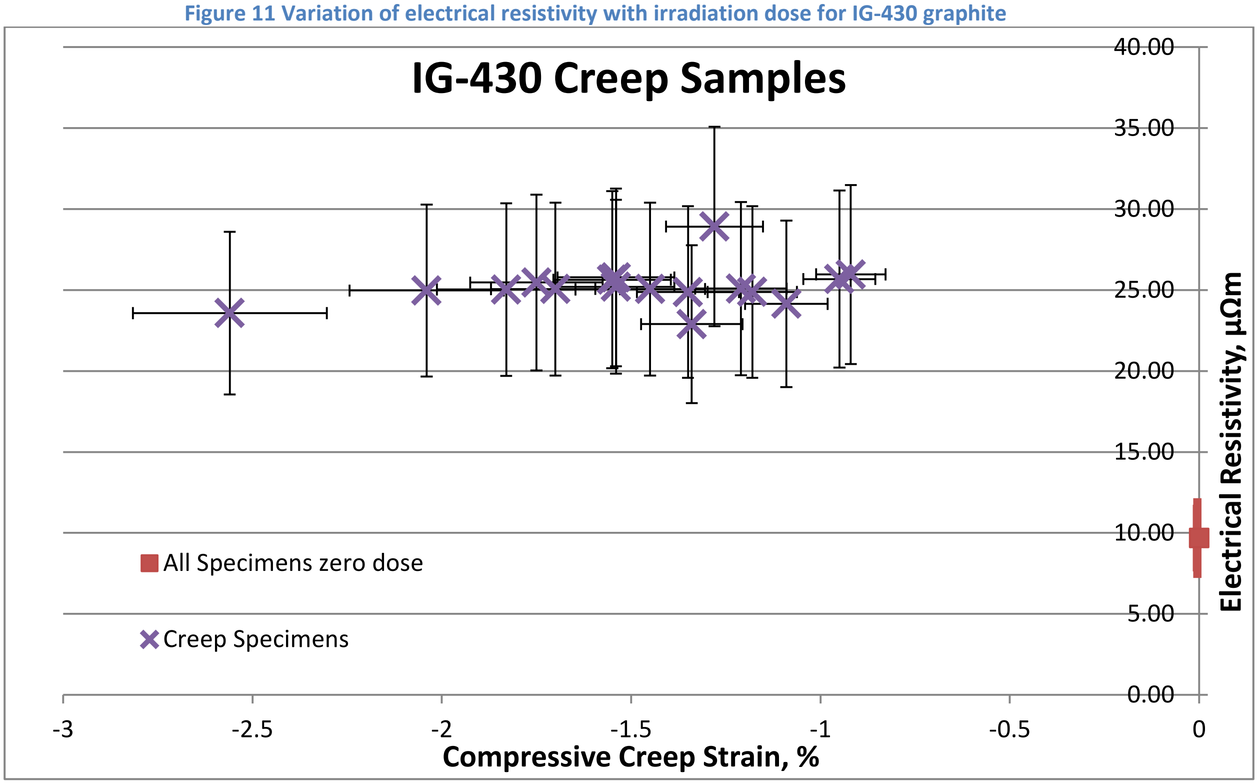

Figure 12 Variation of electrical resistivity with compressive creep strain for IG-430 graphite

3.1.7 Grade Anisotropy Effects on Resistivity

If effects of anisotropy manifest themselves in the electrical resistivity data, they should be visible for the extruded grade PCEA. As expected, the against-grain (AG) PCEA resistivity is greater than the with-grain (WG) PCEA resistivity. This is due to preferred orientation of the filler particle's that have more crystallographic basal planes aligned along their major axis and hence with-grain. Conduction in graphite is via electrons and their preferred pathway is along the basal planes. The mean unirradiated and mean irradiated values of the electrical resistivity are in given in Table 5.

Table 5 the mean electrical resistivity's and mean percentage increase for the major grades irradiated in AGC-1

Grade/Orientation	Mean resistivity, μΩm		Mean % Increase
	Unirradiated	Irradiated	
NBG-17 (AL)	9.87	28.49	188.65
NBG-17 (AW)	10.22	28.63	180.14
NBG-18 (BL)	9.27	27.52	196.87
NBG-18(BW)	9.47	27.98	195.46
H-451 (WG)	6.98	28.68	310.89
PCEA (AG)	8.72	28.99	232.45
PCEA (WG)	8.05	20.63	156.27
IG-110	12.2	25.18	106.39
IG-430	9.68	25.07	158.99

The percent increase of electrical resistivity per grade is shown graphically in Figure 13. The largest percent increase is seen for the extruded grade H-451 and the smallest for the isostatically pressed grades IG-110 and IG-430. It is interesting to compare the WG and AG changes for extruded grade PCEA. In the AG direction the percentage increase was much larger in the WG direction. Both electrical resistivity values appear to be saturated yet the WG increase is far less than the AG increase. This argues for an increased number of electron-scattering centers (i.e., vacancies, interstitials, dislocation loops) forming due to irradiation damage on the prismatic edges of the single crystal (parallel to the c-axis) that are preferentially aligned in the AG direction.

These data suggest that prior to turnaround, damage effects are largely in-crystal or within crystallites, and there is no major re-orientation of the crystals, only the closure of Mrozowski[9] and aligned Mrozowski-like cracks, which one might expect to provide additional conduction path ways. Results from further AGC capsules may shed light on these observed anisotropic effects.

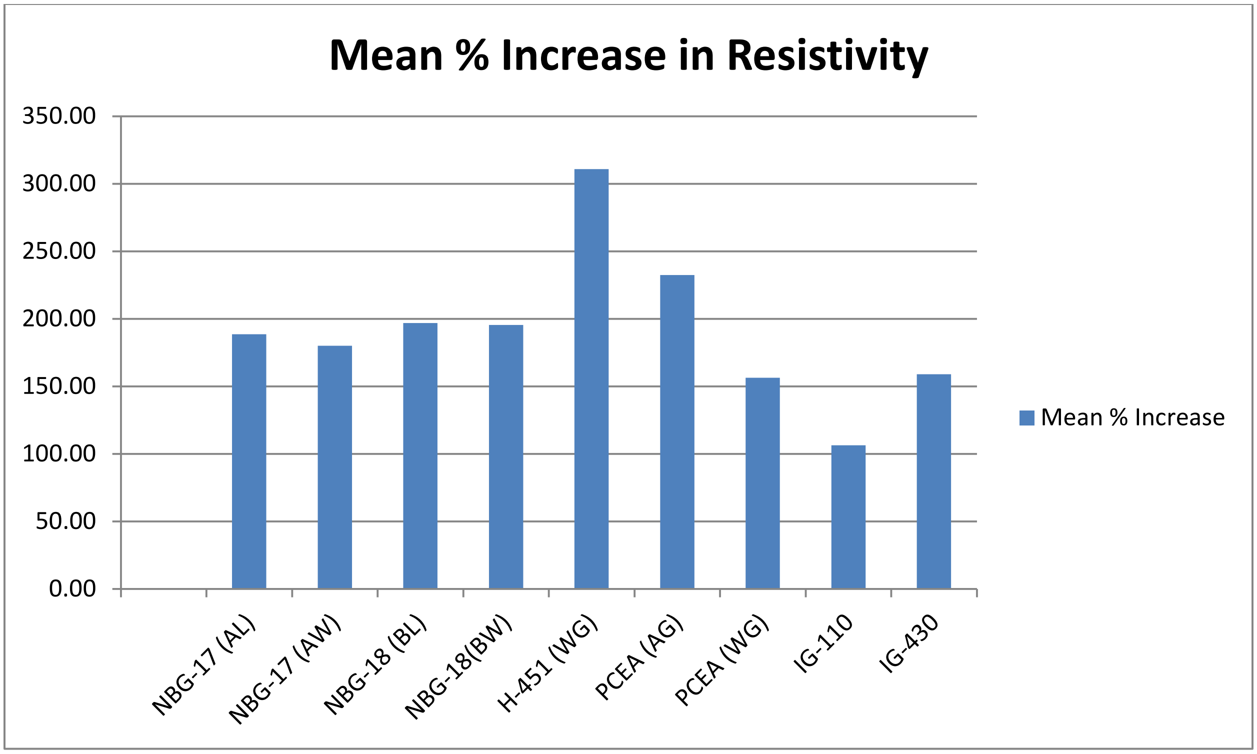

Figure 13 Mean increase in electrical resistivity

3.2 Coefficient of Thermal Expansion

Examples of irradiation effects on the average Coefficient of Thermal Expansion (CTE) are reported for each grade of graphite. To better demonstrate the effects of dose and creep strain on CTE, the mean CTE over a fixed temperature range i.e., 25-500°C has been selected for comparison (i.e., the mean value at 500°C from the temperature dependence curves of mean CTE). A summary of the unirradiated mean $CTE_{(25\text{-}500°C)}$ from pre-irradiation examination[4] is given in Table 2. This temperature range was selected because it was below the AGC-1 irradiation temperature and thus no specimen annealing would have occurred during thermal expansion testing. The values in Table 2 are used as reference values when assessing the effects of dose or dose and stress on CTE. The control and creep CTE values are reported graphically in the subsequent subsections (3.2.2 to 3.2.6 and in tabular form in Appendix 8.2 (Table 21 to Table 26). The error fraction (Table 2) has been used to estimate the error bars in the subsequent plot of CTE (Figure 15 to Figure 26).

3.2.1 Grade A, NBG-17

Figure 14 shows the CTE response to temperature for a matched specimen pair of NBG-17 graphite that received similar neutron dose. The CTE curves for the unirradiated NBG-17 specimens are all similar to that of AW10-03. The initial increase of CTE upon irradiation has been attributed,[10,11,12,13,14] to the c-axis crystal expansion preferentially closing the aligned Mrozowski[9] and Mrozowski-like aligned porosity that forms on cooling from the graphite processing temperature due to thermal contraction of the crystal structure. This type of aligned-acicular porosity internally accommodates the thermal expansion of an individual crystal which can approach 28 $x10^{-6}$/°C in the crystallographic direction perpendicular to the basal planes without the accommodating porosity. This accommodating porosity results in a much lower bulk CTE measurement. Thus, any closure of these pores due to irradiation damage will effectively increase the bulk CTE.

The creep specimen (AW10-03) also underwent -1.9% compressive creep strain and had a larger CTE measured value across the entire test temperature range than the control specimen (i.e., the one that was irradiated unstressed). It appears that compressive creep is closing a larger fraction of the aligned-porosity and further increasing the CTE. To examine this hypothesis more closely, all of the specimens examined in AGC-1 were plotted, taking the mean value of $CTE_{(25\text{-}500°C)}$ as typical of the creep behavior with dose. A reduction of the CTE at higher doses is attributed to pore-creation. The correlations between CTE behavior and other properties that depend upon pore-creation, such as dimensional and volume changes, require further investigation. A similar trend was noted for all of the creep grades examined here.

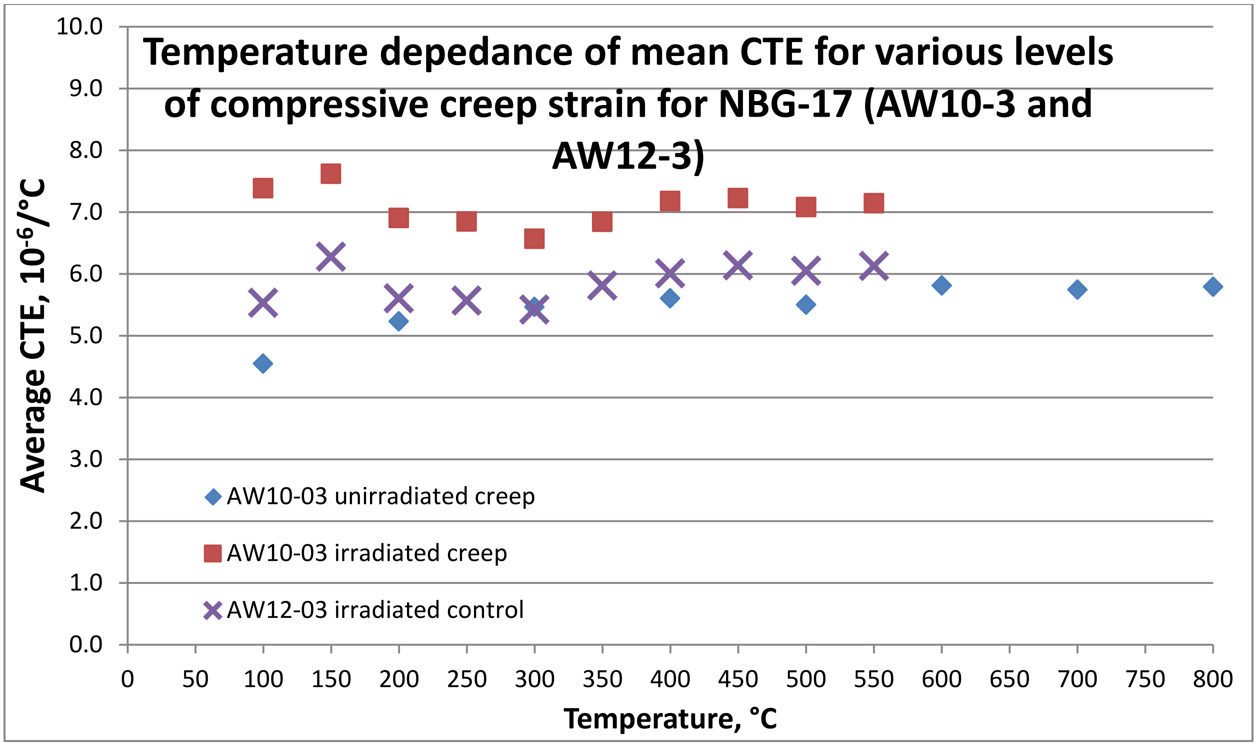

Figure 14 The variation of Average CTE with temperature for NBG-17 (AW) creep specimen AW 10-03 (6.00dpa, -1.893% creep strain, T_{irr} = 670°C) and control specimen 12-03 (5.43 dpa, T_{irr} = 594°C)

All of the NBG-17 irradiated control sample data for the mean $CTE_{(25\text{-}500°C)}$ are plotted in Figure 15. The control CTE is noted to increase prior to dimensional or volume turnaround fluences, but they exhibit a lower mean $CTE_{(25\text{-}500°C)}$ than their companion creep specimens at the same dose (Figure 16).

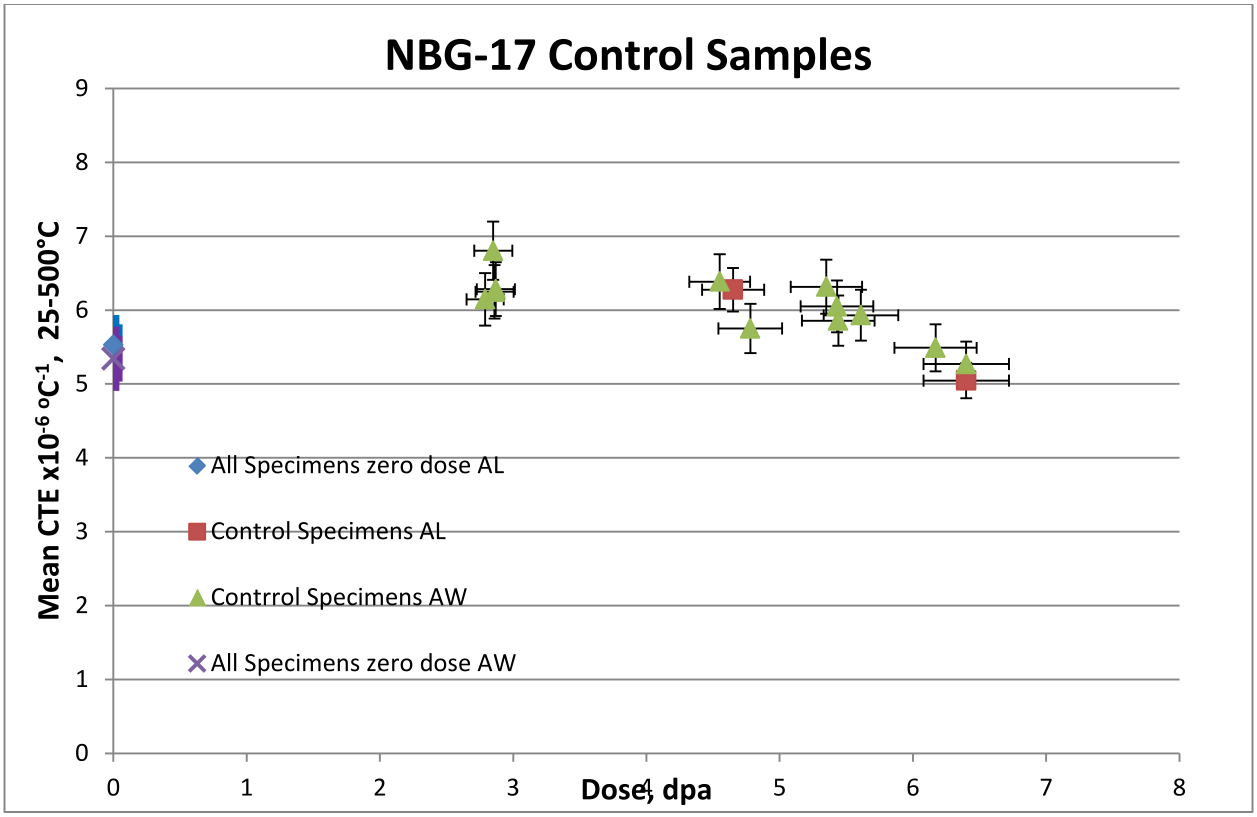

Figure 15 The variation of mean $CTE_{(25\text{-}500°C)}$ with dose for NBG-17(WG) control samples

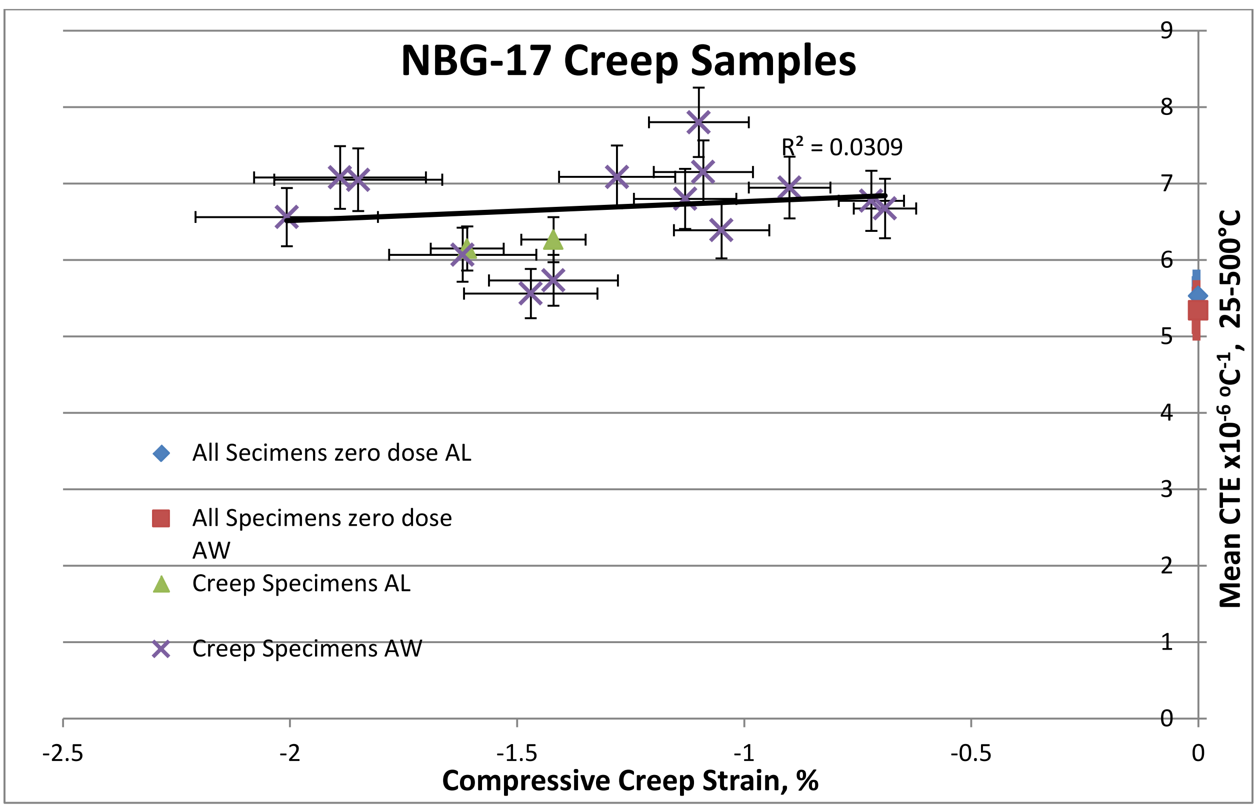

Figure 16 The variation of mean $CTE_{(25\text{-}500°C)}$ with compressive creep strain for NBG-17(WG) creep samples

3.2.2 Grade B, NBG-18

All of the NBG-18 irradiated control sample data for the mean $CTE_{(25\text{-}500°C)}$ are plotted in Figure 17. The control CTE is noted to increase prior to dimensional/volume turnaround fluences, but exhibit a lower mean $CTE_{(25\text{-}500°C)}$ than their companion creep specimens (Figure 18). Again, the creep samples appear to exhibit a larger mean $CTE_{(25\text{-}500°C)}$ than the control specimens.

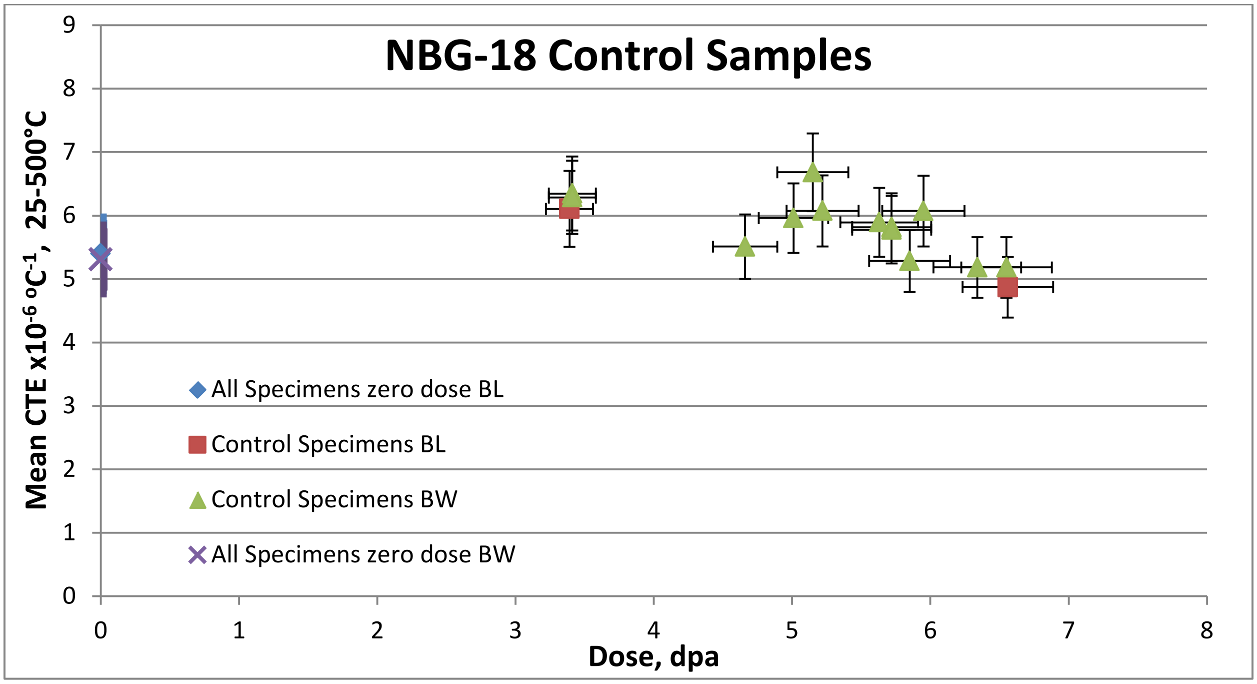

Figure 17 The variation of $CTE_{(25\text{-}500°C)}$ with dose for NBG-18 (WG) control samples

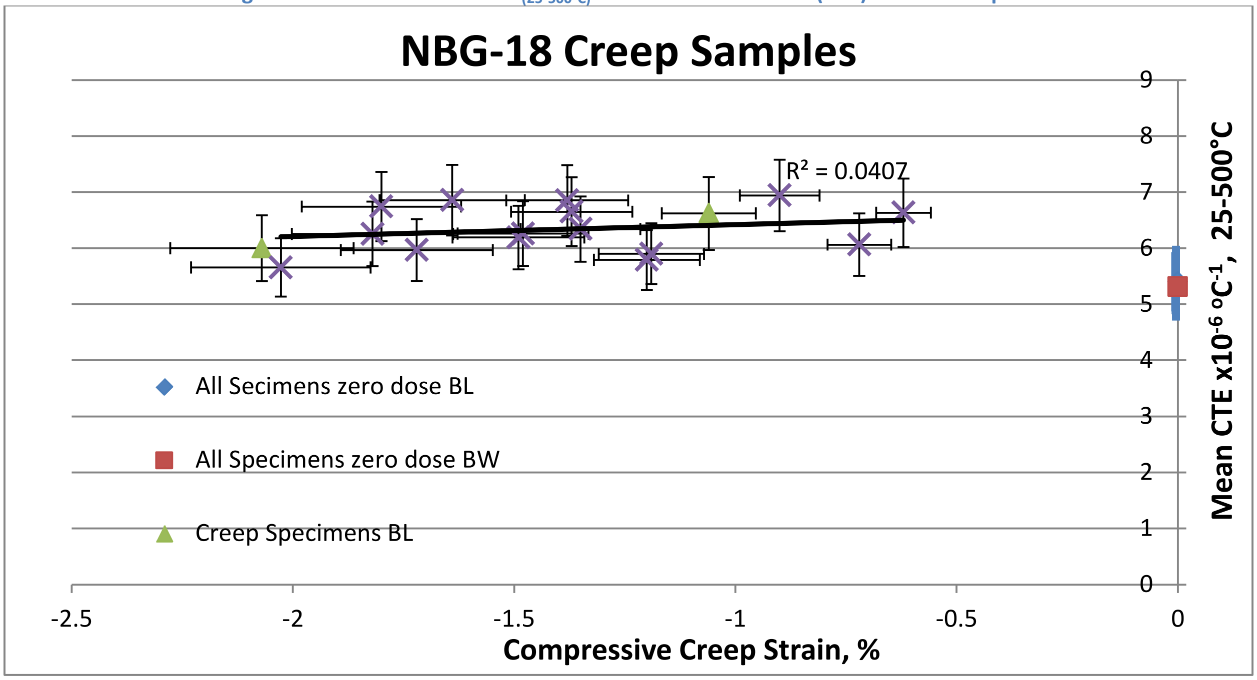

Figure 18 The variation of mean $CTE_{(25\text{-}500°C)}$ with compressive creep strain for NBG-18 (WG) creep samples

3.2.3 Grade C, H-451

All of the H-451 (WG) irradiated control sample data for the mean $CTE_{(25\text{-}500°C)}$ are plotted in Figure 19. The CTE is known to increase prior to dimensional/volume turnaround fluences, but exhibits a lower $CTE_{(25\text{-}500°C)}$ than its companion creep specimens (Figure 20). Again, the creep samples appear to exhibit a larger mean $CTE_{(25\text{-}500°C)}$ than the control specimens.

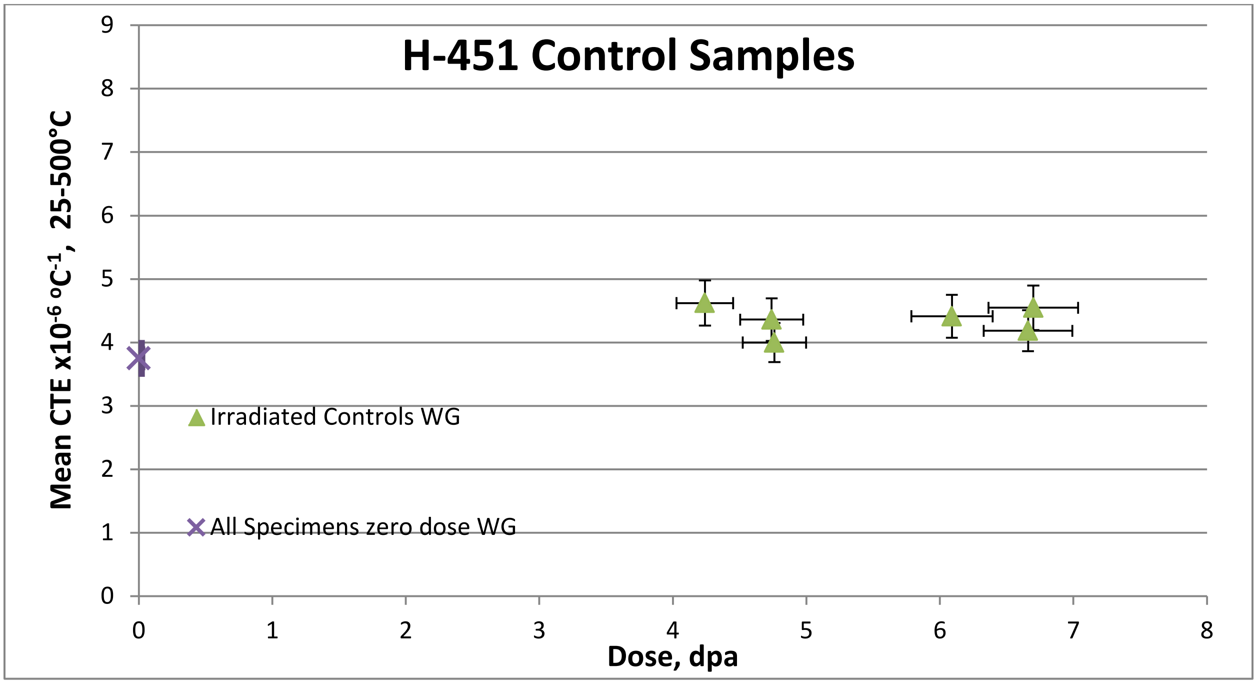

Figure 19 The variation of $CTE_{(25\text{-}500°C)}$ with dose for H-451(WG) control samples

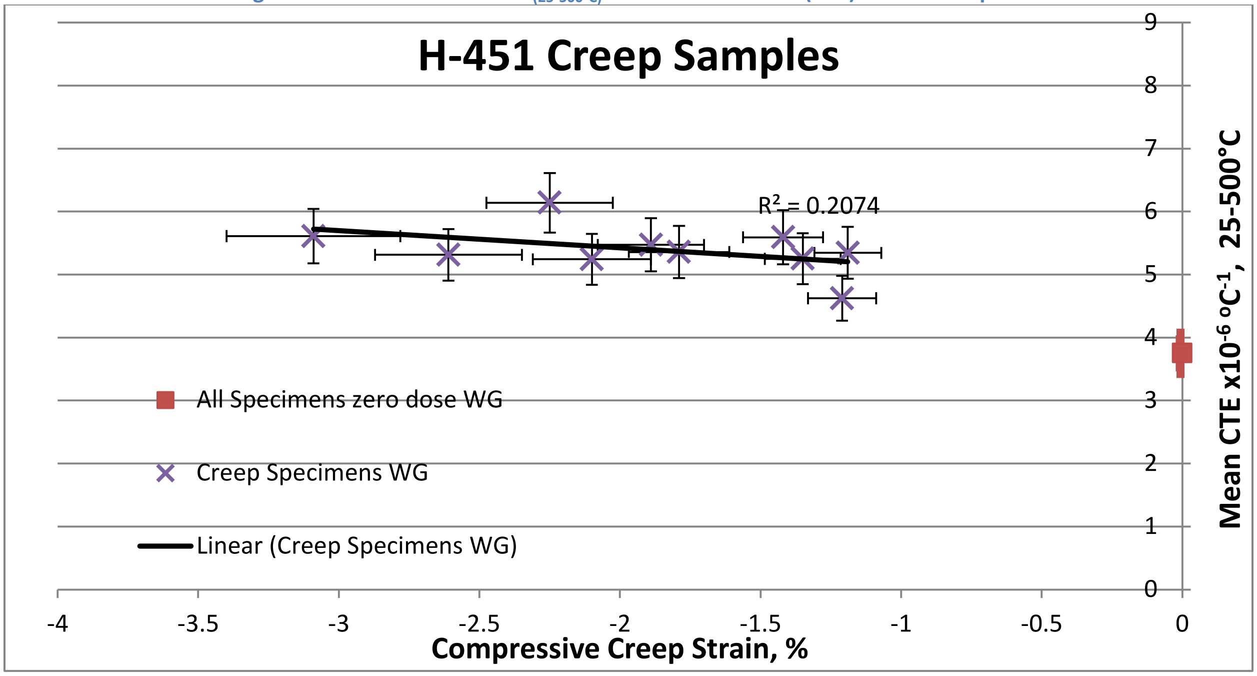

Figure 20 The variation of mean $CTE_{(25\text{-}500°C)}$ with compressive creep strain for H-451(WG) creep samples

3.2.4 Grade D, PCEA

All of the PCEA (WG) irradiated control sample data for the mean $CTE_{(25\text{-}500°C)}$ are plotted in Figure 21. The CTE is noted to increase prior to turnaround fluences, but exhibits a lower $CTE_{(25\text{-}500°C)}$ than its companion creep specimens (Figure 22). Again, the creep samples appear to exhibit a larger $CTE_{(25\text{-}500°C)}$ than the control specimens.

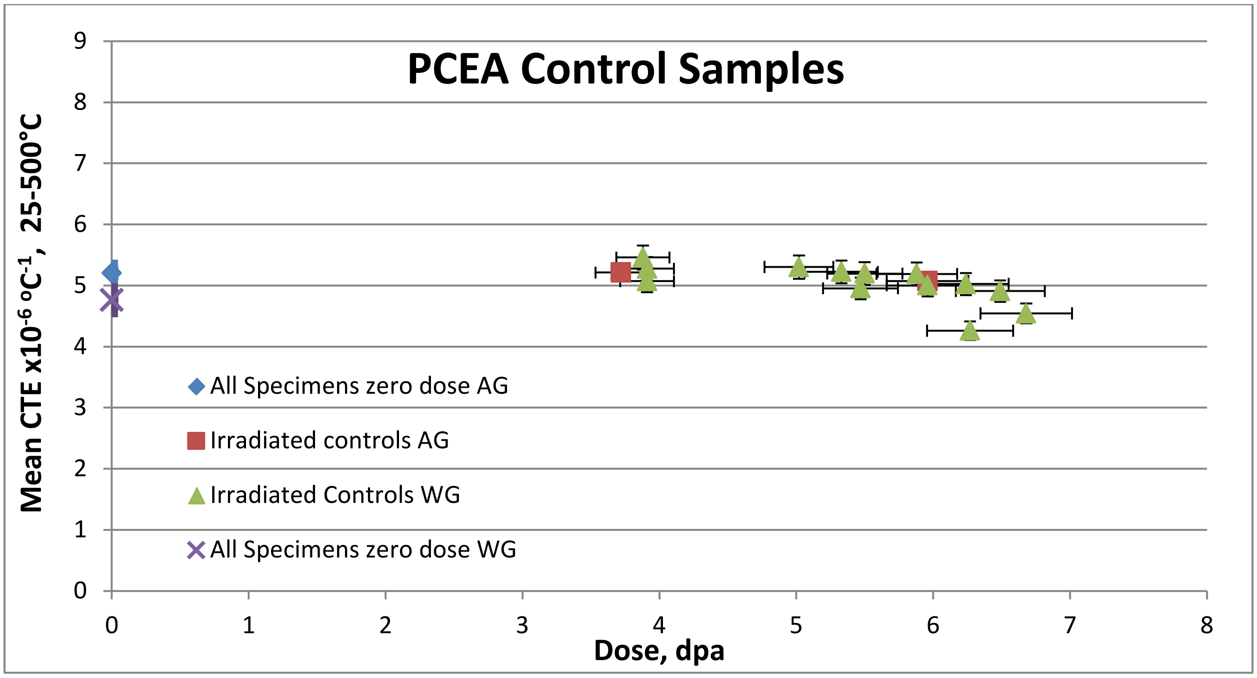

Figure 21 The variation of mean $CTE_{(25\text{-}500°C)}$ with dose for PCEA (WG) control samples

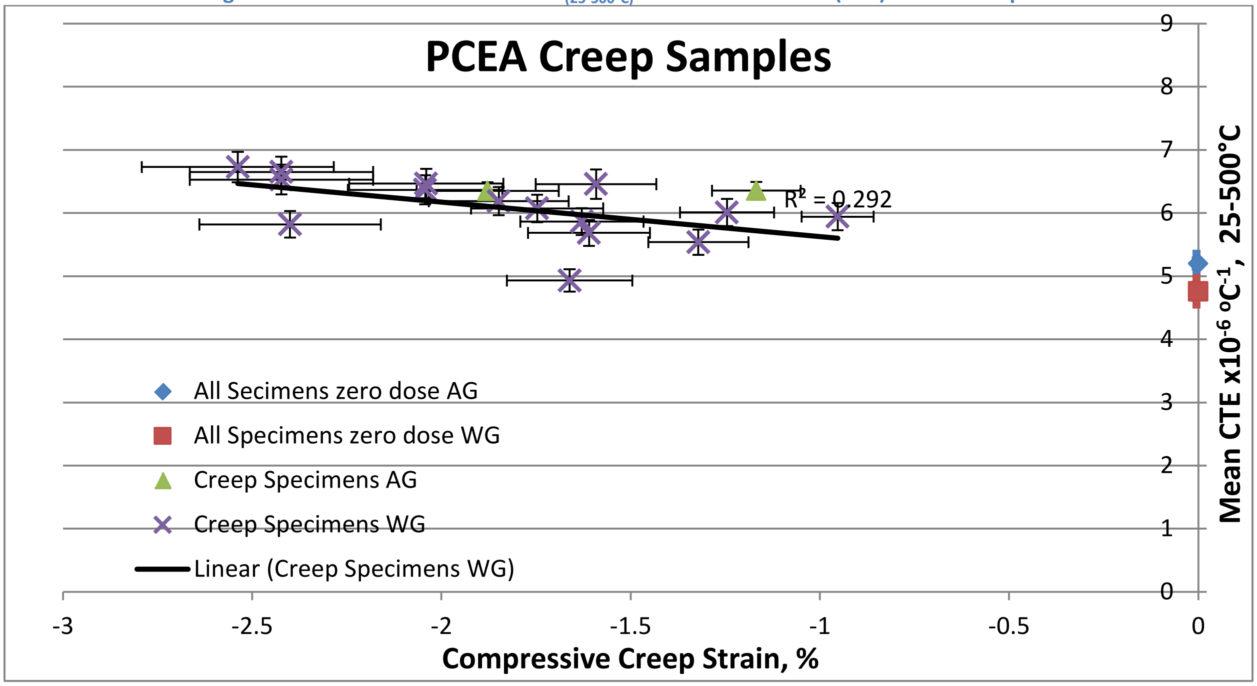

Figure 22 The variation of mean $CTE_{(25\text{-}500°C)}$ with compressive creep strain for PCEA (WG) creep samples

3.2.5 Grade E, IG-110

All of the IG-110 irradiated control sample data for the mean $CTE_{(25\text{-}500°C)}$ are plotted in Figure 23. The CTE is noted to increase prior to turnaround fluences, but exhibits a lower $CTE_{(25\text{-}500°C)}$ than its companion creep specimens (Figure 24). Again, the creep samples appear to exhibit a larger $CTE_{(25\text{-}500°C)}$ than the control specimens.

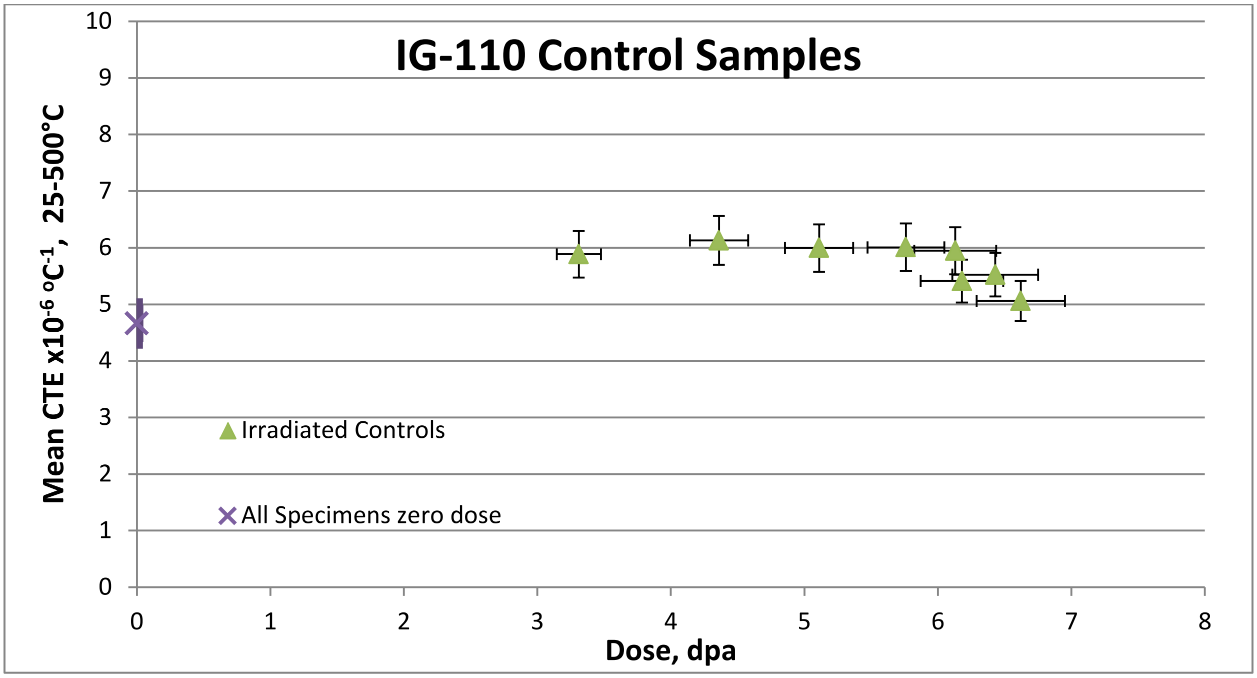

Figure 23 The variation of mean $CTE_{(25\text{-}500°C)}$ with dose for IG-110 control samples

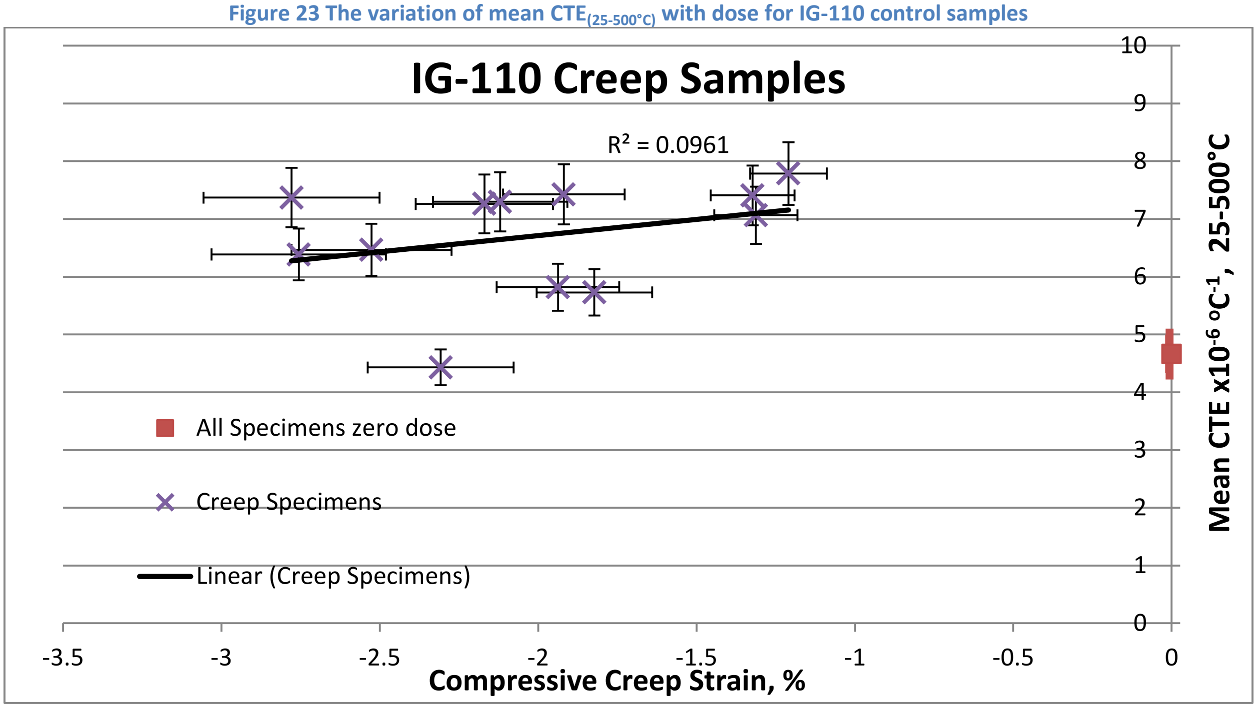

Figure 24 The variation of mean $CTE_{(25\text{-}500°C)}$ with compressive creep strain for IG-110 creep samples

3.2.6 Grade F, IG-430

All of the IG-430 irradiated control sample data for the mean $CTE_{(25\text{-}500°C)}$ are plotted in Figure 25. The CTE is noted to increase prior to turnaround fluences, but exhibits a lower $CTE_{(25\text{-}500°C)}$ than their companion creep specimens (Figure 26). Again, the creep samples appear to exhibit a larger $CTE_{(25\text{-}500°C)}$ than the control specimens.

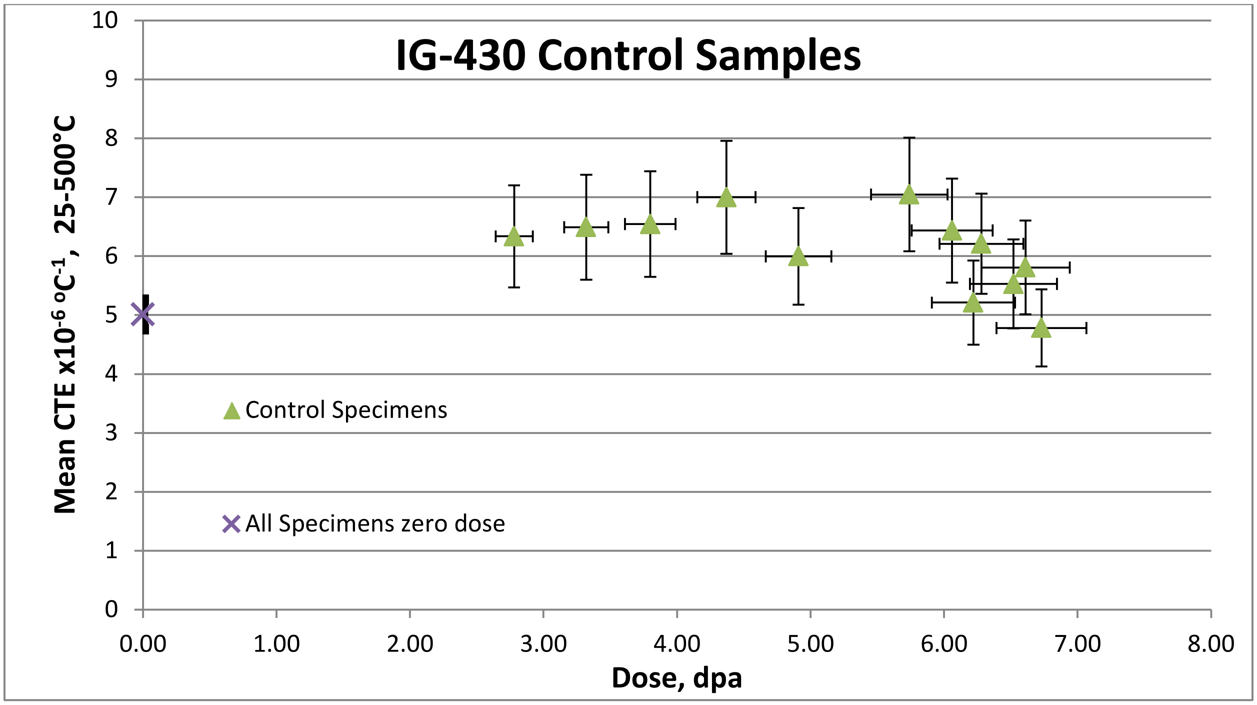

Figure 25 The variation of mean $CTE_{(25\text{-}500°C)}$ with dose for IG-430 control samples

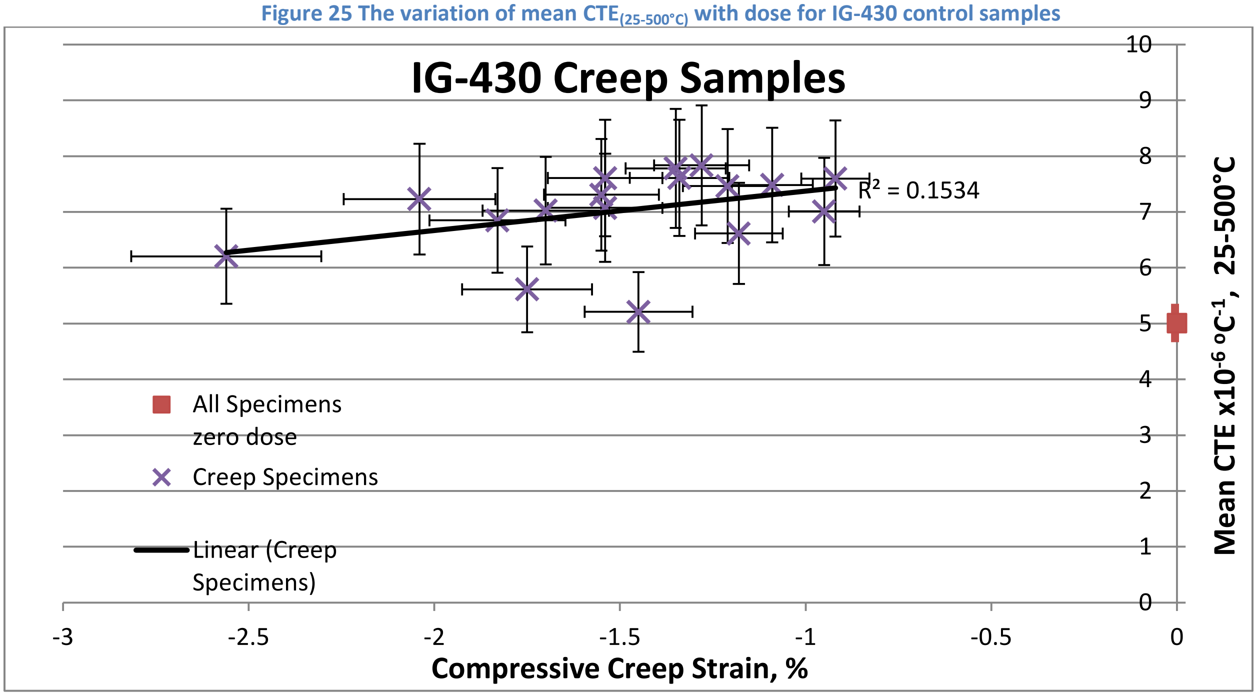

Figure 26 The variation of $CTE_{(25\text{-}500°C)}$ with compressive creep strain for IG-430 creep samples

3.2.7 Stress Direction and Isotropy Effects on Coefficient of Thermal Expansion

The increase in average CTE seen here in the data is likely caused by the irradiation induced closure of thermal shrinkage cracks, such as Mrozowski[9] and Mrozowski-like cracks. Thus, we would expect the effect of CTE to be dependent upon the anisotropy of the grade and the direction and sign of any induced stress, because these will impact the fraction of such porosity available to act as accommodation. In the AGC series of capsules, we measure the expansion along the specimen axis, which is under a compressive stress. In general, we would expect the stress to close the Mrozowski and Mrozowski-like cracks, and therefore increase the CTE. Note, a tensile stress, as in the case of specimens experiencing lateral strains, has been shown to decrease the expansion by opening expansion accommodating Mrozowski and Mrozowski-like cracks. The lateral strain effect is not considered here. Thus, specimens cut across-grain, which have larger fractions of Mrozowski and Mrozowski-like cracks perpendicular the applied stress, might be expected to exhibit larger irradiation induced thermal expansion changes.

However, the crystal anisotropy will also have a large effect on the thermal expansion response of the grade. In extruded graphites, such as PCEA, the anisotropy effect would be more significant than those of isotropic, isostatically pressed grades, such as IG-110 and IG-430. This is because the extrusion process preferentially aligns the filler-coke along the extrusion axis. The filler-coke can be expected to have preferential alignment of its single crystal's along its length and the crystal have a small negative CTE of $\approx$-1 x 10^{-6} °C^{-1} in the crystallographic <a> direction and a CTE of $\approx$ 26 x 10^{-6} °C^{-1} in the crystallographic <c> direction at room temperature. Thus, the WG CTE (with a preferential alignment along the a-axis) should exhibit a lower CTE along its length than the AG direction, which has a preferential alignment of the c-axis along it length. This CTE anisotropy effect was seen in the unirradiated PCEA data.

The observed radiation induced crystal expansion difference creates a great deal of internal stress in the graphite which is relieved by strain (i.e., irradiation induced creep). The build-up of this creep strain with dose must eventually be relieved by Mrozowski crack formation and cracking along the filler/binder interface perpendicular to the crystal basal planes, or <a> direction. This mechanism would additionally provide accommodation for AG thermal expansion and would tend to offset the higher AG expansion initially observed. The thermal expansion behavior of near-isotopic and anisotropic graphite with irradiation dose is a complex interaction of single crystal, bulk structural, and specimen orientation effects, and is particularly difficult to analyze.

The eventual reduction of the CTE by the crystal-strain/crack creation mechanism can be seen in the eventual CTE reduction of IG-430 with dose (Figure 25). Previously[6], we argued the IG-430 was entering into the turnaround (pore generation) regime. The CTE data would appear to corroborate the previous creep strain analysis for IG-430.

3.2.8 The Development of CTE with Creep Strain

The next series of Figures (Figure 27 to Figure 32) illustrates the development of the temperature dependence of CTE with creep strain.

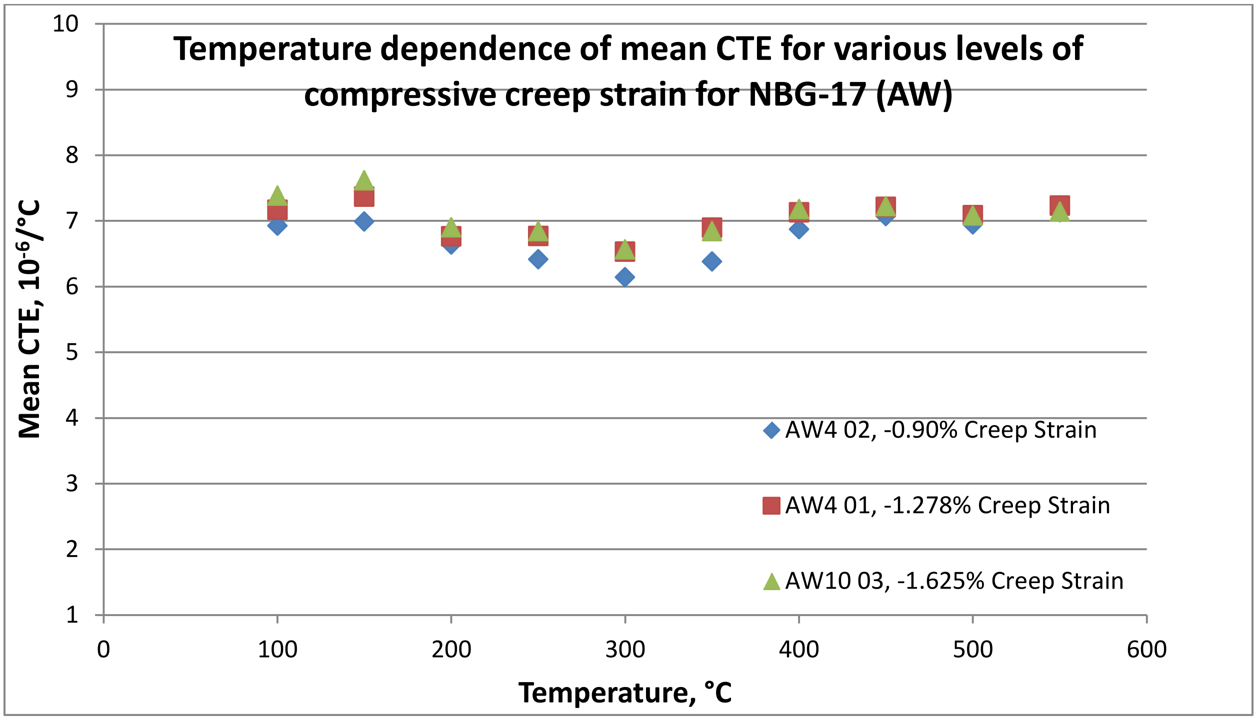

Figure 27 Temperature dependence of mean CTE for various levels of compressive creep strain for NBG-17 (AW)

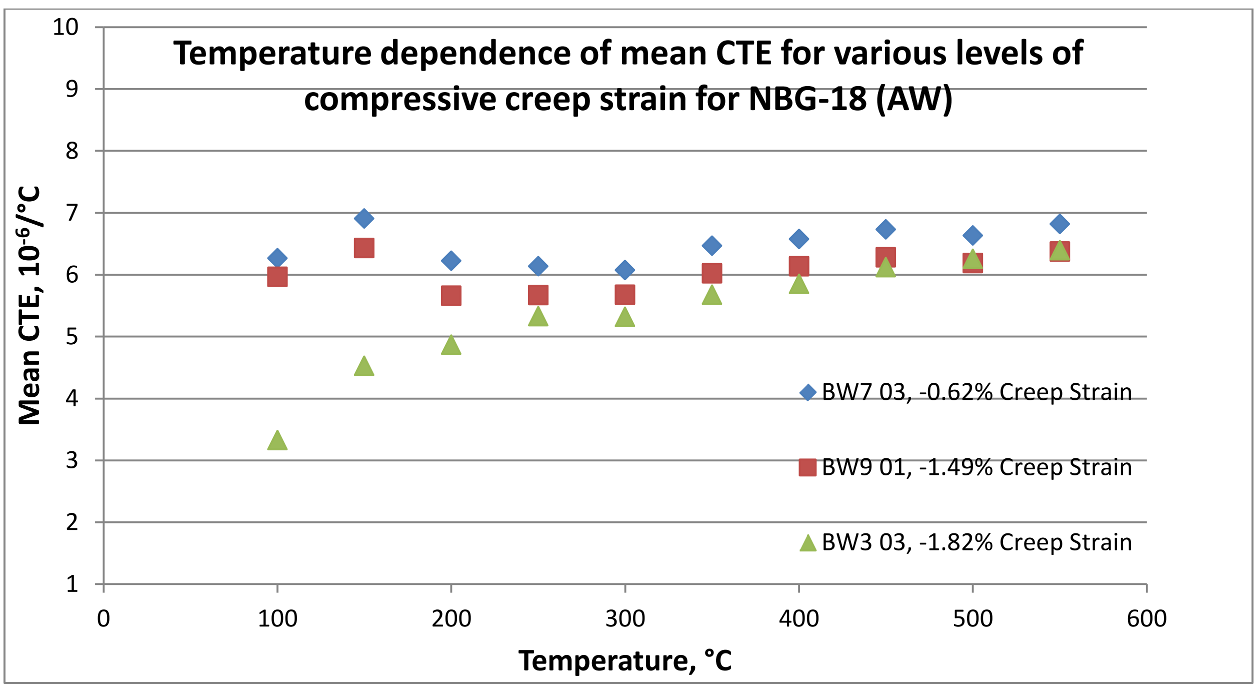

Figure 28 Temperature dependence of mean CTE for various levels of compressive creep strain for NBG-18 (BW)

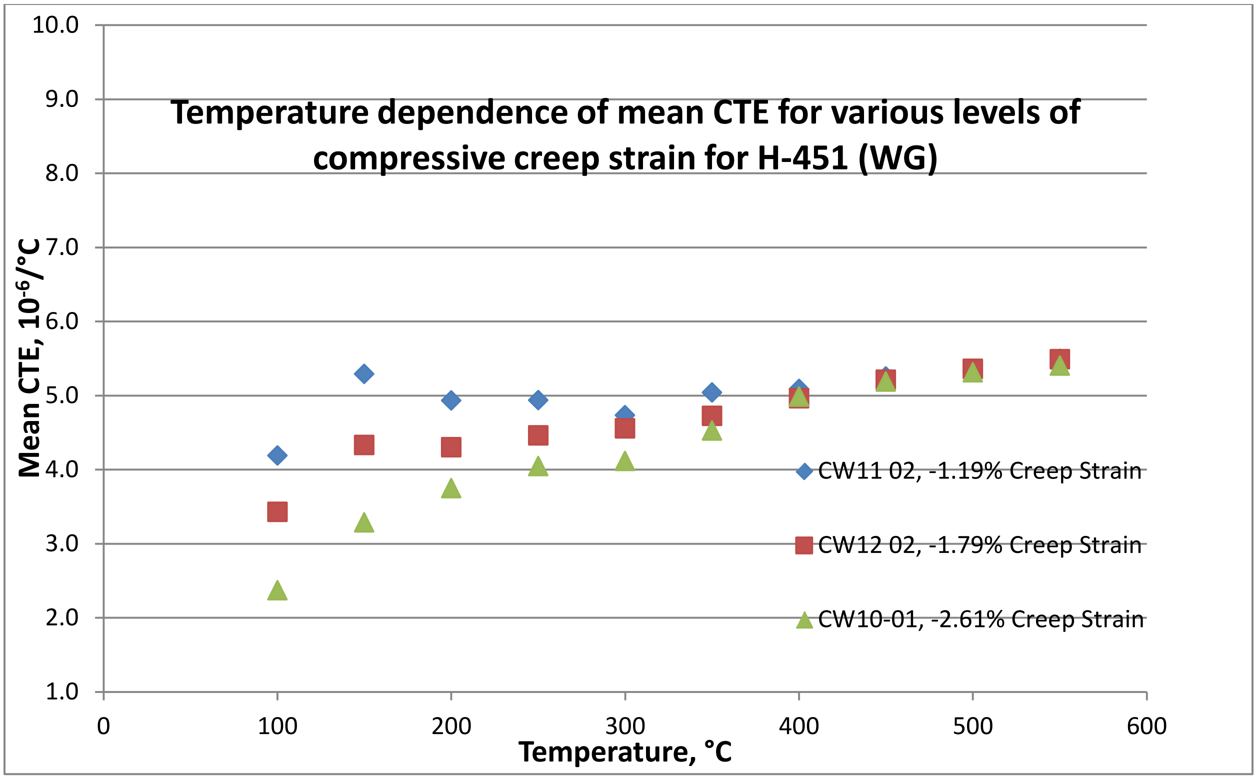

Figure 29 Temperature dependence of mean CTE for various levels of compressive creep strain for H-451 (WG)

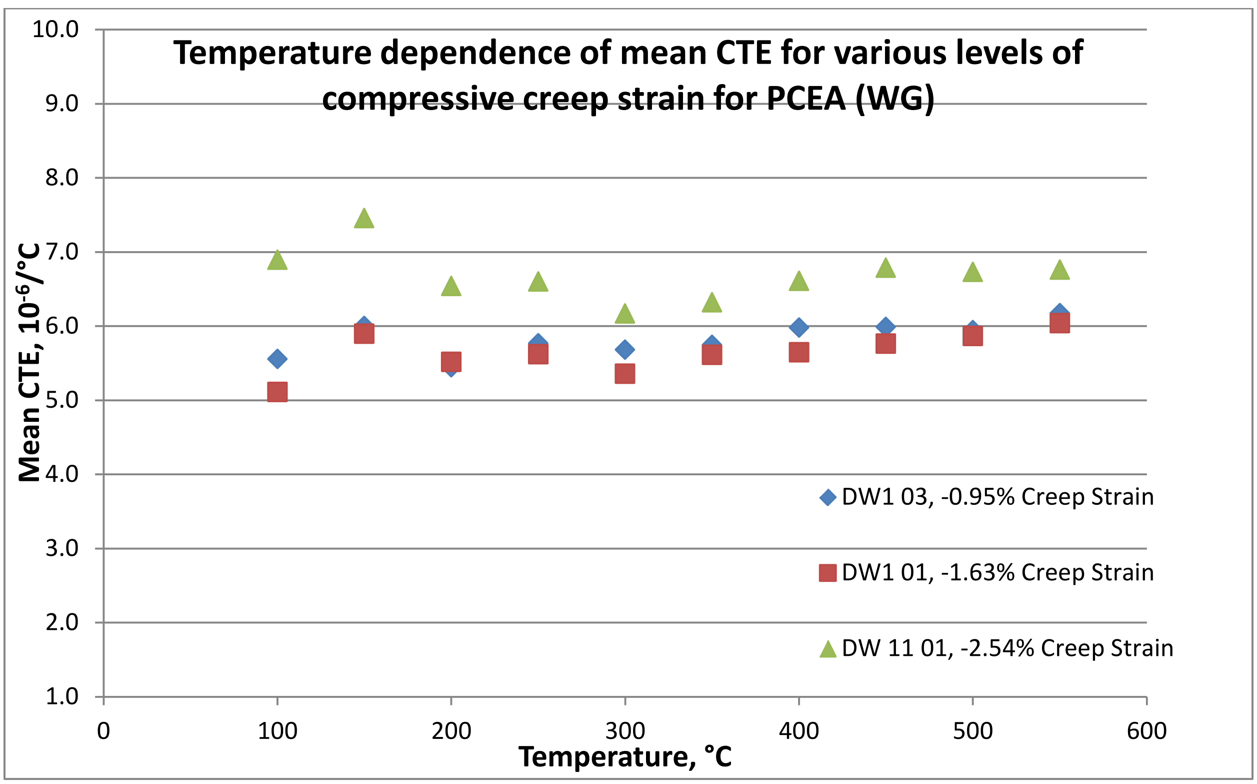

Figure 30 Temperature dependence of mean CTE for various levels of compressive creep strain for PCEA (WG)

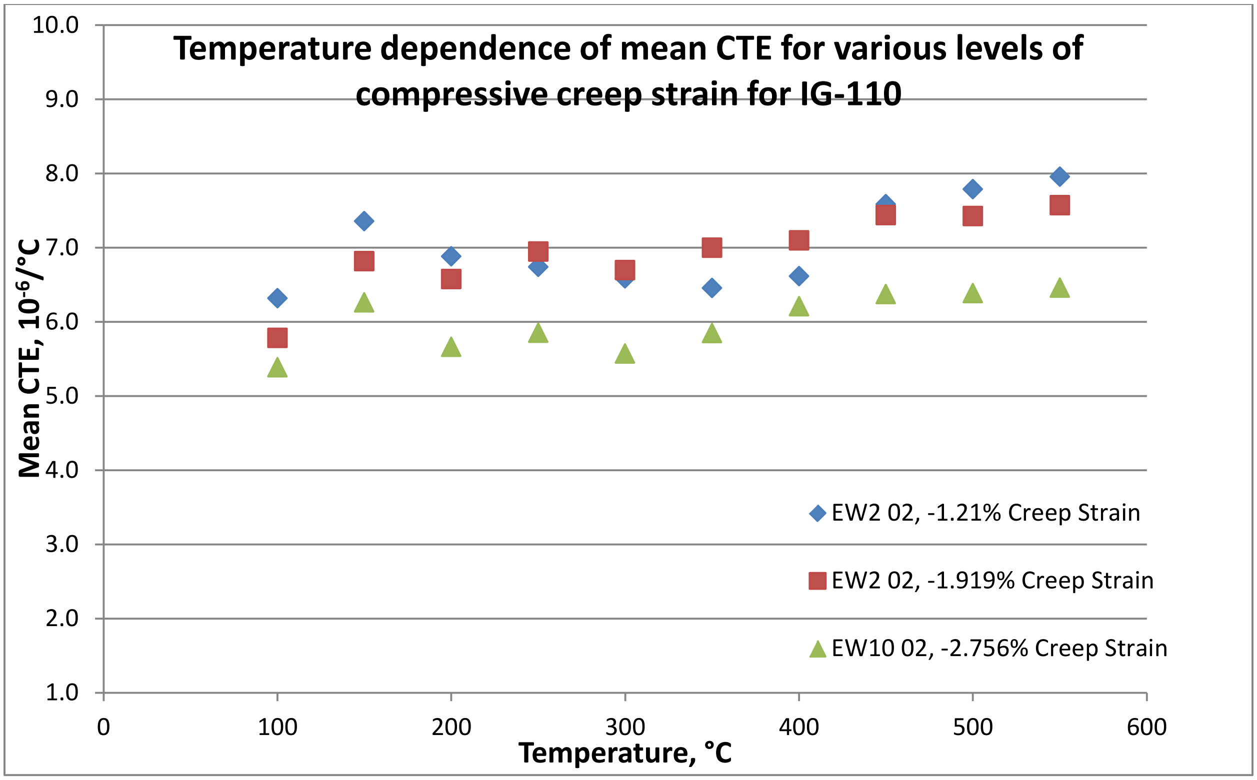

Figure 31 Temperature dependence of mean CTE for various levels of compressive creep strain for IG-110

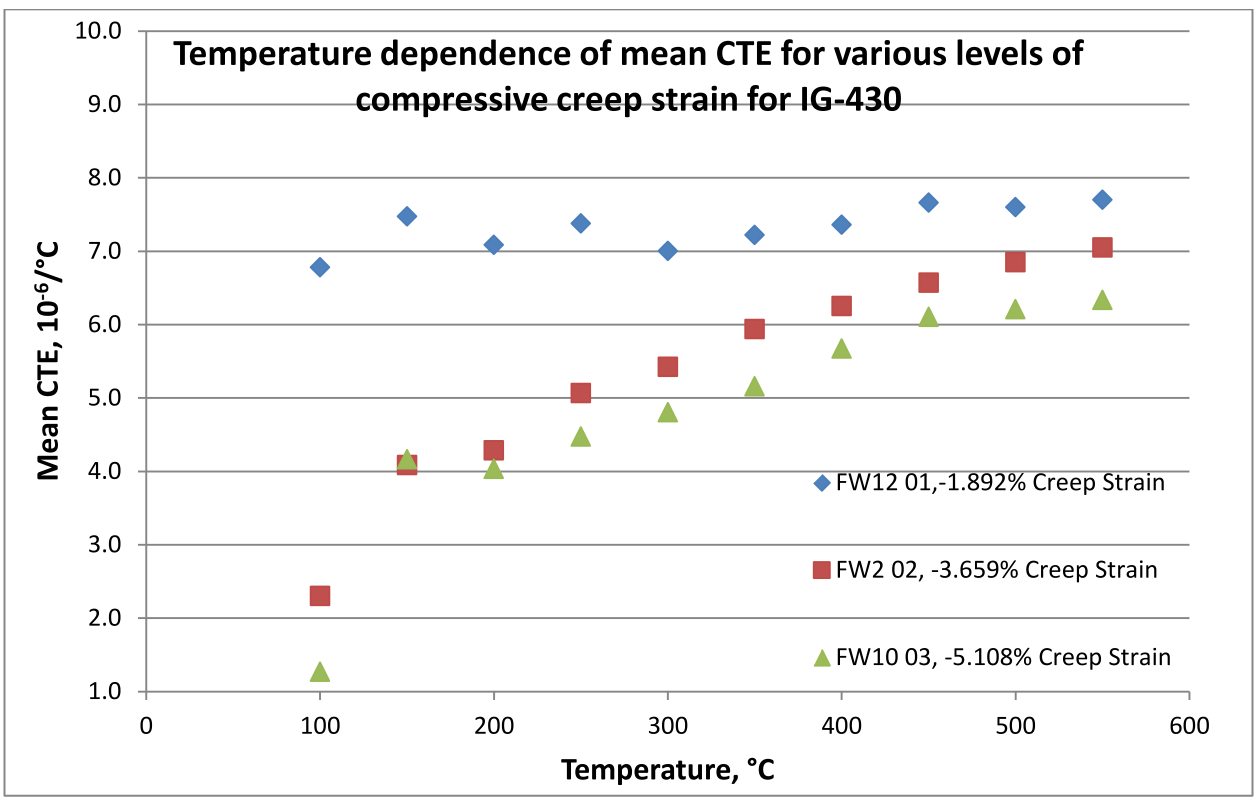

Figure 32 Temperature dependence of mean CTE for various levels of compressive creep strain for IG-430

The development of CTE with creep strain is not the same for each grade studied. In the case of NBG-17 (Figure 27), little effect on the temperature dependence of CTE is seen, whereas for IG-430 a very large effect is seen (Figure 32). In order to more easily see trends in CTE, in Section 4, we have plotted the fractional change in the average CTE at 500°C (i.e., $CTE_{25\text{-}500°C}$) as a function of dose (Figure 39 to Figure 44).

4 Discussion

4.1 Electrical Resistivity

Electrical resistivity appears to saturate at 20-30 μΩm depending on the grade. Generally, extruded graphite grades (WG) have lower electrical resistivity than iso-molded grades, because of the size and alignment of their filler-coke particles. Increases in resistivity after irradiation are expected to arise due to the increased number of irradiation induced damage sites within the crystal structure, which act as electron scattering centers, thus shortening the mean free path of the electrons.

The relative changes between irradiated graphite (control specimens) and irradiated and stressed graphite (creep specimens) are more easily seen when fractional changes in electrical resistivity is plotted. The fractional change in electrical resistivity is given by;

$$\text{Fractional Change} = \frac{\rho_i - \rho_0}{\rho_0}$$

$$= \left(\frac{\rho_i}{\rho_0} - \frac{\rho_0}{\rho_0}\right)$$

$$= \left(\frac{\rho_i}{\rho_0} - 1\right)$$

Where ρ_0 = unirradiated resistivity (μΩm), and

ρ_i = irradiated or irradiated/stressed resistivity (μΩm).

The following sub-sections show the fraction changes in resistivity as a function of dose (dpa) for irradiated (control specimens) and irradiated/stressed (creep) specimens of the six grades of graphite examined here.

4.1.1 Grade A, NBG-17

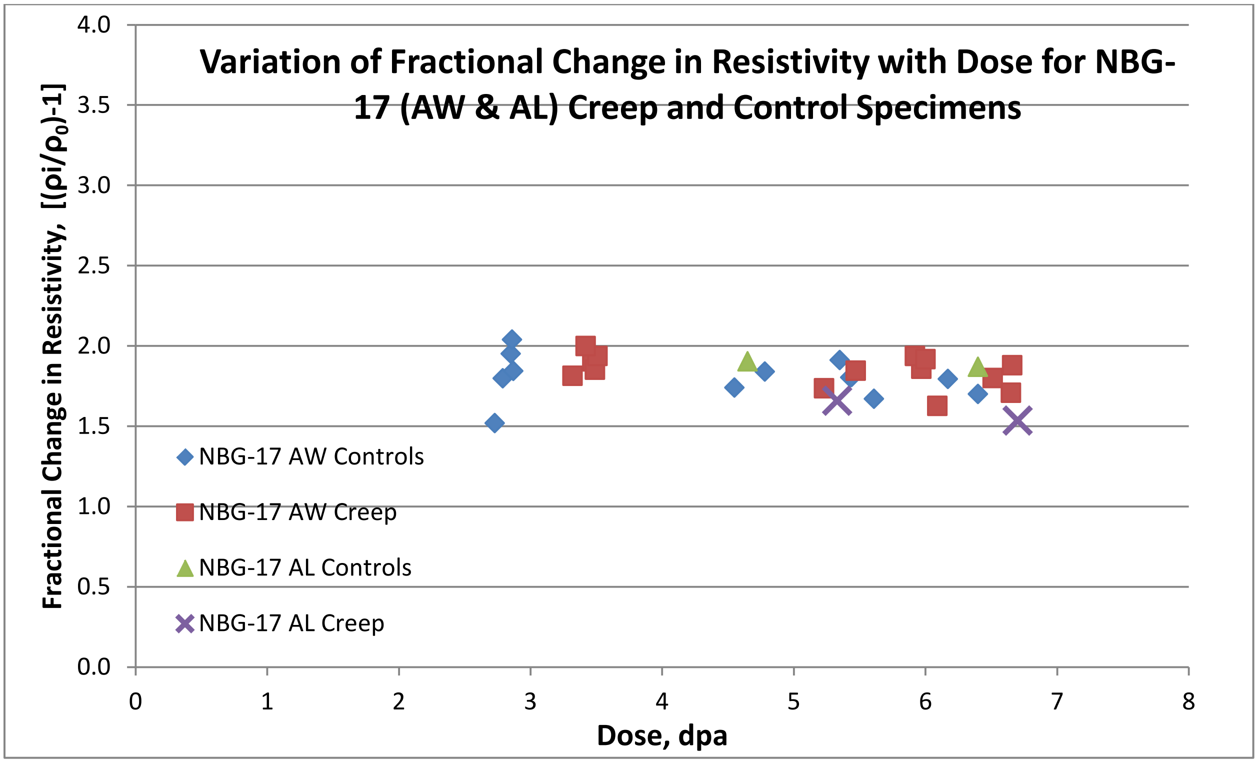

Figure 33 Fractional changes in resistivity for control and creep specimen of NBG-17 (AL) and NBG-17 (AW)

4.1.2 Grade B, NBG-18

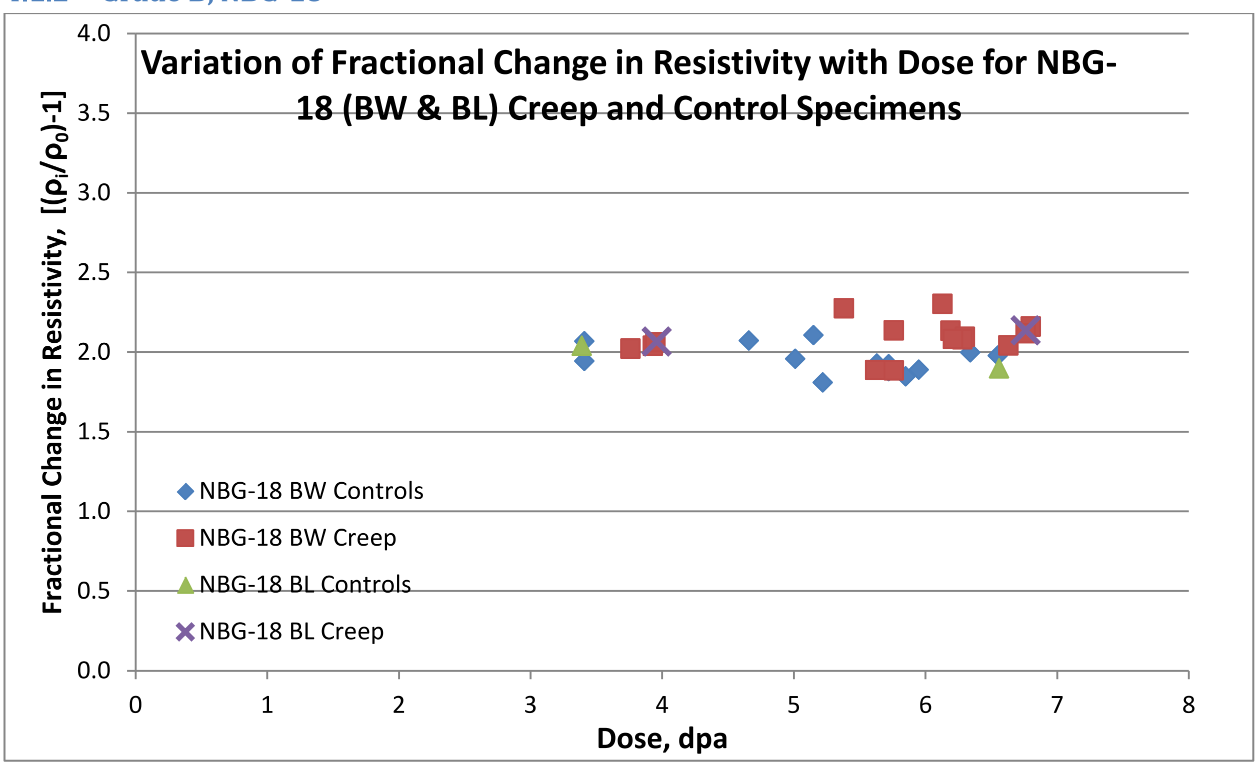

Figure 34 Fractional changes in resistivity for control and creep specimen of NBG-18 (BL) and NBG-18 (BW)

4.1.3 Grade C, H-451

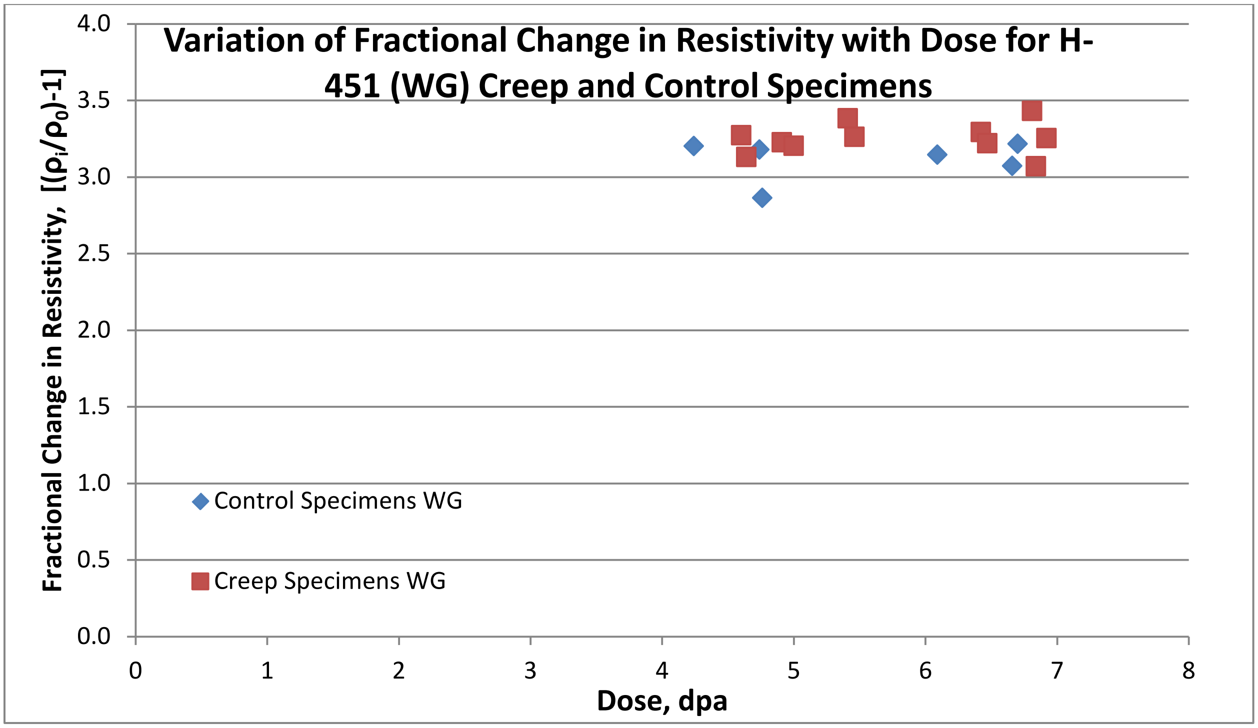

Figure 35 Fractional changes in resistivity for control and creep specimen of H-451 (WG)

4.1.4 Grade D, PCEA

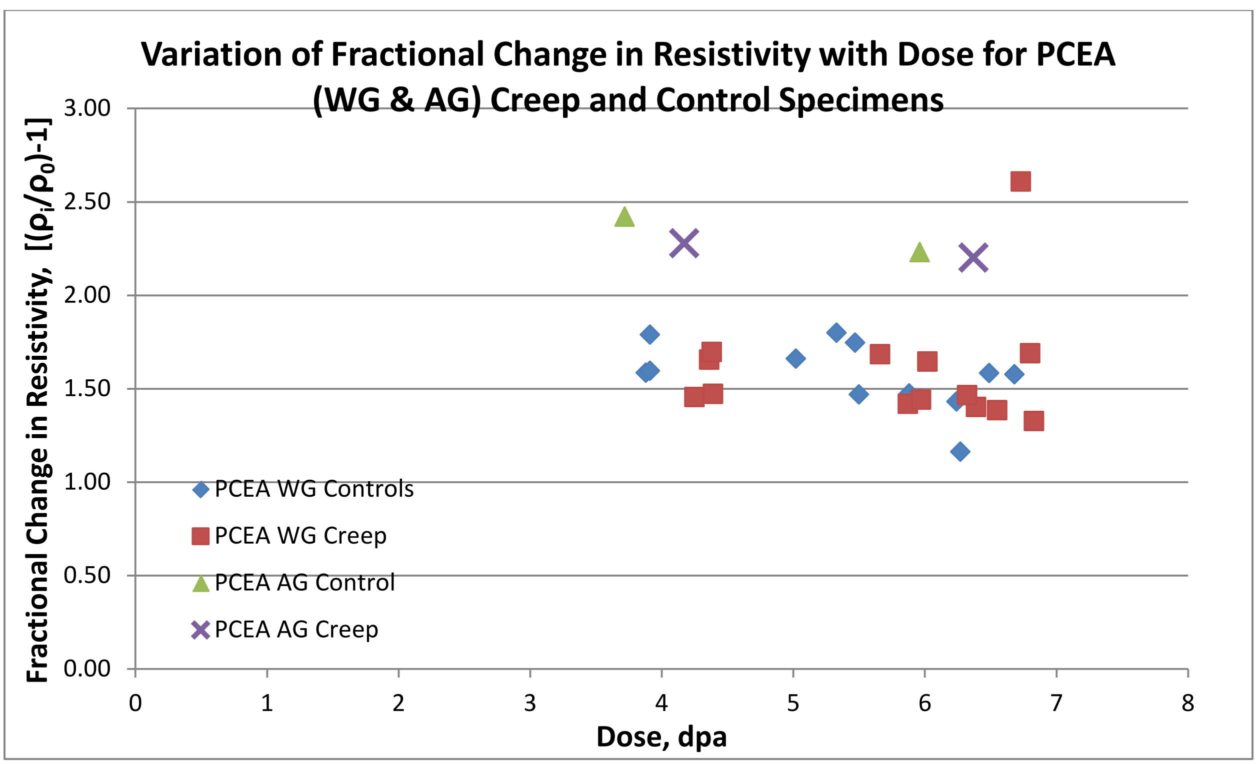

Figure 36 Fractional changes in resistivity for control and creep specimen of PCEA (AG) and PCEA (WG)

4.1.5 Grade E, IG-110

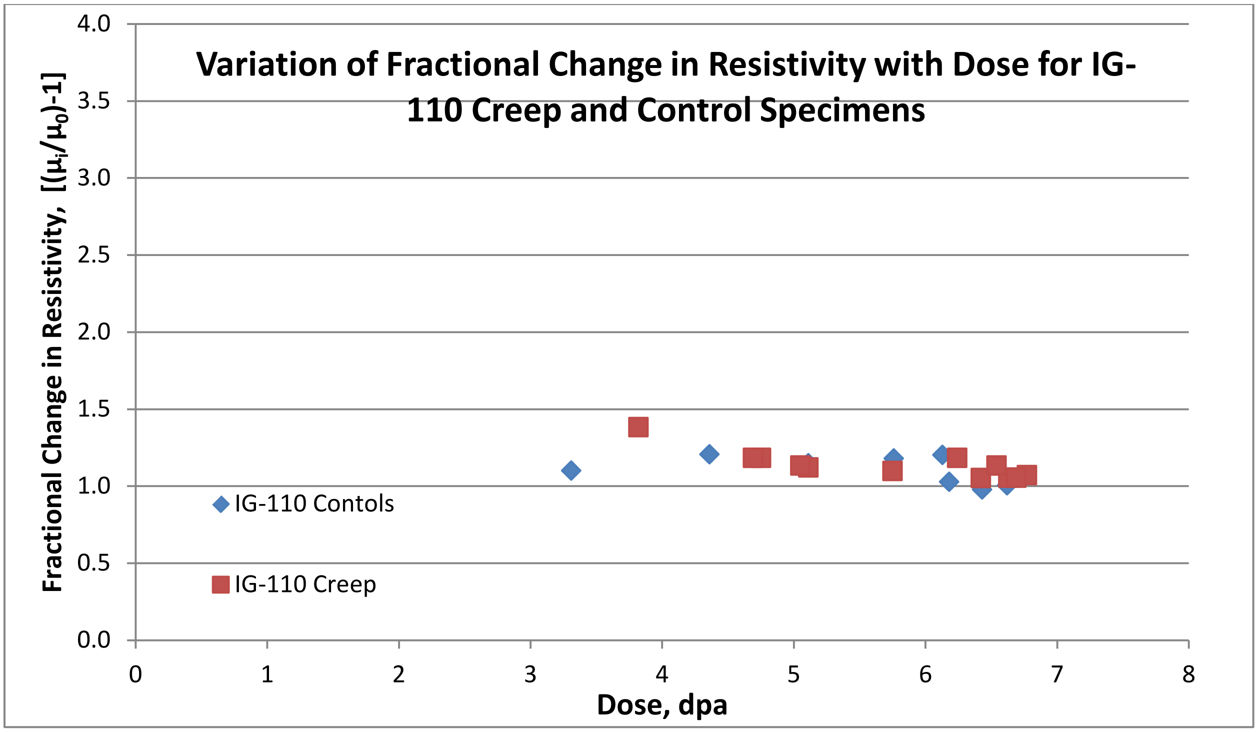

Figure 37 Fractional changes in resistivity for control and creep specimen of IG-110

4.1.6 Grade F, IG-430

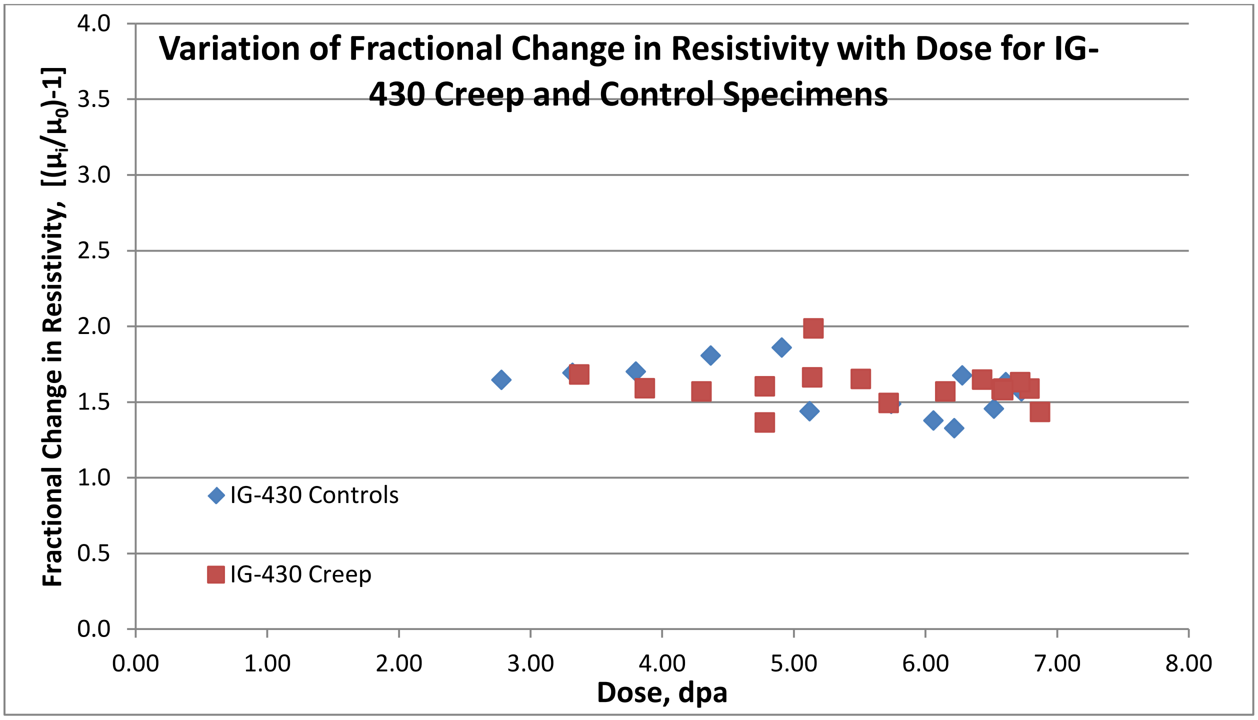

Figure 38 Fractional changes in resistivity for control and creep specimen of IG-430

The largest resistivity fractional changes were observed for the extruded graphite, H-451, and the smallest for the iso-statically molded grade, IG-430. The fractional changes for the creep and control specimens appeared to be very similar for all the graphite grades (subsection 3.1.7).

To determine the actual difference between the creep and control specimens, statistical significance testing[7,8] on the resistivity data was conducted. The means of the three highest doses of the creep and control specimen resistivity for each of the graphite grades were significance tested to see whether they were really different.

4.1.7 Electrical Resistivity Statistical Testing

To analyze the resistivity data a series of significance questions (section 2.4.2) were posed (Table 6).

Table 6 Statistical significance test questions

Question Number	Question
Question/Test i	**Is irradiated resistivity of controls > unirradiated resistivity for grade?**
Question/Test ii	**Is irradiated resistivity of creeps> unirradiated resistivity for grade?**
Question/Test iii	**Is electrical resistivity of the creep and control specimens different?**
Question/Test iv	**Are control resistivity doses and creep resistivity doses similar?**

The resistivity and dose of the three highest dose specimens for creep and control specimen data set (to be significance tested) are given in Table 7.

Table 7 Unirradiated resistivity means and the three highest dose creep and control specimens and their electrical resistivity for each grade of graphite in AGC-1

Grade			Irradiated Resistivity Statistics for "t" Testing				
			Controls (3 highest dose)		Creep (3 highest dose)		
ID	**Name**	**Unirradiated Resistivity, µΩm**	**Resistivity, µΩm**	**dose, dpa**	**Resistivity, µΩm**	**dose, dpa**	**Creep Strain, %**
A	NBG-17 (WG)	n=30	27.29	5.61	28.61	6.51	-1.42
			28.54	6.17	27.68	6.65	-1.63
			27.58	6.4	29.42	6.66	-2.01
	MEAN	10.22	27.80	6.06	28.57	6.61	-1.68
	S.D.	0.24	0.65	0.41	0.87	0.08	0.30
B	NBG-18 (WG)	n=30	27.38	5.95	28.81	6.63	-1.35
			28.40	6.34	29.94	6.80	-1.72
			28.21	6.55	29.54	6.76	-2.03
	MEAN	9.47	28.00	6.28	29.43	6.73	-1.70
	S.D.	0.21	0.54	0.30	0.57	0.09	0.34
C	H-451(WG)	n=22	28.41	6.66	29.67	6.92	-2.10
			29.40	6.7	30.91	6.81	-3.09
			28.91	6.09	28.39	6.84	-1.89
	MEAN	6.98	28.91	6.48	29.66	6.86	-2.36
	S.D.	0.62	0.50	0.34	1.26	0.06	0.64
D	PCEA(WG)	n=31	17.40	6.27	29.04	6.73	-1.63
			20.80	6.49	21.64	6.80	-2.04
			20.74	6.68	18.72	6.83	-2.42
	MEAN	8.05	19.65	6.48	23.13	6.79	-2.03
	S.D.	0.08	1.95	0.21	5.32	0.05	0.40
E	IG-110	n=22	24.72	6.18	25.07	6.63	-1.94
			24.13	6.43	25.05	6.69	-2.76
			24.44	6.62	26.02	6.77	-2.78
	MEAN	12.2	24.43	6.41	25.38	6.70	-2.49
	S.D.	0.62	0.30	0.22	0.55	0.07	0.48
F	IG-430	n=34	23.77	6.52	23.58	6.87	-2.56
			25.48	6.61	25.47	6.72	-1.75
			24.88	6.73	25.06	6.79	-1.70
	MEAN	9.68	24.71	6.62	24.70	6.79	-2.00
	S.D.	0.69	0.87	0.11	0.99	0.08	0.48

Before significance testing the specimen resistivity, it was necessary to establish that the chosen creep and control specimens had comparable irradiation doses. An unpaired Student[7,8] "t" test was employed to test the statistical significance of the differences (Table 6, question iv).

Table 8 "t' tests results for the specimen irradiation dose

UNPAIRED t TEST RESULTS FOR DOSE			
GRADE	TEST	statistics parameter, Two-tailed P	TWO-TAILED TEST RESULT
A(WG)	iv	0.0847	Difference **is not quite** statistically significant
B(WG)	iv	0.0676	Difference **is not quite** statistically significant
C(WG)	iv	0.1293	Difference **is not** statistically significant
D(WG)	iv	0.0677	Difference **is not quite** statistically significant
E	iv	0.0952	Difference **is not quite** statistically significant
F	iv	0.0964	Difference **is not quite** statistically significant

Table 8 gives the results for the t-testing of the specimen doses. In all cases the difference was not statistically significant or was not quite statistically significant. Essentially, we may consider the doses of the creep and control specimens of each graphite grade to be similar. Since the physical property values to be significance tested are a function of neutron dose it was imperative to establish that the doses are comparable. It is now possible to test the resistivity data in Table 7. The results of resistivity significance testing are given in Table 9.

Table 9 Significance testing results for the electrical resistivity data

UNPAIRED t TEST RESULTS FOR RESISTIVITY			
GRADE	TEST	statistics parameter, Two-tailed P	TWO-TAILED TEST RESULT
A(WG)	i	<0.0001	Difference is extremely statistically significant
A(WG)	ii	<0.0001	Difference is extremely statistically significant
A(WG)	iii	0.2867	Difference considered **not** statistically significant
B(WG)	i	<0.0001	Difference is extremely statistically significant
B(WG)	ii	<0.0001	Difference is extremely statistically significant
B(WG)	iii	0.0344	Difference **is** considered statistically significant
C(WG)	i	<0.0001	Difference is extremely statistically significant
C(WG)	ii	<0.0001	Difference is extremely statistically significant
C(WG)	iii	0.3922	Difference considered **not** statistically significant
D(WG)	i	<0.0001	Difference is extremely statistically significant
D(WG)	ii	<0.0001	Difference is extremely statistically significant
D(WG)	iii	0.3474	Difference considered **not** statistically significant
E	i	<0.0001	Difference is extremely statistically significant
E	ii	<0.0001	Difference is extremely statistically significant
E	iii	0.0584	Difference considered **not quite** statistically significant
F	i	<0.0001	Difference is extremely statistically significant
F	ii	<0.0001	Difference is extremely statistically significant
F	iii	0.9901	Difference considered **not** statistically significant

In all cases, the resistivity of the irradiated (control) or irradiated/stressed (creep) specimen was significantly greater than the unirradiated resistivity (questions i and ii). This clearly indicates that irradiation increases the electrical resistivity. In five of the six cases tested, the two data sets (i.e., the creep and control specimens) were not or not quite significantly different (question iii). This suggests that irradiation creep has no additional effect on the electrical resistivity over the dose range examined in AGC-1. This observation, along with the observation that creep at these doses appears to be volume conserving[6], that is, creep and control specimens exhibit similar volume changes on irradiation, support the hypothesis that creep prior to volume turnaround is largely an in-crystal phenomena.

4.2 Coefficient of Thermal Expansion

All of the graphite grades examined here had an unirradiated $CTE_{(25\text{-}500°C)}$ of approximately $\approx 5.0\times10^{-6}$/°C, with the exception of H-451 which had a mean $CTE_{(25\text{-}500°C)}$ closer to 4×10^{-6}/°C. The CTE of the creep specimens exceed the CTE of controls specimens.

Utilizing linear regression techniques, it is seen that, with the exception of the two extruded grades, H-451 (Figure 20) and PCEA (Figure 22), the value of $CTE_{(25\text{-}500°C)}$ appears to decrease or stay relatively constant after approximately -1% compressive creep strain (Figure 16, Figure 18, Figure 24, and Figure 26). The linear regression correlation coefficients are very small, and do not indicate good correlations. However, this CTE saturation observation with increasing creep strain is in agreement with recent UK modelling[15] and disagrees with previous analysis where the CTE was believed to increase linearly with creep strain[16]. Unfortunately, we only have the benefit of pre volume turnaround data in the AGC-1 experiment (with the possible exception of IG-430).

The observation that H-451 CTE increases with increasing compressive creep strain is dramatically different from observed behavior for the other AGC-1 graphite grades, but is in agreement with Kelly's previous analysis[16]. The effect of creep on CTE is perplexing; previous work[16] on H-451 was over the same pre-turnaround dose range as reported here. It may be possible the observed relationship between CTE behavior and creep strain is specific to the forming method used during the graphite grade manufacture. Given the known behavior of CTE, a continually increasing or saturated crept CTE seems implausible. Further analysis is necessary to determine the underlying mechanisms for the CTE behavior. This will allow more accurate predictions of the thermal expansion performance for nuclear graphite.

Since CTE is a continuous function of irradiation dose, it is impossible to calculate a mean percentage change over a wide fluence range. The change of CTE, as dose increases, is best seen by examining the fractional changes with irradiation dose. Consequently, the relative changes between control sample graphite and creep sample graphite are reported here. The fractional change in mean $CTE_{(25\text{-}500°C)}$ is given by;

$$\text{Fractional Change} = \frac{\left[CTE_{(25-500°C)}\right]_i - \left[CTE_{(25-500°C)}\right]_0}{\left[CTE_{(25-500°C)}\right]_0}$$

$$= \left(\frac{\left[CTE_{(25-500°C)}\right]_i}{\left[CTE_{(25-500°C)}\right]_0} - \frac{\left[CTE_{(25-500°C)}\right]_0}{\left[CTE_{(25-500°C)}\right]_0}\right)$$

$$= \left(\frac{\left[CTE_{(25-500°C)}\right]_i}{\left[CTE_{(25-500°C)}\right]_0} - 1\right)$$

$$\text{Fractional change in CTE} = \left(\frac{\alpha_i}{\alpha_0} - 1\right)$$

Where $\alpha_0 = [CTE_{(25\text{-}500°C)}]_0$ = unirradiated mean CTE from 25 to 500°C, µm/m/°C, and

$\alpha_i = [CTE_{(25\text{-}500°C)}]_i$ = irradiated or irradiated/crept mean CTE from 25 to 500°C, µm/m/°C .

The following sub-sections illustrate the fractional changes in mean CTE from 25 to 500°C as a function of dose (dpa) for control and creep specimens for the six grades of graphite examined here.

4.2.1 Grade A, NBG-17

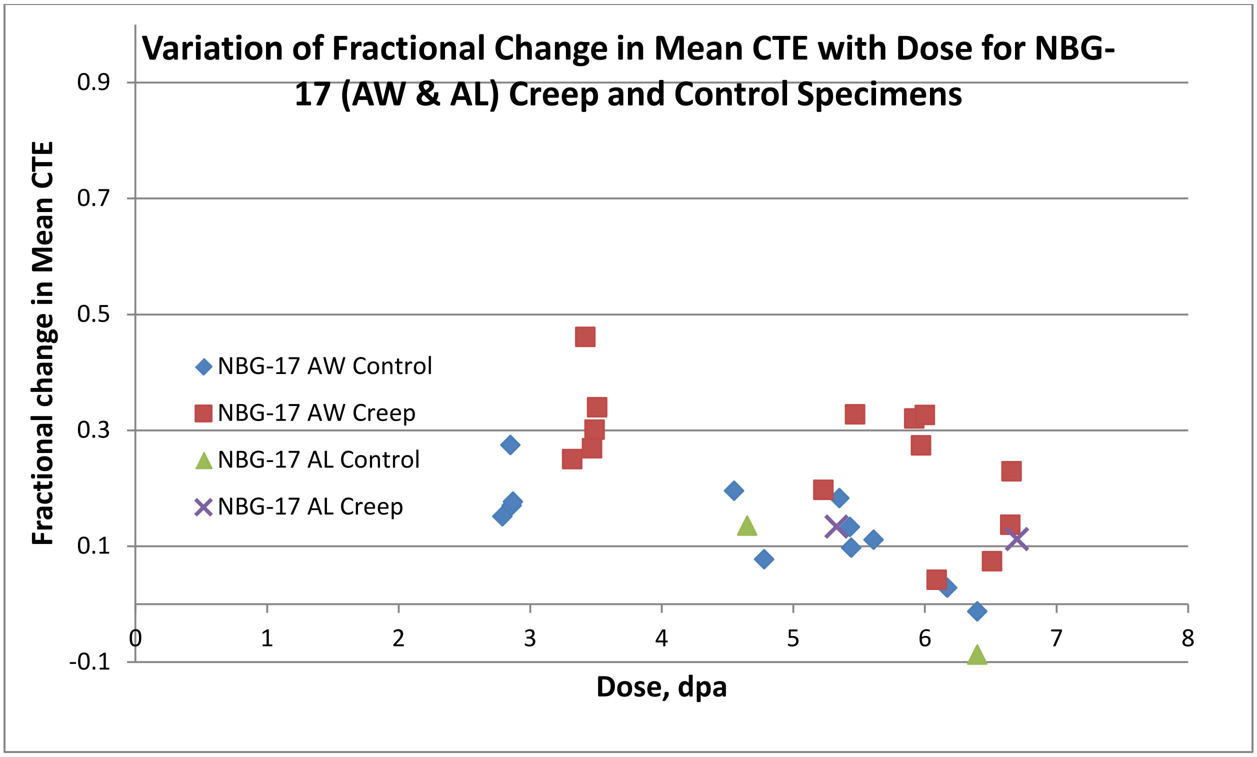

Figure 39 Fractional changes in CTE for control and creep specimen of NBG-17 (AW) and NBG-17 (AL)

4.2.2 Grade B, NBG-18

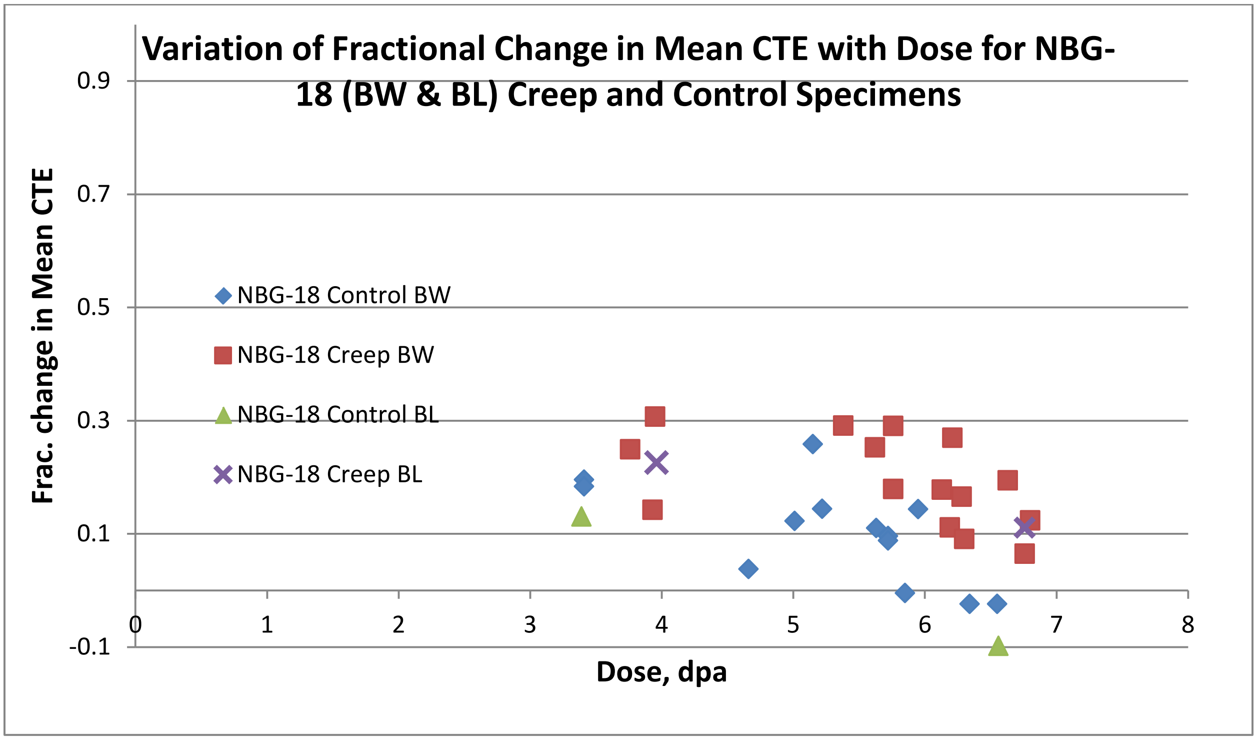

Figure 40 Fractional changes in CTE for control and creep specimen of NBG-18 (BW) and NBG-18 (BL)

4.2.3 Grade C, H-451

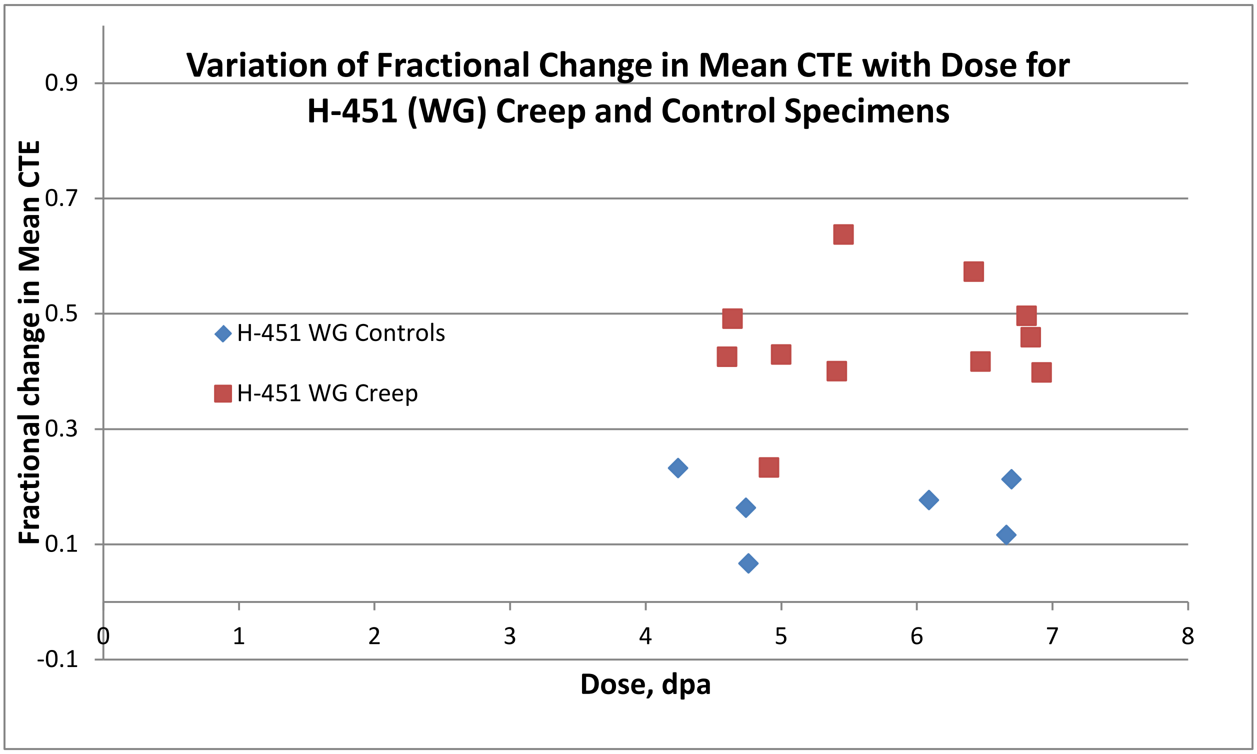

Figure 41 Fractional changes in CTE for control and creep specimen of H-451 (WG)

4.2.4 Grade D, PCEA

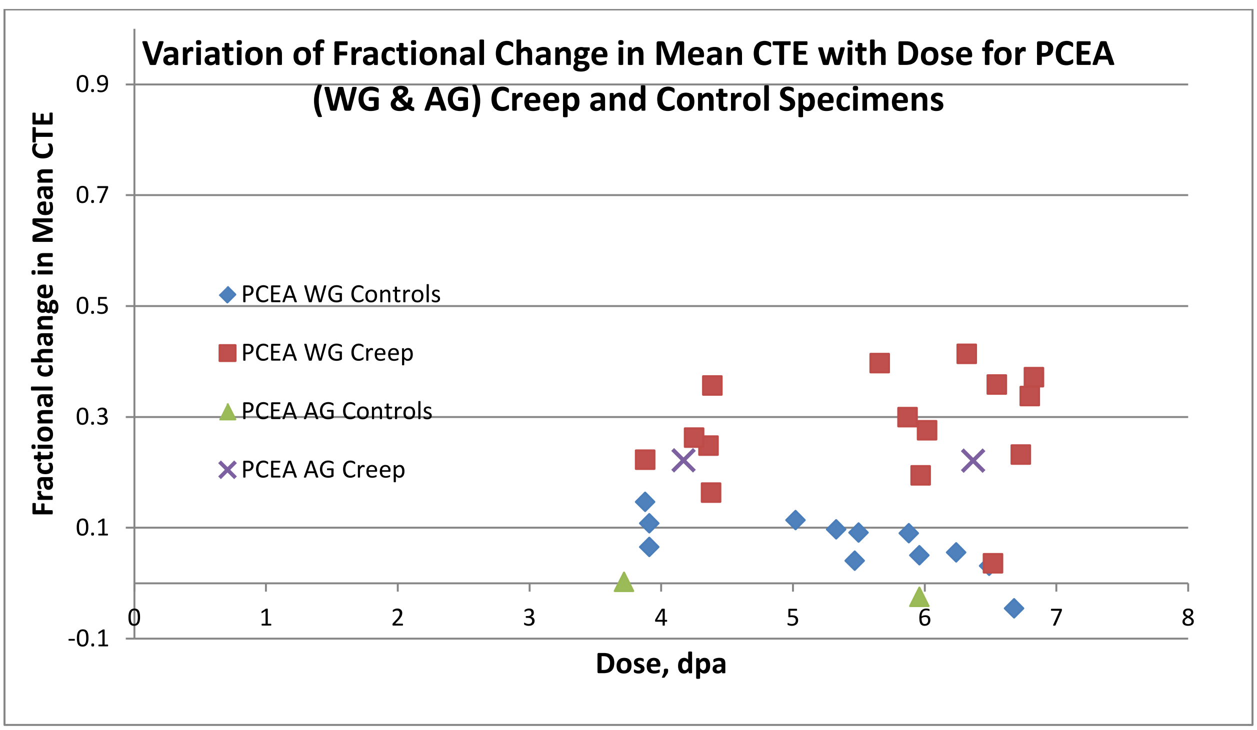

Figure 42 Fractional changes in CTE for control and creep specimen of PCEA (AG) and PCEA (WG)

4.2.5 Grade E, IG-110

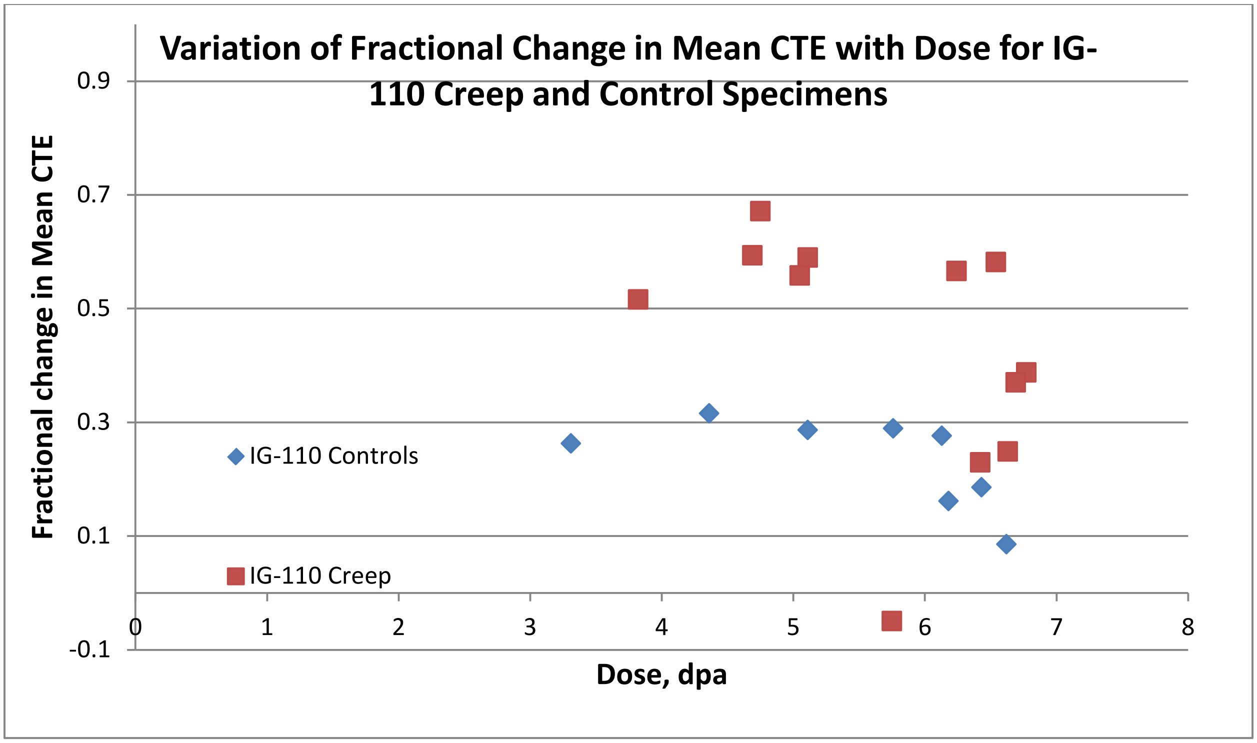

Figure 43 Fractional changes in CTE for control and creep specimen of IG-110

4.2.6 Grade F, IG-430

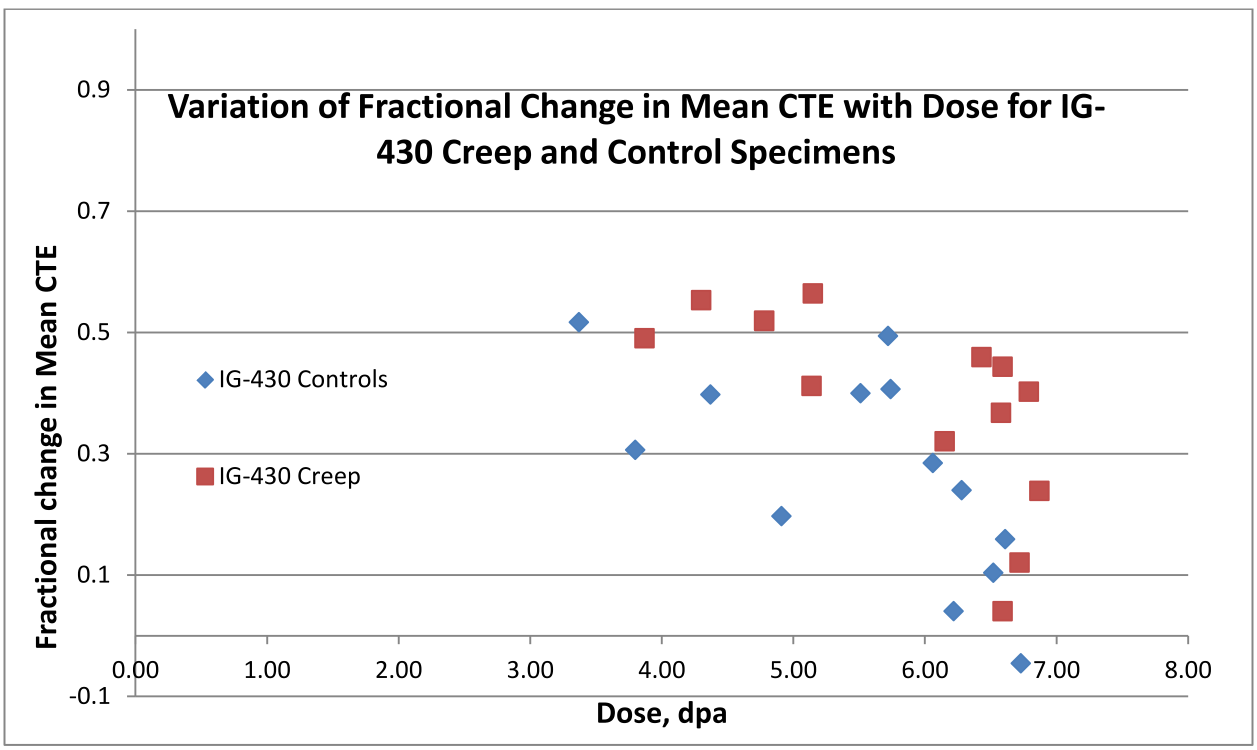

Figure 44 Fractional changes in CTE for control and creep specimen of IG-430

Although the dose range reported here did not commence from zero, but began at three dpa the expected property changes with dose were observed for this dose range. In the case of IG-430, we suspect the graphite had begun dimensional turnaround[6] and the creep CTE at higher dose should have approached the unirradiated value (Figure 25).

4.2.7 CTE Statistical Testing

In each of the cases in Figure 39 to Figure 44, the fractional change of CTE appears greater in the crept specimens compared to the control specimens. To test whether this is actually true, significance testing[7,8] (subsection 2.4.2) has been conducted on the mean of the $CTE_{(25\text{-}500°C)}$ of the three creep and control specimens with the largest neutron dose and on mean of the $CTE_{(25\text{-}500°C)}$ of the three creep and control specimens with the largest $CTE_{(25\text{-}500°C)}$ values.

Once again, we posed the same questions (Table 6) to determine whether the value of mean $CTE_{(25\text{-}500°C)}$ increased on irradiation and whether the mean $CTE_{(25\text{-}500°C)}$ for the creep specimens was greater than the mean $CTE_{(25\text{-}500°C)}$ for control specimen. The means and standard deviations of the mean $CTE_{(25\text{-}500°C)}$ for the selected specimen groups are in presented in Table 10 and Table 12.

Since the physical property values to be tested are a function of neutron dose, it was imperative to establish that the doses are comparable. Differences in dose were previously established (subsection 4.1.6, Table 8), where dose levels of the creep and control specimens could be considered as identical for the largest dose specimens. For the three largest creep and control $CTE_{(50\text{-}500°C)}$ specimens the results of "t" testing showed the difference in flux in five of the six cases was not statistically significant (Table 12 and Table 13). Thus we may consider the doses to be similar for the 3 creep and control specimens with the largest $CTE_{(50\text{-}500°C)}$. Similar to significance testing for Electrical Resistivity, the mean $CTE_{(25\text{-}500°C)}$ values and dose levels for the three highest irradiated dose specimens for creep and control data sets are presented in Table 10.

Three questions were posed:

1. Are irradiated mean $CTE_{(RT\text{-}500°C)}$ of controls greater than unirradiated mean $CTE_{(RT\text{-}500°C)}$ for grade?
2. Are irradiated mean $CTE_{(RT\text{-}500°C)}$ of creeps greater than unirradiated mean CTE($_{RT\text{-}500°C)}$ for grade?
3. Are mean $CTE_{(RT\text{-}500°C)}$ of the creep and control specimens different?

The results of mean $CTE_{(25\text{-}500°C)}$ significance testing results are presented in Table 11. In 11 of 12 cases (questions 1 and 2) the difference between the control and creep specimen CTE and the unirradiated specimen $CTE_{(50\text{-}500°C)}$ was either very significant or significant. Inspection of the mean values in Table 10 shows that in the vast majority of cases, for the dose range examined in AGC-1, the control or creep CTE exceeded the unirradiated value. Moreover, significance testing (Table 11) showed that for four of the six graphite grades examined the creep specimens had a larger $CTE_{(25\text{-}500°C)}$ than the control samples.

Table 10 Unirradiated $CTE_{(25\text{-}500°C)}$ and the three largest values doses specimens and their corresponding values of $CTE_{(25\text{-}500°C)}$ for the creep and control specimens for each major grade of graphite in AGC-1

ID	NAME	CTE x10^{-6} °C^{-1}, 25-500°C	Controls (3 highest Dose)		Creep (3 highest Dose)		
			CTE x10^{-6} °C^{-1}, 25-500°C	dose, dpa	CTE x10^{-6} °C^{-1}, 25-500°C	dose, dpa	Creep Strain, %
A	NBG-17 (WG)	n=30	5.93	5.61	5.73	5.61	-1.42
			5.49	6.17	6.07	6.65	-1.62
			5.27	6.4	6.56	6.66	-2.01
	MEAN	5.34	5.56	6.06	6.12	6.31	-1.68
	S.D.	0.104	0.34	0.41	0.42	0.60	0.30
B	NBG-18 (WG)	n=30	6.07	5.95	6.34	6.63	-1.35
			5.18	6.34	5.97	6.80	-1.72
			5.18	6.55	5.66	6.76	-2.03
	MEAN	5.31	5.48	6.28	5.99	6.73	-1.70
	S.D.	0.163	0.51	0.30	0.34	0.09	0.34
C	H-451(WG)	n=22	4.41	6.09	5.47	6.84	-1.89
			4.18	6.66	5.24	6.92	-2.10
			4.55	6.7	5.61	6.81	-3.09
	MEAN	3.75	4.38	6.48	5.44	6.86	-2.36
	S.D.	0.096	0.19	0.34	0.19	0.06	0.64
D	PCEA(WG)	n=33	4.26	6.27	5.87	6.73	-1.63
			4.91	6.49	6.37	6.80	-2.04
			4.54	6.68	6.53	6.83	-2.42
	MEAN	4.76	4.57	6.48	6.26	6.79	-2.03
	S.D.	0.057	0.33	0.21	0.34	0.05	0.40
E	IG-110	n=22	5.41	6.18	5.82	6.63	-1.94
			5.52	6.43	6.47	6.77	-2.53
			5.06	6.62	6.39	6.69	-2.76
	MEAN	4.66	5.33	6.41	6.23	6.70	-2.41
	S.D.	0.109	0.24	0.22	0.35	0.07	0.42
F	IG-430	n=34	5.53	6.53	7.02	6.79	-1.70
			5.81	6.61	5.61	6.72	-1.75
			4.78	6.73	6.21	6.87	-2.56
	MEAN	5.01	5.37	6.62	6.28	6.79	-2.00
	S.D.	0.299	0.53	0.10	0.71	0.08	0.48

Table 11 Significance testing results for the mean coefficient of thermal expansion (25-500°C) with largest dose from AGC-1

UNPAIRED t TEST RESULTS FOR CTE			
GRADE	TEST	Statistics parameter, two-tailed P	TWO-TAILED TEST RESULT
A(WG)	i	0.0101	Difference is statistically significant
A(WG)	ii	<0.0001	Difference is extremely statistically significant
A(WG)	iii	0.1471	Difference is considered to be **not** statistically significant
B(WG)	i	0.1787	Difference is considered to be **not** statistically significant
B(WG)	ii	<0.0001	Difference is extremely statistically significant
B(WG)	iii	0.223	Difference is considered to be **not** statistically significant
C(WG)	i	<0.0001	Difference is extremely statistically significant
C(WG)	iii	<0.0001	Difference is extremely statistically significant
C(WG)	iii	0.0258	Difference **is** considered **very** statistically significant
D(WG)	i	0.0027	Difference is considered to be **very** statistically significant
D(WG)	ii	<0.0001	Difference is extremely statistically significant
D(WG)	iii	0.0035	Difference **is** considered **very** statistically significant
E	i	<0.0001	Difference is extremely statistically significant
E	ii	<0.0001	Difference is extremely statistically significant
E	iii	0.0213	Difference **is** considered statistically significant
F	i	<0.0001	Difference is **not quite** statistically significant
F	ii	<0.0001	Difference is extremely statistically significant
F	iii	0.0415	Difference **is** considered **extremely** statistically significant

To further assess the differences between CTE$_{(RT\text{-}500°C)}$ of the creep and control specimens we significance tested the means of the three specimens with the largest CTE$_{(RT\text{-}500°C)}$ (Table 12). First, we established that the specimen doses were comparable (Table 13). The outcome of the significance testing showed (Table 14) that for all of the six grades neutron irradiation either with or without imposed load, i.e., creep vs. control, was to increase the CTE$_{(RT\text{-}500°C)}$ value. Significantly, in five out of the six grades tested, the creep specimens had a higher CTE$_{(RT\text{-}500°C)}$ than the control specimens (Table 14).

Table 12 Unirradiated $CTE_{(25\text{-}500°C)}$ and the three largest values of $CTE_{(25\text{-}500°C)}$ for the creep and control specimens and their doses for each major grade of graphite in AGC-1

GRADE		Virgin	Irradiated CTE Test Statistics				
			Controls (3 highest CTE Values)		Creep (3 highest CTE Values)		
ID	NAME	CTE x10^{-6} °C^{-1}, 25-500°C	CTE x10^{-6} °C^{-1}, 25-500°C	dose, dpa	CTE x10^{-6} °C^{-1}, 25-500°C	dose, dpa	Creep Strain, %
A	NBG-17 (WG)	n=30	6.32	5.35	7.09	5.47	-1.28
			6.38	4.55	7.15	3.51	-1.09
			6.80	2.65	7.80	3.42	-1.10
	MEAN	5.34	6.50	4.18	7.35	4.13	-1.16
	S.D.	0.104	0.26	1.39	0.39	1.16	0.11
B	NBG-18 (WG)	n=30	6.29	3.41	6.85	5.76	-1.38
			6.35	3.41	6.86	5.38	-1.64
			6.68	5.15	6.94	3.95	-0.09
	MEAN	5.31	6.44	3.99	6.88	5.03	-1.04
	S.D.	0.163	0.21	1.00	0.05	0.95	0.83
C	H-451(WG)	n=22	4.41	6.09	5.59	4.64	-1.42
			4.55	6.7	5.61	6.81	-3.09
			4.62	4.24	6.14	5.56	-2.25
	MEAN	3.75	4.53	5.68	5.78	5.67	-2.25
	S.D.	0.096	0.11	1.28	0.31	1.09	0.84
D	PCEA(WG)	n=33	5.28	3.91	6.53	6.83	-2.42
			5.30	5.02	6.65	5.66	-2.42
			5.46	3.88	6.73	6.62	-2.54
	MEAN	4.76	5.35	4.27	6.64	6.37	-2.46
	S.D.	0.057	0.10	0.65	0.10	0.62	0.07
E	IG-110	n=22	5.99	5.11	7.41	5.11	-1.32
			6.01	5.76	7.42	4.69	-1.92
			6.13	4.36	7.79	4.75	-1.21
	MEAN	4.66	6.04	5.08	7.54	4.85	-1.48
	S.D.	0.109	0.08	0.70	0.22	0.23	0.38
F	IG-430	n=34	6.54	3.8	7.61	4.78	-1.34
			7.00	4.37	7.78	4.30	-1.35
			7.05	5.74	7.84	5.15	-1.28
	MEAN	5.01	6.86	4.64	7.74	4.74	-1.32
	S.D.	0.299	0.28	1.00	0.12	0.43	0.04

Table 13 "t' tests results for the specimen irradiation dose of the three specimens with the largest $CTE_{(25\text{-}500°C)}$

UNPAIRED t TEST RESULTS FOR DOSE OF THE 3 LARGEST CTE $\times 10^{-6}$ °C^{-1}, (25-500°C) VALUES			
GRADE	TEST	Statistics parameter, Two-tailed P	TWO-TAILED TEST RESULT
A(WG)	iv	0.9697	Difference is considered to be **not** statistically significant
B(WG)	iv	0.2616	Difference is considered to be **not** statistically significant
C(WG)	iv	0.9923	Difference is considered to be **not** statistically significant
D(WG)	iv	0.0155	Difference is considered to be statistically significant
E	iv	0.6174	Difference is considered to be **not** statistically significant
F	iv	0.8813	Difference is considered to be **not** statistically significant

Table 14 Significance testing results for the three largest mean coefficient of thermal expansion (25-500°C) from AGC-1

UNPAIRED t TEST RESULTS FOR CTE			
GRADE	TEST	Statistics parameter, two-tailed P	TWO-TAILED TEST RESULT
A(WG)	i	<0.0001	Difference is extremely statistically significant
A(WG)	ii	<0.0001	Difference is extremely statistically significant
A(WG)	iii	0.0348	Difference **is** considered to be statistically significant
B(WG)	i	<0.0001	Difference is extremely statistically significant
B(WG)	ii	<0.0001	Difference is extremely statistically significant
B(WG)	iii	0.0242	Difference **is** considered to be statistically significant
C(WG)	i	<0.0001	Difference is extremely statistically significant
C(WG)	iii	<0.0001	Difference is extremely statistically significant
C(WG)	iii	0.0028	Difference **is** considered to be **very** statistically significant
D(WG)	i	<0.0001	Difference is extremely statistically significant
D(WG)	ii	<0.0001	Difference is extremely statistically significant
D(WG)	iii	<0.0001	Cannot Test
E	i	<0.0001	Difference is extremely statistically significant
E	ii	<0.0001	Difference is extremely statistically significant
E	iii	0.0004	Difference **is** considered to be **extremely** statistically significant
F	i	<0.0001	Difference is extremely statistically significant
F	ii	<0.0001	Difference is extremely statistically significant
F	iii	0.0075	Difference **is** considered to be **very** statistically significant

Clearly, irradiation creep has an effect on the CTE behavior of graphite in excess of that caused by the neutron damage alone.

5 Quality Assurance

The described technical work scope and related activities were conducted in accordance with the applicable quality assurance requirements of ASME NQA-1-2008/1a-2009*, Quality Assurance Requirements for Nuclear Facilities*. Work scope at ORNL was performed under the activity-specific requirements of the applicable ORNL nuclear R&D quality assurance plan (QAP) numbered QAP-ORNL-NR&D-01 and entitled *Quality Assurance Plan for Nuclear Research and Development Conducted at the Oak Ridge National Laboratory*. This QAP is based on and compliant with ASME NQA-1-2008/1a-2009.

6 Conclusions

The electrical resistivity of irradiated graphite greatly exceeds that of unirradiated graphite. Moreover, the resistivity appears to saturate over the dose range examined here, which is similar to behavior reported previously in past electrical resistivity studies. There is no additional effect of creep strain on electrical resistivity over the studied dose range.

All of the graphite grades examined here had an unirradiated mean $CTE_{(25\text{-}500°C)}$ of ≈$5.0x10^{-6}$/°C, with the exception of H-451 which has a mean $CTE_{(25\text{-}500°C)}$ closer to $4x10^{-6}$/°C. In the dose range of AGC-1, the mean CTE was expected to increase with increasing dose and reach a maximum when the individual graphite grades begin to approach dimensional turnaround levels. This behavior was observed.

The CTE of the creep specimens appears to exceed the mean CTE of controls specimens. Clearly, creep has an additional effect on mean CTE in excess of the change observed for neutron irradiation alone.

The exact relationship between CTE and irradiation induced compressive creep remains ill-defined. For grade H-451, previous trends[16] were confirmed. However, other AGC-1 graphite grades exhibited a contrary trend with compressive creep strain.

7 Acknowledgements

This work is sponsored by the U.S. Department of Energy, Office of Nuclear Energy Science and Technology under a Memorandum Purchase Order with Idaho National Laboratory at Oak Ridge National Laboratories managed by UT-Battelle, LLC

The author wishes to thank Ashli Clark for her diligence performing AGC-1 experimental measurements.

8 Appendices

8.1 Electrical Resistivity

The data for each graphite grade are tabulated here in ascending dose, and the creep and control population are separated.

8.1.1 NBG-17

Table 15 Electrical resistivity data for irradiated and crept samples of NBG-17 graphite

Sample ID	GRADE	Dose, DPA	Irr Temp,°C	SPEC TYPE	creep strain, %	Electrical Resistivity μΩm	Fractional change $[(\rho_i/\rho_0)-1]$
AL8-02	NBG-17 AG	4.65	585	Control	0	28.66	1.90
AL6-01	NBG-17 AG	6.4	667	Control	0	28.32	1.87
AL8-01	NBG-17 AG	5.33	655	Creep	-1.42	26.24	1.66
AL6-02	NBG-17 AG	6.7	703	Creep	-1.61	25.02	1.54
AW7-02	NBG-17 WG	2.73	473	Control	0	25.73	1.52
AW6-01	NBG-17 WG	2.79	472	Control	0	28.59	1.80
AW13-01	NBG-17 WG	2.85	470	Control	0	30.16	1.95
AW5-01	NBG-17 WG	2.86	470	Control	0	31.06	2.04
AW2-03	NBG-17 WG	2.87	468	Control	0	29.06	1.84
AW7-01	NBG-17 WG	4.55	587	Control	0	28.00	1.74
AW4-03	NBG-17 WG	4.78	582	Control	0	29.02	1.84
AW5-03	NBG-17 WG	5.35	597	Control	0	29.76	1.91
AW12-03	NBG-17 WG	5.43	594	Control	0	28.65	1.80
AW2-02	NBG-17 WG	5.44	592	Control	0	28.68	1.81
AW10-01	NBG-17 WG	5.61	617	Control	0	27.29	1.67
AW2-01	NBG-17 WG	6.17	650	Control	0	28.54	1.79
AW9-03	NBG-17 WG	6.4	678	Control	0	27.58	1.70
	NBG-17 WG						
AW 6-03	NBG-17 WG	3.32	594	Creep	-0.69	28.76	1.81
AW1-03	NBG-17 WG	3.47	589	Creep	-0.72	29.66	1.90
AW4-02	NBG-17 WG	3.49	592	Creep	-0.90	29.14	1.85
AW6-02	NBG-17 WG	5.23	656	Creep	-1.05	27.96	1.74
AW12-01	NBG-17 WG	3.51	593	Creep	-1.09	30.02	1.94
AW5-02	NBG-17 WG	3.42	594	Creep	-1.10	30.65	2.00
AW1-02	NBG-17 WG	5.97	668	Creep	-1.13	29.20	1.86
AW4-01	NBG-17 WG	5.47	653	Creep	-1.28	29.08	1.85
AW1-01	NBG-17 WG	6.51	690	Creep	-1.42	28.61	1.80
AW9-01	NBG-17 WG	6.09	677	Creep	-1.47	26.83	1.63
AW7-03	NBG-17 WG	6.65	712	Creep	-1.62	27.68	1.71
AW13-02	NBG-17 WG	5.92	674	Creep	-1.85	30.01	1.94
AW10-03	NBG-17 WG	6	670	Creep	-1.89	29.80	1.92
AW10-02	NBG-17 WG	6.66	703	Creep	-2.007	29.42	1.88

8.1.2 NBG-18

Table 16 Electrical resistivity data for irradiated and crept samples of NBG-18 graphite

Sample ID	GRADE	DOSE	Irr. Temp	SPEC TYPE	CREEP STRAIN	Electrical Resistivity μΩm	Fractional change $[(\rho_i/\rho_0)-1]$
BL7-02	NBG-18 AG	3.39	505	Control	0	28.18	2.04
BL6-02	NBG-18 AG	6.56	678	Control	0	26.86	1.90
BL7-01	NBG-18 AG	3.96	599	Creep	-1.06	28.43	2.07
BL6-03	NBG-18 AG	6.76	714	Creep	-2.07	29.08	2.14
BW1-02	NBG-18 WG	3.41	504	Control	0	27.89	1.94
BW11-02	NBG-18 WG	3.41	505	Control	0	29.06	2.07
BW7-01	NBG-18 WG	4.66	585	Control	0	29.10	2.07
BW10-02	NBG-18 WG	5.01	585	Control	0	28.02	1.96
BW3-01	NBG-18 WG	5.15	582	Control	0	29.42	2.11
BW8-02	NBG-18 WG	5.22	599	Control	0	26.61	1.81
BW5-03	NBG-18 WG	5.63	617	Control	0	27.74	1.93
BW12-01	NBG-18 WG	5.72	613	Control	0	27.28	1.88
BW5-02	NBG-18 WG	5.72	611	Control	0	27.70	1.92
BW10-01	NBG-18 WG	5.85	638	Control	0	26.97	1.85
BW8-01	NBG-18 WG	5.95	658	Control	0	27.38	1.89
BW1-03	NBG-18 WG	6.34	664	Control	0	28.40	2.00
BW2-03	NBG-18 WG	6.55	675	Control	0	28.21	1.98
BW7-03	NBG-18 WG	3.76	603	Creep	-0.62	28.62	2.02
BW12-02	NBG-18 WG	3.93	597	Creep	-0.72	28.80	2.04
BW9-03	NBG-18 WG	3.95	599	Creep	-0.90	29.00	2.06
BW3-02	NBG-18 WG	6.19	671	Creep	-1.19	29.70	2.13
BW7-02	NBG-18 WG	6.3	698	Creep	-1.20	29.34	2.10
BW1-01	NBG-18 WG	6.63	700	Creep	-1.35	28.81	2.04
BW9-02	NBG-18 WG	5.62	668	Creep	-1.37	27.34	1.89
BW2-02	NBG-18 WG	5.76	665	Creep	-1.38	29.71	2.14
BW12-03	NBG-18 WG	5.76	675	Creep	-1.48	27.34	1.89
BW9-01	NBG-18 WG	6.28	686	Creep	-1.49	29.17	2.08
BW5-01	NBG-18 WG	5.38	656	Creep	-1.64	31.03	2.28
BW2-01	NBG-18 WG	6.8	709	Creep	-1.72	29.94	2.16
BW11-01	NBG-18 WG	6.21	674	Creep	-1.80	29.20	2.08
BW3-03	NBG-18 WG	6.13	678	Creep	-1.82	31.30	2.30
BW10-03	NBG-18 WG	6.76	709	Creep	-2.03	29.54	2.12

8.1.3 H-451

Table 17 Electrical resistivity data for irradiated and crept samples of H-451 graphite

Sample ID	GRADE	DOSE dpa	Irr. Temp °C	SPEC TYPE	CREEP STRAIN %	Electrical Resistivity μΩm	Fractional change $[(\rho_i/\rho_0)-1]$
CW13-01	H-451 (WG)	4.24	567	Control	0	29.30	3.20
CW14-02	H-451 (WG)	4.74	582	Control	0	29.14	3.18
CW8-03	H-451 (WG)	4.76	580	Control	0	26.95	2.86
CW10-03	H-451 (WG)	6.09	657	Control	0	28.91	3.14
CW10-02	H-451 (WG)	6.66	681	Control	0	28.41	3.07
CW8-02	H-451 (WG)	6.7	674	Control	0	29.40	3.22
CW9-01	H-451 (WG)	6.42	683	Creep	unknown	29.94	3.29
CW11-02	H-451 (WG)	4.6	628	Creep	-1.19	29.80	3.27
CW11-01	H-451 (WG)	4.91	642	Creep	-1.21	29.48	3.23
CW7-03	H-451 (WG)	5.41	649	Creep	-1.35	30.57	3.38
CW14-01	H-451 (WG)	4.64	627	Creep	-1.42	28.80	3.13
CW12-02	H-451 (WG)	5	641	Creep	-1.79	29.32	3.20
CW7-01	H-451 (WG)	6.84	706	Creep	-1.89	28.39	3.07
CW13-02	H-451 (WG)	6.92	708	Creep	-2.1	29.67	3.25
CW13-03	H-451 (WG)	5.46	653	Creep	-2.25	29.73	3.26
CW10-01	H-451 (WG)	6.47	697	Creep	-2.61	29.44	3.22
CW9-03	H-451 (WG)	6.81	712	Creep	-3.09	30.91	3.43

8.1.4 PCEA

Table 18 Electrical resistivity data for irradiated and crept samples of PCEA graphite

Sample ID	GRADE	DOSE dpa	Irr. Temp °C	SPEC TYPE	CREEP STRAIN %	Electrical Resistivity μΩm	Fractional change $[(\rho_i/\rho_0)-1]$
DA702	PCEA (AG)	3.72	538	Control	0	29.82	2.42
DA601	PCEA (AG)	5.96	632	Control	0	28.16	2.23
DA701	PCEA (AG)	4.17	612	Creep	-1.17	28.59	2.28
DA602	PCEA (AG)	6.37	680	Creep	-1.88	27.90	2.20
DW10-02	PCEA (WG)	3.88	534	Control	0	20.81	1.58
DW2-03	PCEA (WG)	3.91	533	Control	0	20.89	1.59
DW5-01	PCEA (WG)	3.91	534	Control	0	22.45	1.79
DW6-01	PCEA (WG)	5.02	585	Control	0	21.42	1.66
DW9-01	PCEA (WG)	5.33	597	Control	0	22.53	1.80
DW4-01	PCEA (WG)	5.47	594	Control	0	22.10	1.74
DW7-02	PCEA (WG)	5.5	618	Control	0	19.87	1.47
DW5-03	PCEA (WG)	5.88	638	Control	0	19.91	1.47
DW2-02	PCEA (WG)	5.96	634	Control	0	19.69	1.45
DW8-03	PCEA (WG)	6.24	670	Control	0	19.57	1.43
DW7-01	PCEA (WG)	6.27	679	Control	0	17.40	1.16
DW2-01	PCEA (WG)	6.49	672	Control	0	20.80	1.58
DW4-03	PCEA (WG)	6.68	674	Control	0	20.74	1.58
DW1-03	PCEA (WG)	4.36	606	Creep	-0.95	21.38	1.66
DW8-02	PCEA (WG)	4.25	611	Creep	-1.25	19.76	1.45
DW3-03	PCEA (WG)	4.38	609	Creep	-1.32	21.70	1.69
DW10-01	PCEA (WG)	4.39	610	Creep	-1.59	19.89	1.47
DW1-01	PCEA (WG)	6.73	706	Creep	-1.63	29.04	2.61
DW6-03	PCEA (WG)	6.52	714	Creep	-1.66	18.72	1.32
DW3-02	PCEA (WG)	6.02	670	Creep	-1.75	21.29	1.64
DW8-01	PCEA (WG)	5.87	674	Creep	-1.85	19.46	1.42
DW7-03	PCEA (WG)	6.55	706	Creep	-2.04	19.20	1.38
DW3-01	PCEA (WG)	6.8	711	Creep	-2.04	21.64	1.69
DW1-02	PCEA (WG)	6.39	683	Creep	-2.40	19.33	1.40
DW9-03	PCEA (WG)	6.83	710	Creep	-2.42	18.72	1.33
DW5-02	PCEA (WG)	5.66	669	Creep	-2.42	21.61	1.68
DW11-01	PCEA (WG)	6.32	687	Creep	-2.54	19.84	1.46
DW6-02	PCEA (WG)	5.97	679	Creep	unknown	19.65	1.44

8.1.5 IG-110

Table 19 Electrical resistivity data for irradiated and crept samples of IG-110 graphite

Sample ID	GRADE	DOSE dpa	Irr. Temp °C	SPEC TYPE	CREEP STRAIN %	Electrical Resistivity μΩm	Fractional change $[(\mu_i/\mu_0)-1]$
EW9-02	IG-110	3.31	507	Control	0	25.62	1.10
EW2-03	IG-110	4.36	562	Control	0	26.90	1.20
EW10-01	IG-110	5.11	582	Control	0	26.18	1.15
EW5-03	IG-110	5.76	613	Control	0	26.56	1.18
EW8-01	IG-110	6.13	671	Control	0	26.85	1.20
EW5-02	IG-110	6.18	653	Control	0	24.72	1.03
EW10-03	IG-110	6.43	678	Control	0	24.13	0.98
EW9-01	IG-110	6.62	681	Control	0	24.44	1.00
EW2-02	IG-110	4.75	621	Creep	-1.21	26.62	1.18
EW8-03	IG-110	3.82	601	Creep	-1.31	29.06	1.38
EW2-01	IG-110	5.11	635	Creep	-1.32	25.87	1.12
EW7-01	IG-110	6.42	708	Creep	-1.82	25.02	1.05
EW4-01	IG-110	4.69	628	Creep	-1.92	26.62	1.18
EW6-03	IG-110	6.63	713	Creep	-1.94	25.07	1.05
EW5-01	IG-110	6.24	674	Creep	-2.12	26.62	1.18
EW6-01	IG-110	5.05	642	Creep	-2.17	26.02	1.13
EW9-03	IG-110	5.75	666	Creep	-2.31	25.59	1.10
EW8-02	IG-110	6.77	712	Creep	-2.53	25.26	1.07
EW10-02	IG-110	6.69	713	Creep	-2.76	25.05	1.05
EW4-02	IG-110	6.54	693	Creep	-2.78	26.02	1.13

8.1.6 IG-430

Table 20 Electrical resistivity data for irradiated and crept samples of IG-430 graphite

Sample ID	GRADE	DOSE dpa	Irr. Temp °C	SPEC TYPE	CREEP STRAIN %	Electrical Resistivity μΩm	Mean Fractional change [(Ω$_i$/Ω$_0$)-1]
FW4-01	IG-430	2.78	472	Control	0	25.61	1.65
FW7-03	IG-430	3.32	508	Control	0	26.07	1.69
FW7-02	IG-430	3.80	537	Control	0	26.14	1.70
FW3-03	IG-430	4.37	564	Control	0	27.17	1.81
FW9-01	IG-430	4.91	587	Control	0	27.68	1.86
FW2-01	IG-430	5.12	580	Control	0	23.62	1.44
FW5-03	IG-430	5.74	639	Control	0	24.09	1.49
FW10-02	IG-430	6.06	656	Control	0	23.03	1.38
FW3-02	IG-430	6.22	653	Control	0	22.53	1.33
FW7-01	IG-430	6.28	670	Control	0	25.91	1.68
FW10-01	IG-430	6.52	678	Control	0	23.77	1.45
FW1-03	IG-430	6.61	672	Control	0	25.48	1.63
FW11-03	IG-430	6.73	677	Control	0	24.88	1.57
FW12-01	IG-430	3.37	593	Creep	-0.92	25.96	1.68
FW8-02	IG-430	5.51	669	Creep	-0.95	25.68	1.65
FW13-01	IG-430	5.72	662	Creep	-1.09	24.15	1.49
FW4-02	IG-430	6.15	688	Creep	-1.18	24.88	1.57
FW5-02	IG-430	3.87	602	Creep	-1.21	25.09	1.59
FW2-03	IG-430	5.15	639	Creep	-1.28	28.92	1.99
FW3-01	IG-430	4.78	625	Creep	-1.34	22.90	1.36
FW5-01	IG-430	4.30	612	Creep	-1.35	24.87	1.57
FW8-01	IG-430	6.59	716	Creep	-1.45	25.06	1.59
FW11-01	IG-430	5.14	639	Creep	-1.54	25.78	1.66
FW11-02	IG-430	4.78	626	Creep	-1.54	25.21	1.60
FW9-03	IG-430	6.43	697	Creep	-1.55	25.64	1.65
FW1-01	IG-430	6.79	708	Creep	-1.70	25.06	1.59
FW9-02	IG-430	6.72	714	Creep	-1.75	25.47	1.63
FW2-02	IG-430	6.58	693	Creep	-1.83	25.03	1.59
FW4-03	IG-430	6.59	707	Creep	-2.04	24.97	1.58
FW10-03	IG-430	6.87	708	Creep	-2.56	23.58	1.44

8.2 Coefficient of Thermal Expansion

8.2.1 NBG-17

Table 21 Average Coefficient of Thermal Expansion (α) over the temperature range RT - 500°C for irradiated and crept NBG-17 Graphite

Sample ID	GRADE	Dose, DPA	Irr Temp,°C	SPEC TYPE	creep strain, %	Mean CTE $x10^{-6}\,^{o}C^{-1}$, 25-500°C	Fractional change $[(\alpha_i/\alpha_0)-1]$
AL8-02	NBG-17 AG	4.65	585	Control	0	6.28	0.13
AL6-01	NBG-17 AG	6.4	667	Control	0	5.05	-0.09
AL8-01	NBG-17 AG	5.33	655	Creep	-1.42	6.27	0.13
AL6-02	NBG-17 AG	6.7	703	Creep	-1.61	6.15	0.11
AW7-02	NBG-17 WG	2.73	473	Control	0		
AW6-01	NBG-17 WG	2.79	472	Control	0	6.15	0.15
AW13-01	NBG-17 WG	2.85	470	Control	0	6.80	0.27
AW5-01	NBG-17 WG	2.86	470	Control	0	6.25	0.17
AW2-03	NBG-17 WG	2.87	468	Control	0	6.28	0.18
AW7-01	NBG-17 WG	4.55	587	Control	0	6.38	0.20
AW4-03	NBG-17 WG	4.78	582	Control	0	5.75	0.08
AW5-03	NBG-17 WG	5.35	597	Control	0	6.32	0.18
AW12-03	NBG-17 WG	5.43	594	Control	0	6.05	0.13
AW2-02	NBG-17 WG	5.44	592	Control	0	5.86	0.10
AW10-01	NBG-17 WG	5.61	617	Control	0	5.93	0.11
AW2-01	NBG-17 WG	6.17	650	Control	0	5.49	0.03
AW9-03	NBG-17 WG	6.4	678	Control	0	5.27	-0.01
	NBG-17 WG						
AW 6-03	NBG-17 WG	3.32	594	Creep	-0.69	6.67	0.25
AW1-03	NBG-17 WG	3.47	589	Creep	-0.72	6.78	0.27
AW4-02	NBG-17 WG	3.49	592	Creep	-0.90	6.95	0.30
AW6-02	NBG-17 WG	5.23	656	Creep	-1.05	6.39	0.20
AW12-01	NBG-17 WG	3.51	593	Creep	-1.09	7.15	0.34
AW5-02	NBG-17 WG	3.42	594	Creep	-1.10	7.80	0.46
AW1-02	NBG-17 WG	5.97	668	Creep	-1.13	6.80	0.27
AW4-01	NBG-17 WG	5.47	653	Creep	-1.28	7.09	0.33
AW1-01	NBG-17 WG	6.51	690	Creep	-1.42	5.73	0.07
AW9-01	NBG-17 WG	6.09	677	Creep	-1.47	5.56	0.04
AW7-03	NBG-17 WG	6.65	712	Creep	-1.62	6.07	0.14
AW13-02	NBG-17 WG	5.92	674	Creep	-1.85	7.05	0.32
AW10-03	NBG-17 WG	6	670	Creep	-1.89	7.08	0.33
AW10-02	NBG-17 WG	6.66	703	Creep	-2.007	6.56	0.23

8.2.2 NBG-18

Table 22 Average Coefficient of Thermal Expansion (α) over the temperature range RT - 500°C for irradiated and crept NBG-18 Graphite

Sample ID	GRADE	DOSE	Irr. Temp °C	SPEC TYPE	CREEP STRAIN %	Mean CTE $x10^{-6}\ {}^{o}C^{-1}$, 25-500°C	Fractional change $[(\alpha_i/\alpha_0)-1]$
BL7-02	NBG-18 AG	3.39	505	Control	0	6.11	0.13
BL6-02	NBG-18 AG	6.56	678	Control	0	4.87	-0.10
BL7-01	NBG-18 AG	3.96	599	Creep	-1.06	6.62	0.23
BL6-03	NBG-18 AG	6.76	714	Creep	-2.07	6.00	0.11
BW1-02	NBG-18 WG	3.41	504	Control	0	6.35	0.20
BW11-02	NBG-18 WG	3.41	505	Control	0	6.29	0.18
BW7-01	NBG-18 WG	4.66	585	Control	0	5.51	0.04
BW10-02	NBG-18 WG	5.01	585	Control	0	5.96	0.12
BW3-01	NBG-18 WG	5.15	582	Control	0	6.68	0.26
BW8-02	NBG-18 WG	5.22	599	Control	0	6.07	0.14
BW5-03	NBG-18 WG	5.63	617	Control	0	5.89	0.11
BW12-01	NBG-18 WG	5.72	613	Control	0	5.82	0.10
BW5-02	NBG-18 WG	5.72	611	Control	0	5.78	0.09
BW10-01	NBG-18 WG	5.85	638	Control	0	5.28	0.00
BW8-01	NBG-18 WG	5.95	658	Control	0	6.07	0.14
BW1-03	NBG-18 WG	6.34	664	Control	0	5.18	-0.02
BW2-03	NBG-18 WG	6.55	675	Control	0	5.18	-0.02
BW7-03	NBG-18 WG	3.76	603	Creep	-0.62	6.63	0.25
BW12-02	NBG-18 WG	3.93	597	Creep	-0.72	6.06	0.14
BW9-03	NBG-18 WG	3.95	599	Creep	-0.90	6.94	0.31
BW3-02	NBG-18 WG	6.19	671	Creep	-1.19	5.90	0.11
BW7-02	NBG-18 WG	6.3	698	Creep	-1.20	5.79	0.09
BW1-01	NBG-18 WG	6.63	700	Creep	-1.35	6.34	0.19
BW9-02	NBG-18 WG	5.62	668	Creep	-1.37	6.65	0.25
BW2-02	NBG-18 WG	5.76	665	Creep	-1.38	6.85	0.29
BW12-03	NBG-18 WG	5.76	675	Creep	-1.48	6.26	0.18
BW9-01	NBG-18 WG	6.28	686	Creep	-1.49	6.19	0.17
BW5-01	NBG-18 WG	5.38	656	Creep	-1.64	6.86	0.29
BW2-01	NBG-18 WG	6.8	709	Creep	-1.72	5.97	0.12
BW11-01	NBG-18 WG	6.21	674	Creep	-1.80	6.74	0.27
BW3-03	NBG-18 WG	6.13	678	Creep	-1.82	6.25	0.18
BW10-03	NBG-18 BW	6.76	709	Creep	-2.03	5.66	0.06

8.2.3 H-451

Table 23 Average Coefficient of Thermal Expansion (α) over the temperature range RT - 500°C for irradiated and crept H-451 Graphite

Sample ID	GRADE	DOSE dpa	Irr. Temp °C	SPEC TYPE	CREEP STRAIN %	Mean CTE $x10^{-6}\,{}^{o}C^{-1}$, 25-500°C	Fractional change $[(\alpha_i/\alpha_0)-1]$
CW13-01	H-451 (WG)	4.24	567	Control	0	4.62	0.23
CW14-02	H-451 (WG)	4.74	582	Control	0	4.36	0.16
CW8-03	H-451 (WG)	4.76	580	Control	0	4.00	0.07
CW10-03	H-451 (WG)	6.09	657	Control	0	4.41	0.18
CW10-02	H-451 (WG)	6.66	681	Control	0	4.18	0.12
CW8-02	H-451 (WG)	6.7	674	Control	0	4.55	0.21
CW9-01	H-451 (WG)	6.42	683	Creep	unknown	5.90	0.57
CW11-02	H-451 (WG)	4.6	628	Creep	-1.19	5.34	0.43
CW11-01	H-451 (WG)	4.91	642	Creep	-1.21	4.62	0.23
CW7-03	H-451 (WG)	5.41	649	Creep	-1.35	5.25	0.40
CW14-01	H-451 (WG)	4.64	627	Creep	-1.42	5.59	0.49
CW12-02	H-451 (WG)	5	641	Creep	-1.79	5.36	0.43
CW7-01	H-451 (WG)	6.84	706	Creep	-1.89	5.47	0.46
CW13-02	H-451 (WG)	6.92	708	Creep	-2.1	5.24	0.40
CW13-03	H-451 (WG)	5.46	653	Creep	-2.25	6.14	0.64
CW10-01	H-451 (WG)	6.47	697	Creep	-2.61	5.31	0.42
CW9-03	H-451 (WG)	6.81	712	Creep	-3.09	5.61	0.50

8.2.4 PCEA

Table 24 Average Coefficient of Thermal Expansion (α) over the temperature range RT - 500°C for irradiated and crept PCEA Graphite

Sample ID	GRADE	DOSE dpa	Irr. Temp °C	SPEC TYPE	CREEP STRAIN %	Mean CTE $x10^{-6}\,^{o}C^{-1}$, 25-500°C	Fractional change $[(\alpha_i/\alpha_0)-1]$
DA702	PCEA (AG)	3.72	538	Control	0	5.21	0.00
DA601	PCEA (AG)	5.96	632	Control	0	5.07	-0.02
DA701	PCEA (AG)	4.17	612	Creep	-1.17	6.35	0.22
DA602	PCEA (AG)	6.37	680	Creep	-1.88	6.35	0.22
DW10-02	PCEA (WG)	3.88	534	Control	0	5.46	0.15
DW2-03	PCEA (WG)	3.91	533	Control	0	5.28	0.11
DW5-01	PCEA (WG)	3.91	534	Control	0	5.07	0.07
DW6-01	PCEA (WG)	5.02	585	Control	0	5.30	0.11
DW9-01	PCEA (WG)	5.33	597	Control	0	5.22	0.10
DW4-01	PCEA (WG)	5.47	594	Control	0	4.95	0.04
DW7-02	PCEA (WG)	5.5	618	Control	0	5.20	0.09
DW5-03	PCEA (WG)	5.88	638	Control	0	5.19	0.09
DW2-02	PCEA (WG)	5.96	634	Control	0	5.00	0.05
DW8-03	PCEA (WG)	6.24	670	Control	0	5.03	0.06
DW7-01	PCEA (WG)	6.27	679	Control	0	4.26	-0.10
DW2-01	PCEA (WG)	6.49	672	Control	0	4.91	0.03
DW4-03	PCEA (WG)	6.68	674	Control	0	4.54	-0.05
DW1-03	PCEA (WG)	4.36	606	Creep	-0.95	5.94	0.25
DW8-02	PCEA (WG)	4.25	611	Creep	-1.25	6.01	0.26
DW3-03	PCEA (WG)	4.38	609	Creep	-1.32	5.54	0.16
DW10-01	PCEA (WG)	4.39	610	Creep	-1.59	6.46	0.36
DW6-02	PCEA (WG)	5.97	679	Creep	-1.61	5.69	0.19
DW1-01	PCEA (WG)	6.73	706	Creep	-1.63	5.87	0.23
DW6-03	PCEA (WG)	6.52	714	Creep	-1.66	4.93	0.04
DW3-02	PCEA (WG)	6.02	670	Creep	-1.75	6.07	0.28
DW8-01	PCEA (WG)	5.87	674	Creep	-1.85	6.19	0.30
DW7-03	PCEA (WG)	6.55	706	Creep	-2.04	6.47	0.36
DW3-01	PCEA (WG)	6.8	711	Creep	-2.04	6.37	0.34
DW1-02	PCEA (WG)	6.39	683	Creep	-2.40	5.82	0.22
DW9-03	PCEA (WG)	6.83	710	Creep	-2.42	6.53	0.37
DW5-02	PCEA (WG)	5.66	669	Creep	-2.42	6.65	0.40
DW11-01	PCEA (WG)	6.32	687	Creep	-2.54	6.73	0.41

8.2.5 IG-110

Table 25 Average Coefficient of Thermal Expansion (α) over the temperature range RT - 500°C for irradiated and crept IG-110 Graphite

Sample ID	GRADE	DOSE dpa	Irr. Temp °C	SPEC TYPE	CREEP STRAIN %	Mean CTE $x10^{-6}\,^{o}C^{-1}$, 25-500°C	Fractional change $[(\alpha_i/\alpha_0)-1]$
EW9-02	IG-110	3.31	507	Control	0.00	5.88	0.26
EW2-03	IG-110	4.36	562	Control	0.00	6.13	0.32
EW10-01	IG-110	5.11	582	Control	0.00	5.99	0.29
EW5-03	IG-110	5.76	613	Control	0.00	6.01	0.29
EW8-01	IG-110	6.13	671	Control	0.00	5.95	0.28
EW5-02	IG-110	6.18	653	Control	0.00	5.41	0.16
EW10-03	IG-110	6.43	678	Control	0.00	5.52	0.19
EW9-01	IG-110	6.62	681	Control	0.00	5.06	0.09
EW2-02	IG-110	4.75	621	Creep	-1.21	7.79	0.67
EW8-03	IG-110	3.82	601	Creep	-1.31	7.06	0.52
EW2-01	IG-110	5.11	635	Creep	-1.32	7.41	0.59
EW7-01	IG-110	6.42	708	Creep	-1.82	5.73	0.23
EW4-01	IG-110	4.69	628	Creep	-1.92	7.42	0.59
EW6-03	IG-110	6.63	713	Creep	-1.94	5.82	0.25
EW5-01	IG-110	6.24	674	Creep	-2.12	7.30	0.57
EW6-01	IG-110	5.05	642	Creep	-2.17	7.26	0.56
EW9-03	IG-110	5.75	666	Creep	-2.31	4.43	-0.05
EW8-02	IG-110	6.77	712	Creep	-2.53	6.47	0.39
EW10-02	IG-110	6.69	713	Creep	-2.76	6.39	0.37
EW4-02	IG-110	6.54	693	Creep	-2.78	7.37	0.58

8.2.6 IG-430

Table 26 Average Coefficient of Thermal Expansion (α) over the temperature range RT - 500°C for irradiated and crept IG-430 Graphite

Sample ID	GRADE	DOSE dpa	Irr. Temp °C	SPEC TYPE	CREEP STRAIN %	Mean CTE $x10^{-6}$ $^oC^{-1}$, 25-500°C	Fractional change $[(\alpha_i/\alpha_0)-1]$
FW4-01	IG-430	2.78	472	Control	0	6.34	0.26
FW7-03	IG-430	3.32	508	Control	0	6.49	0.30
FW7-02	IG-430	3.80	537	Control	0	6.54	0.31
FW3-03	IG-430	4.37	564	Control	0	7.00	0.40
FW9-01	IG-430	4.91	587	Control	0	6.00	0.20
FW5-03	IG-430	5.74	639	Control	0	7.05	0.41
FW10-02	IG-430	6.06	656	Control	0	6.44	0.28
FW3-02	IG-430	6.22	653	Control	0	5.21	0.04
FW7-01	IG-430	6.28	670	Control	0	6.21	0.24
FW10-01	IG-430	6.52	678	Control	0	5.53	0.10
FW1-03	IG-430	6.61	672	Control	0	5.81	0.16
FW11-03	IG-430	6.73	677	Control	0	4.78	-0.05
FW12-01	IG-430	3.37	593	Creep	-0.92	7.60	0.52
FW8-02	IG-430	5.51	669	Creep	-0.95	7.01	0.40
FW13-01	IG-430	5.72	662	Creep	-1.09	7.48	0.49
FW4-02	IG-430	6.15	688	Creep	-1.18	6.62	0.32
FW5-02	IG-430	3.87	602	Creep	-1.21	7.47	0.49
FW2-03	IG-430	5.15	639	Creep	-1.28	7.84	0.56
FW3-01	IG-430	4.78	625	Creep	-1.34	7.61	0.52
FW5-01	IG-430	4.30	612	Creep	-1.35	7.78	0.55
FW8-01	IG-430	6.59	716	Creep	-1.45	5.21	0.04
FW11-01	IG-430	5.14	639	Creep	-1.54	7.07	0.41
FW11-02	IG-430	4.78	626	Creep	-1.54	7.61	0.52
FW9-03	IG-430	6.43	697	Creep	-1.55	7.31	0.46
FW1-01	IG-430	6.79	708	Creep	-1.70	7.02	0.40
FW9-02	IG-430	6.72	714	Creep	-1.75	5.61	0.12
FW2-02	IG-430	6.58	693	Creep	-1.83	6.85	0.37
FW4-03	IG-430	6.59	707	Creep	-2.04	7.23	0.44
FW10-03	IG-430	6.87	708	Creep	-2.56	6.21	0.24

9 Distribution

ORNL	INL	DOE
Tim Burchell	Judy Mount	William Corwin
Anne Campbell	Larry Hull	Tom O'Conner
Cristian Contescu	Travis Mitchell	
Yutai Katoh	David Swank	
Mark Vance	David Petti	
Wei Ju Ren	William Windes	

10 References

[1] ORNL/TM-2015/378, Tim Burchell, "AGC-1 irradiation induced property changes analysis report B: Elastic Constants", August 2015
[2] ORNL/TM-2005/505 Timothy Burchell and Robert Bratton "Graphite irradiation creep capsule AGC-1 experimental plan", September 2006
[3] ORNL/TM-2009/009, Timothy D. Burchell' "A revised AGC-1 creep capsule layout", November 2010
[4] ORNL/TM-2010/285, Tim Burchell, Joe Strizak and Marie Williams, "AGC-1 Specimen Pre-irradiation Data Report" October 2010
[5] ORNL/TM-2013/242, Tim Burchell "AGC-1 Specimen Post Irradiation Data Report", Sept 2013
[6] ORNL/TM-2014/255, Tim Burchell, "AGC-1 Creep Strain Data Analysis" September 2014
[7] Student (William S. Gossett), "The Probable Error of a Mean", BIOMETRIKA Vol.6, No. 1pp. 1-25 (1908)
[8] GraphPad Software, QuickCalcs, t test. http://www.graphpad.com/quickcalcs/ttest1/?Format=SD
[9] Mrozowski, S. In Proceedings First and Second Conference on Carbon, Pergamon Press, p. 31 (1956)
[10] R. E. Nightingale., "Nuclear Graphite", Pub., Academic Press, New York (1962)
[11] J. H. W. Simmons, "Radiation Damage in Graphite". Pub. Pergamon Press, Oxford (1965)
[12] B. T. Kelly., "Physics of Graphite" Pub. Applied Science Publishers. (London (1981)
[13] T.D. Burchell, "Radiation Effects in Graphite and Carbon-Based Materials", *MRS Bulletin*, Volume XXII, No. 2 pp. 29-35, February 1997
[14] Burchell , T. D., Radiation Effects in Graphite. In Konings, R.J.M., (ed.) Comprehensive Nuclear Materials, volume 4, pp. 299-324 Amsterdam; Elsevier (2012).
[15] Davies, M. A. and Bradford, M. R., "Modelling Graphite Aging: Black Art of Forensic Science? In: Management of Ageing Processes in Graphite Reactor Cores. G.B Neighbour, Ed., Pub. RSC Publishing, pp.100-107 (2007)
[16] Kelly, B.T. and Burchell, T.D., "The Analysis of Irradiation Creep Experiments on Nuclear Reactor Graphites"' Carbon, Vol. 32, No.1, pp. 119- 125 (1994)